

STRUCTURE AND FUNCTION OF CYTOCHROME

c550 OF *SYNECHOCYSTIS* sp. PCC6803:

FACTORS CONTROLLING

REDOX POTENTIAL

By

HEATHER L. ANDREWS

Bachelor of Science

Missouri Southern State University

Joplin, Missouri

2000

**Submitted to the Faculty of the
Graduate College of the
Oklahoma State University
in partial fulfillment of
the requirement for
the Degree of
MASTER OF SCIENCE
December, 2003**

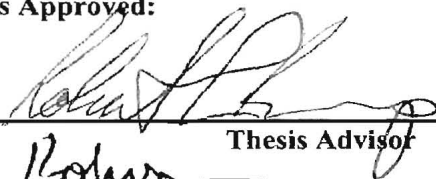
STRUCTURE AND FUNCTION OF CYTOCHROME

c550 OF *SYNECHOCYSTIS* sp. PCC6803:

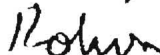
FACTORS CONTROLLING

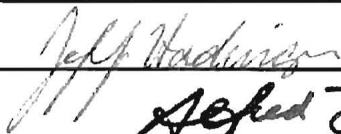
REDOX POTENTIAL

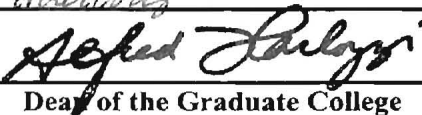
Thesis Approved:



Thesis Advisor







Dean of the Graduate College

ACKNOWLEDGMENTS

I wish to express my sincere appreciation to my major advisor, Dr. Robert Burnap, for his constructive guidance and input, encouragement, and for instilling confidence in me to conduct my research. My sincere appreciation also extends to Dr. Xhaolang Li for working by my side throughout my project as a mentor and educator. I am in debt to him for being extremely patient and for providing extra guidance with every aspect of my project whenever I needed it. My appreciation extends to my other committee members, Dr. Robert Miller, and Dr. Jeffery Hadwiger, whose time, advice and assistance were also invaluable. My appreciation extends to Dr. Mario Rivera who was our collaborator, for dedicating his time, expertise, and excellent guidance to my project. I also want to thank Dr. Rivera and his lab members for allowing me to use their lab, while making it one of the most pleasurable working experiences. My thanks goes to Adriana Altuve, Gregori Caignan, and Christopher Damaso, as all of your friendships and assistance were greatly appreciated.

A special thanks is due to my colleagues and friends in Dr. Burnap's lab: Dr. Hong-Liang Wang, Bradley Postier, Jessica Klahn and Lori Impson for not only their help in my research, but for creating an enjoyable and pleasant work environment.

I would also like to give a very special thanks to my parents and brother Adam who have always been there for me under any circumstances and who have always

managed to keep me on track and help me to not lose site of my goals and dreams. I also want to thank Ira Burnett who has been with me throughout my graduate experience for being patient, kind and loving towards me. Your companionship has been essential in me making it through this process. Lastly, I extend my appreciation to all of my other family and friends. A person could not ask for a group of more supportive and loving individuals, and I feel blessed to be surrounded by them.

TABLE OF CONTENTS

Chapter	Page
1. GENERAL INTRODUCTION.....	1
2. LITERATURE REVIEW.....	3
<i>Photosystem II</i>	4
<i>Synechocystis sp. PCC6803</i>	7
<i>Cytochrome c550</i>	8
<i>Experimental background</i>	12
<i>Redox properties of cytochromes</i>	16
<i>Comparisons of c-type cytochromes</i>	18
<i>Selection of mutation target sites</i>	25
3. OBJECTIVES.....	28
4. MATERIALS AND METHODS.....	29
Construction of pETC550 plasmid vector.....	29
Mutagenic primer design.....	31
Site-directed mutagenesis using polymerase chain reaction (PCR).....	32
Transformation of mutant PCR products into <i>Epicurian Coli</i> XL-1 Blue Supercompetent Cells.....	35
Mini-plasmid preparations.....	35
Restriction Enzyme Digests.....	36
Transformation into BL-21 (DE3) <i>E.coli</i> containing pEC86.....	37
The over-expression of pETC550 in BL-21 (DE3) <i>E.coli</i> with pEC86.....	37
Periplasmic fraction preparation.....	38
Crude extract protein preparation.....	39
Column chromatography protein purification.....	39
SDS-page gel analysis.....	40
Spectroelectrochemistry.....	40
5. EXPRESSION AND PURIFICATION OF CYT. c550.....	43
Introduction.....	43
Mutagenesis.....	44
Over-expression of cyt. c550 using a binary plasmid system in <i>E.coli</i>	48

Optimization of Expression.....	49
Purification.....	58
6. REDOX PROPERTIES OF CYTOCHROME c550 AND MUTANTS.....	64
Introduction.....	64
Results and Discussion.....	66
Cyt. c550.....	68
Cyt. c550-T48I.....	72
Cyt. c550-L91I.....	74
Cyt. c550H.....	76
Cyt Hc550.....	78
Cyt. c550-P93A and P93G.....	82
Cyt. c550-N49L and N49D.....	85
Cyt. c550-H92M.....	89
7. SUMMARY.....	91
BIBLIOGRAPHY.....	96
APPENDIX.....	102

LIST OF TABLES

Table	Page
1. Plasmids.....	31
2. Bacterial strains.....	31
3. Mutagenic primer design.....	32
4. Redox mediators used for spectroelectrochemistry.....	42
5. Successfully mutagenized cytochromes.....	44
6. Expression conditions of Cyt. c550.....	50
7. Concentrations and yields of the 3 column chromatography purification.....	59
8. Concentrations of proteins after crude extract purification.....	63
9. Results of the sodium dithionite titrations of cyt. c550 and mutants.....	68

LIST OF FIGURES

Figure	Page
1. Photosystem II complex	7
2. Heme environment of cytochrome c550.....	10
3. Sequence alignment of cyt. c550 and vcyt. C6.....	19
4. Structural alignment of cyt. c550 of <i>Synechocystis</i> sp. PCC6803 and cyt. c6 of <i>Arthrospira maxima</i>	21
5. Structural alignment of cyt. c550 of <i>Synechocystis</i> sp. PCC6803 and cyt. c6 of <i>Arthrospira maxima</i> with spacefill.....	23
6. Cytochrome c550 asparagine 49 mutant.....	26
7. Cytochrome c550 with bis-histidine axial ligation and his-met axial ligation.....	27
8. Cytochrome c550 proline 93 mutant.....	27
9. pET22 with <i>psbV</i> insert.....	30
10. pETC550 plasmid map.....	30
11. Site-directed mutagenesis flow-chart.....	34
12. Restriction enzyme digest of Cyt. c550-N49D with <i>PstI</i>	46
13. The pEC86 plasmid used to overexpress Cyt. c550 in <i>E. coli</i>	49
14. Characteristic spectra of periplasmic fraction preparation after the addition of sodium dithionite.....	51
15. Absorbance of Cyt. c550-P93A under varying IPTG concentrations as a percentage of the control.....	53

16. The induction by IPTG given at varying concentrations on the expression of Cyt. c550-P93A in <i>E.coli</i> at 28°C.....	54
17. The induction by IPTG given at varying concentrations on the expression of Cyt. c550-P93A in <i>E.coli</i> at 37°C.....	55
18. The induction by IPTG given at varying concentrations on the expression of Cyt. c550-H92M in <i>E.coli</i> at 37°C.....	56
19. The induction by IPTG given at varying concentrations on the expression of Cyt. c550-H92M in <i>E.coli</i> at 28°C.....	56
20. The effects of 0.5mM IPTG, 2.5mM Betaine, and 300mM Sucrose on the expression of Cyt. c550-H92M in <i>E.coli</i> at 28°C.....	57
21. Ion exchange profile with 500mM NaCl salt gradient for Cyt. c550 after purification through DEAE cellulose column.....	60
22. Ion exchange profile for Cyt. c550 after purification through the DEAE sephacel column.....	60
23. Elution profile of Cyt. c550 after purification through the gel permeation column (G-75 superdex).....	61
24. SDS-page: FPLC purification of Cyt.C550 on Ni-NTA Superflow.....	62
25. Redox titration spectrum at 550nm.....	65
26. Graphs of spectroelectrochemical titration of cyt. c550 using sodium dithionite.....	71
27. Graphs of spectroelectrochemical titration of cyt. c550-T48I using sodium dithionite.....	73
28. Graphs of spectroelectrochemical titration of cyt. c550-L91I using sodium dithionite.....	75
29. Graphs of spectroelectrochemical titration of cyt. c550H using sodium dithionite.....	77

30. Effects of dithiothreitol concentration and the position of his-tag on the electrophoretic behavior of cyt. c550.....	78
31. Graphs of spectroelectrochemical titration of cyt. Hc550 using sodium dithionite.....	79
32. MALDI-TOF mass spectra of cyt. c550 with a C-terminal his-tag and a N-terminal his-tag from <i>Synechocystis</i> sp. PCC6803.....	81
33. Graphs of spectroelectrochemical titration of cyt. c550-P93A using sodium dithionite.....	84
34. Graphs of spectroelectrochemical titration of cyt. c550-N49L using sodium dithionite.....	87
35. Graphs of spectroelectrochemical titration of cyt. c550-N49D using sodium dithionite.....	88
36. Graphs of spectroelectrochemical titration of cyt. c550-H92M using sodium dithionite.....	90

ABBREVIATIONS AND SYMBOLS

1. **PSII**..... photosystem II
2. **c550**.....cytochrome c550
3. **Cyt**.....cytochrome
4. **PSI**..... photosystem I
5. **OEC**..... oxygen evolving complex
6. **Nmole**..... nano mole
8. **mM**..... milli mole
9. **μ** micro
10. **pETC550**..... pET22bC550
11. **OEA**.....oxygen evolving activity
12. **kDa**.....kilodalton
13. **mV**.....millivolts
14. **Å**.....Angstrom
15. **α**alpha
17. **β**beta
16. **δ**imidazole
17. **MP**.....midpoint potential

CHAPTER 1

GENERAL INTRODUCTION

Photosynthesis is responsible for the conversion of the energy in sunlight into usable forms of energy, therefore making it arguably the most important biological process on earth. Photosynthesis converts carbon dioxide from the air into sugars, starches and other high-energy carbohydrates while also releasing oxygen. Photosynthesis directly or indirectly, fulfills all of our food requirements and many of our needs for fiber and building materials. In addition, the energy stored in petroleum, natural gas and coal all come from the sun via photosynthesis, as does the energy in firewood, which is major source of fuel in many parts of the world. Hence, this phenomenal process of liberating oxygen and fixing carbon dioxide has transformed the world into the hospitable environment we live in today (Gust, 1996).

One of the reaction centers of oxygenic photosynthesis is photosystem II (PSII), where light energy is used to split water into oxygen, protons and electrons. This process can be studied in model organisms such as the cyanobacterium *Synechocystis* sp. PCC6803 (*Synechocystis* 6803). One evolutionarily conserved protein of *Synechocystis* PSII with an unknown function is cytochrome c550. This unique protein is a mono-heme cytochrome with bis-histidine coordination and an unusually low redox midpoint potential of -250mV. Therefore, it is important to study c550's structure to see how it applies to this very negative redox potential, and to answer questions regarding the

unknown functional role of cyt. c550 in PSII, and additionally achieve a better understanding of other redox proteins.

CHAPTER 2

LITERATURE REVIEW

Photosynthesis

Photosynthesis is responsible for the conversion of the energy in sunlight into usable forms of energy, therefore making it arguably the most important biological process on earth. Photosynthesis converts carbon dioxide from the air into sugars, starches and other high-energy carbohydrates while also releasing oxygen. Photosynthesis directly or indirectly, fulfills all of our food requirements and many of our needs for fiber and building materials. In addition, the energy stored in petroleum, natural gas and coal all come from the sun via photosynthesis, as does the energy in firewood, which is major source of fuel in many parts of the world. Hence, this phenomenal process of liberating oxygen and fixing carbon dioxide has transformed the world into the hospitable environment we live in today (Gust, 1996).

Oxygenic photosynthesis is the principal energy converter on earth, and in plants, algae and cyanobacteria, it is driven by two reaction centers containing integral membrane protein complexes, photosystem I (PSI) and photosystem II (PS II). These two large protein-cofactor complexes located in the thylakoid membrane are involved in the initial steps of the conversion of solar energy into usable chemical energy that is released into the biosphere (Zouni *et al.*, 2000). It is therefore important to study photosynthesis in simpler forms to find out more about the origin, evolution, and influence of life on this planet. Fossil records show filamentous cyanobacteria of

3.4×10^9 years of age while the earth's age is $4.4\text{-}4.8 \times 10^9$. Cyanobacteria and early eukaryotic algae produced oxygen and over several billion years, brought the atmosphere to its present condition in which life predominates. The cytochromes that function in photosynthesis in cyanobacteria, algae and plants have, like other photosynthetic catalysts, been largely conserved in their structure and function during evolution (Rutherford & Faller, 2001). By studying such intricacies of photosynthesis we can learn how to enhance this process and harness it for the betterment of mankind.

Photosystem II (PSII)

One key reaction center of photosynthesis is PSII, which is the site of photosynthetic water oxidation that accounts for nearly all oxygen in the atmosphere and indirectly nearly all the biomass on the earth (Debus, 2000). PSII is variously referred to as the oxygen-evolving complex, water-oxidizing complex or the water-plastoquinone photo-oxidoreductase. PSII water oxidation, which takes place near the luminal surface of the thylakoid membranes in plants, algae, and cyanobacteria, is catalyzed by the oxygen evolving complex (OEC) (Meentemeyer *et al.*, 1999). Oxygenic photosynthesis depends upon the ability of the PSII complex to utilize water as a source of electrons to be used for reductive metabolism. Electrons are generated when water is cleaved and molecular oxygen is produced in the water-splitting complex of PSII (Kato *et al.*, 2001).

The PSII complex is an integral membrane protein that utilizes solar energy to reduce plastoquinone to extract electrons and protons from water (Debus, 2000) with the simultaneous evolution of molecular oxygen. Therefore the oxygen evolution of PSII, in order to evolve one molecule of oxygen, and two molecules of water, CO_2 must be

decomposed with the concomitant extraction of four electrons and four protons (Shen *et al.*, 1998). During each catalytic cycle, two plastoquinone molecules are reduced and protonated, four protons are removed from the stroma, and four protons are deposited into the lumen. These protons contribute to the transmembrane proton gradient that is utilized for ATP formation. PSII therefore provides the reducing equivalents and much of the electrochemical potential that is required for the synthesis of organic compounds from carbon dioxide (Debus, 2000). The conversion of light to chemical energy in PSII is associated with this charge separation across the thylakoid membrane (Zouni, *et al.*, 2000).

PSII is a large complex with many subunits, most of which are integral membrane proteins and others which are peripherally located (Fig. 1) (Seidler, 1996). In vivo, the PSII complex contains nearly 30 different polypeptides, including those involved in light harvesting. Of these polypeptides, about 25 are considered the PSII core proteins and are encoded by the *psb* genes, most of which are located on the chloroplast genome (Debus, 2000). Although the minimum number of protein subunits required for water oxidation is not currently confirmed, there are varying opinions regarding the matter. Both the PSII complexes from cyanobacteria and higher plants consist of the D1 and D2 reaction center proteins, the 47 and 43 kDa CP proteins that serve as proximal antennae, the 33kDa extrinsic protein that stabilizes the Mn cluster, the alpha and beta subunits of cyt. b559 and several other low molecular weight polypeptides whose functions are not well established (Shen & Inoue, 1993). The extrinsic 33kDa protein is referred to as the manganese-stabilizing protein (MSP) and is encoded for by the *psbO* gene. In addition to membrane spanning polypeptides, it is believed that at least 3 extrinsic proteins including

the aforementioned MSP, are required for optimum activity of the water oxidation complex (Franzao *et al.*, 2001). In higher plants and green algae the other two extrinsic proteins are the 24 and 18 kDa proteins encoded by the *psbP* and *psbQ* genes respectively. In cyanobacteria and non-green algae, the extrinsic proteins associated with the water oxidation reaction are MSP, cytochrome c550 and an 8-12kDa protein. Cyt. c550 and the 8-12 kDa protein are encoded by the *psbV* and *psbU* genes, respectively.

Photosynthetic oxygen evolution in cyanobacteria, algae and plants is catalyzed by the tetranuclear Mn cluster ligated to several polypeptides of the PSII complex (Franzao *et al.*, 2001). The Mn cluster accumulates oxidizing equivalents in response to photochemical events within PSII, then catalyzes the oxidation of 2 molecules of water, releasing one molecule of oxygen as a byproduct (Debus, 2000). There are three inorganic ions, manganese, calcium and chloride serve as the cofactors of the OEC (Meentemeyer *et al.*, 1999).

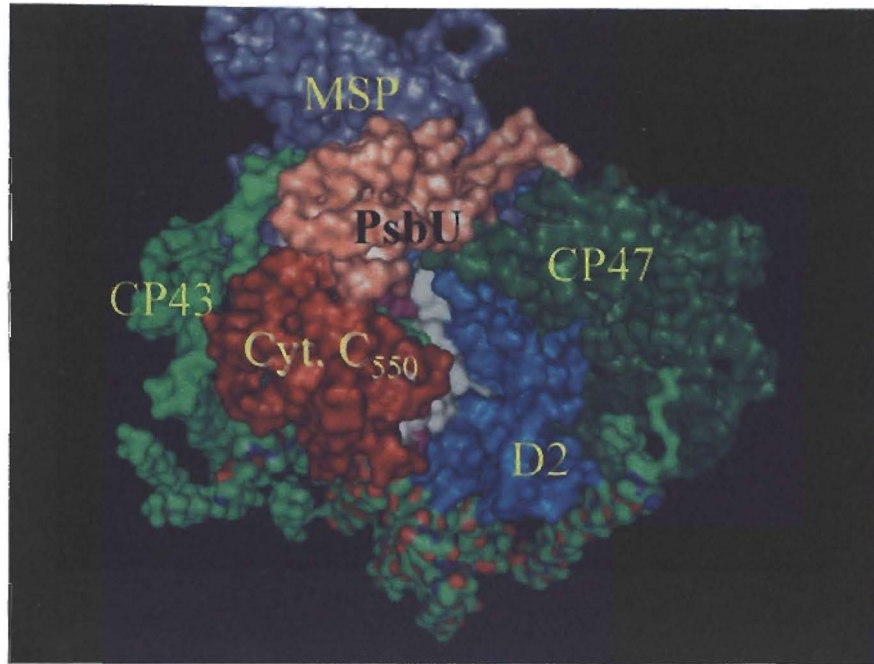


Figure 1: PSII complex. The PSII complex is composed of the DI and DII reaction center proteins, the CP43 and CP47 antennae proteins, the 33kDa manganese-stabilizing protein (MSP), the 12kDa *psbU* protein, and cytochrome c550.

Synechocystis sp. PCC6803

Since PSII is functionally and structurally similar in the chloroplasts of higher plants and in cyanobacteria (Pakrasi *et al.*, 1985), organisms such as *Synechocystis* 6803 can be used as easily engineered model systems to study this process. No such methodology exists for molecular analysis of PSII in higher plants. *Synechocystis* 6803 is a halotolerant cyanobacterium that is mesophilic. It serves as an excellent model to study photosynthesis because it has a naturally occurring genetic transformation system and it possesses the ability to grow photoheterotrophically on glucose (Williams, 1988). So far, four specific c-type cytochromes have been isolated from *Synechocystis* 6803; cyt. f, cyt. c6, cyt. c550 and cyt. Cm of which has an unknown function. The particular cytochrome

of interest to my project is the low-potential cyt. c550. By using site-directed mutagenesis, genes in cyt c550 can be deleted and replaced with modified copies to study the molecular processes of photosynthesis in a cyanobacterium.

Cytochrome c550 (cyt. c550)

Cytochromes are hemoproteins, the activity of which depends on an association between the cofactor and the polypeptide chain. C-type cyts. can be defined as having one or several hemes bound to the protein moiety by one, or more thioether bonds involving sulfhydryl groups of cysteine residues and the propionate groups of the heme moiety (Dolla *et al.*, 1994). Based on this characterization, four classes of c-type cyts. have been identified. Class I includes classical soluble cyt. c of mitochondria and bacteria, with the heme binding site towards the N- terminus and the sixth axial ligand provided by a methionine residues (Dolla *et al.*, 1994). Class II includes cyts. having their heme binding site close to the C-terminal part, and are typically found as the high spin state of the heme iron. Class III are distinguished by their multi-heme nature and very low redox potentials, while class IV involves complex proteins having distinct prosthetic groups in the same molecule. C-cytochromes are one of the most thoroughly documented oxidoreductase proteins (Dolla *et al.*, 1994). One unique c-type cytochrome is c550 which is essential to the structure of PSII (Shen & Inoue, 1993) and has been found in cyanobacteria and algae but not in higher plants. Cytochrome c550 is one of the major c-type cytochromes found in cyanobacterial cells when whole cell extracts are electrophoretically separated and viewed by heme staining (Shen *et al.*, 1995). Cyt. c550 has been found in *Synechococcus vulcanus* (Shen *et al.*, 1992) the red algae *Cyanidium caldarium* (Enami *et al.*, 1995) and in our model organism, *Synechocystis* 6803 (Shen *et*

al., 1995). C550 functions in PSII and is encoded for by the *psbV* gene which has been sequenced by Shen *et al.* From the most probable start codon, gene *psbV* codes for 160 amino acid residues which includes a cleavable N-terminal leader sequence of 25 residues. The leader sequence has an Arg-Asn-Arg sequence immediately before the cleavage site that is characteristic of transit peptides in prokaryotes (Shen *et al.*, 1995). This transit sequence is responsible for directing the newly synthesized cyt. into the thylakoid lumen.

Some unique features of the water soluble c550 as seen in (Fig. 2), are its single heme with low-spin *bis*-histidine coordination at the fifth and sixth axial ligands, (Diner & Babcock, 1996) and a very low reduction potential of -250mV, therefore classifying it as a low-potential c-cytochrome (Shen *et al.*, 1995). Thus far, c550 has the lowest redox potential of any monoheme cytochrome (Sawaya *et al.*, 2001). Cyt. c550 shows a maximum absorption between 548 and 550nm in its reduced form corresponding to the alpha band (Frazao *et al.*, 2001) and has an acid isoelectric point of 3.9 (Navarro *et al.*, 1995). Cyt. c550 is an extrinsic protein associated with PSII in cyanobacteria and lower eukaryotic algae and has been proposed to play an important role in the water splitting reaction (Kerfeld and Krogman, 1998, Shen *et al.*, 1992). However, the physiological function and physical localization of c550 inside the cells are still controversial (Navarro *et al.*, 1995).

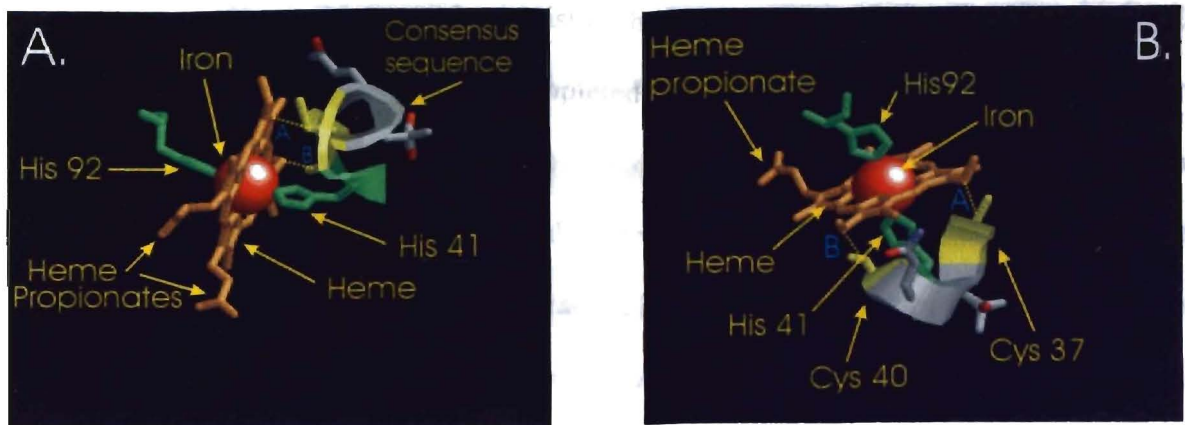


Figure 2: Heme environment of cytochrome c550. Shown above are two different views of the heme environment of cyt. c550. **2A:** Labeled are the heme with iron, the *bis*-histidine (His41 & His92) axial ligation, the heme consensus binding sequence (CXXCH), and the heme propionates. The dotted lines labeled by letters A and B represent the thio-ether bonds from the two cysteines (Cys38 & Cys40) to the heme, that were not drawn in on the original (PDB 1E29) obtained from the entry by Sawaya *et al.* **2B:** A different view of the heme environment that also shows the heme with iron, the *bis*-histidine coordination of the heme, and the heme propionates. Once again the dotted lines labeled by letters A and B represent the thio-ether bonds from Cys37 and Cys 40 of the consensus binding sequence to the heme.

A number of roles have been proposed for c550: as an electron carrier in cyclic photophosphorylation (Kienzl *et al.*, 1983), sulfide oxidation (Ho *et al.*, 1979), and nitrate reduction (Alam *et al.*, 1984) and as enzyme with peroxidase activity (Kang *et al.*, 1994). Krogman *et al.*, and Kang *et al.*, have proposed a role for c550 in unicellular cyanobacteria as an electron carrier between reduced ferredoxin or flavodoxin and hydrogenase during the fermentative process that occurs under prolonged periods of dark and anaerobiosis. It has additionally been proposed that the membrane bound cyt. c550 is involved in regulation of S-state transitions in the water-splitting reaction of PSII (Navarro *et al.*, 1995). Cyt. c550 has been shown to accept electrons from ferredoxin II in cell extracts in the presence of dithionite *in vitro*. Therefore, c550 could function in removing excess electrons generated in cells grown under anaerobic conditions by reducing ferredoxin (Shen & Inoue, 1993).

Since many questions exist in the research community regarding cyt. c550, a number of experiments have been completed to provide further insight into its structure and function. Furthermore, its unique low redox potential raises fundamental questions on the factors governing redox potential in heme proteins. The crystal structure of cyt. c550 has been solved by Frazao *et al.*, at 1.21 Å resolution confirming that c550 is the first structural cyt. of a monodomain, monoheme soluble c cyt. with *bis*-histidine axial coordination. The resolved structure shows c550 with 1104 N or O atoms plus 1 Fe and 2S atoms. The Fe atom is coordinated by a heme porphyrin which, in turn, is covalently attached to the characteristic Cys-Gly-Gly-Cys-His sequence motif via two thioether linkages with the cysteines. The model contained 227 solvent molecules initially assigned as waters where three near the protein surface at the first solvent layer were assigned as calciums. A hairpin motif, an anti-parallel β -sheet connected by a β -hairpin is found near the N-terminus. Since mono-heme c-cyts. are almost exclusively α -helical structures, this seems to be an unusual feature (Frazao *et al.*, 2001).

Amino acids that are highly conserved in the primary structures of c550 cluster into three different regions of the protein. Most of these are found in the interior of the protein near the N-terminus, where many of these residues may be involved in stabilizing interhelical interactions (Sawaya *et al.*, 2001). The structure of c550 shows the typical hydrophobic inner core of monoheme c cyts. with three helices forming a nest for the prosthetic heme group (Frazao *et al.*, 2001). Cyt. c550 heme nestles in an essentially conserved hydrophobic pocket but exposes one of its edges to the solvent, for 9.7% (Sawaya *et al.*, 2001) of heme surface exposure. As mentioned above, the c550 heme is covalently bound to the polypeptide chain through cysteines (Cys37 & Cys40)

which are localized within the conserved C-X-X-C-H binding motif, while the heme iron coordinates to His41 and His92. The only other known structure of a monoheme cyt. with bis-histidine coordination is cyt. cd1, which is found in the nitrite reductase complex of *Thiosphaera panthotropha*. The stereochemistry of the imidazole planes of His41 and His92 are maintained by h-bonds between ND1 of their imidazole rings to carbonyls of Lys45 or Pro93 respectively. A large number of bis-histidine c-cyts. have been characterized, but are not related to c550 as they harbor several heme groups and show different folding features, while one property in common is a very low redox potential (Frazao *et al*, 2001).

Experimental Background

A number of studies have been completed which have unveiled some interesting experimental results regarding the function of photosynthetic cyt. c550. Shen, Inoue, and their colleagues have isolated a PSII core complex from *Synechococcus vulcanis*, while retaining the PSII extrinsic proteins using gentle detergents (Shen *et al.*, 1993). After a wash with high salt concentration, three extrinsic proteins were released from the particles. The released proteins include a 33kDa protein found in higher plants and two other unique proteins of 17 and 12kDa. The 33kDa protein is the manganese stabilizing protein while the 17kDa protein is representative of cyt. c550. It is likely that these two proteins replace the 23 and 17kDa proteins found in higher plants since features of binding of the 17 and 12kDa protein to cyanobacterial PSII resemble those of the extrinsic 23 and 17kDa proteins to higher plant PSII (Finazzi *et al.*, 1997). There are some functional similarities between the two cyanobacterial proteins and the two higher

plant proteins. Both of them play some regulatory roles in oxygen evolution, while the underlying nature of their function varies, and c550 and the 12kDa protein may be functional equivalents in cyanobacteria to the 17 and 23kDa proteins in higher plants (Shen & Inoue, 1993). However, there is no sequence similarity between the two small extrinsic proteins of cyanobacteria with those from higher plants (Kerfeld & Krogman 1998).

In rebinding studies, c550 has been found to bind appreciably to the PSII core in the absence of the 33 and 12kDa proteins, but their presence facilitates full rebinding (Shen & Inoue, 1993). Cyt. c550 can rebind to PSII in spite of the absence of the 12 or 33kDa proteins, whereas rebinding of the 12kDa protein requires co-rebinding of the 33kDa and 17kDa (c550) proteins. These results are fully consistent with the PSII crystal structure which shows that the 12kDa protein binds into a crevice formed by the 33kDa and c550 proteins. Cyt c550 is unable to restore oxygen evolving activity (OEA) alone, however, if the 33kDa protein is present, partial restoration occurs and when the 33kDa and 12kDa proteins were both present, maximum restoration of OEA close to the original level is obtained (Shen & Inoue, 1993). Based on its close interaction with the 33 and 12kDa proteins in rebinding to the PSII core complex, c550 is likely associated with PSII at the luminal surface of the thylakoid membrane (Shen & Inoue, 1993). Therefore, c550's transport into the lumen likely contributes to the optimal functional stability of PSII in cyanobacteria (Shen *et al.*, 1995). In addition, single-particle image analysis of PSII has shown c550 at the luminal side and in close contact with the core and the 12 and 33kDa proteins (Kuhl *et al.*, 1999). The finding of c550 as an extrinsic protein functioning at the donor side of PSII may suggest a possible evolutionary link at the

donor side of reaction centers between photosynthetic purple bacteria and cyanobacteria. In purple bacteria it is known that cyt. C2 functions at the donor side of the reaction center (Shen *et al.*, 1995).

In cross-linking studies by Han *et al.*, c550 has been found to cross link to both the 12 and 33kDa proteins and to both the 12kDa and the D2 proteins that holds elements of the reaction center. Cyt. c550 is likely very close to the electron transfer catalysts in PSII, but no evidence exists thus far indicating that it undergoes any reduction or oxidation in this location (Kerfeld & Krogman, 1998). That is why c550's electron transfer activity, which involves an association between the heme group and the polypeptide chain, therefore corresponding to the redox potential of the heme group, is an important feature to experimentally investigate.

Mutant strains with either insertion or deletion of c550 (*psbV*) seem to be capable of photoautotrophic growth but at a reduced rate, while they contain only half the amount of PSII found in the wild type. On a chlorophyll basis, oxygen evolving activity of the mutant was found to be around 42% of the wild type (Seidler, 1996). This major reduction of OEA is due to decreased stability of the PSII reaction center, and the activity per reaction center is not, or only slightly diminished (Shen *et al.*, 1995). Therefore, rather than c550 being directly involved in enzyme activity itself, it seems to be necessary for the conformational integrity and stability of PSII. Additionally, the c550 deletion mutant was unable to grow in the absence of Ca^{2+} and Cl^- in growth medium and showed a rapid deactivation of OEA in the dark that could be photoactivated upon light illumination with a very high efficiency (Shen *et al.*, 1998). In algal PSII, c550 has been shown to maintain optimal concentrations of Ca^{2+} and Cl^- ions near the Mn cluster and

protect the Mn cluster from endogenous reductants to stabilize and optimize its catalytic activity (Debus, 2000). A similar role for c550 could be hypothesized.

The results of double deletion studies of both *psbV* (c550) and *psbO* (33kDa) results suggest a role for c550 in cyanobacterial PSII to support oxygen evolution and photoautotrophic growth that can bind and function independently. The double deletion mutants show almost no OEA and are unable to grow photoautotrophically. With one or the other protein present, oxygen evolution still exists, but both are required for a normal, maximal rate of OEA in cyanobacterial PSII. It was also found that the destabilizing effect caused by the loss of c550 is more pronounced in the absence of the 33kDa protein (Shen *et al.*, 1995). These results do indicate that c550 has a functional role in OEA, although its direct function in the electron transfer reaction mechanism of water-oxidation seems unlikely.

In *Synechococcus vulcanus*, c550 has been detected only in the thylakoid membrane fraction being tightly bound to thylakoids, where removal has required sonication in the presence of 1M CaCl₂. Upon further fractionation of the thylakoids into PSI and PSII, c550 is exclusively concentrated in the crude PSII fraction together with cyt. f, with no significant amount being detected in PSI. Therefore, c550 binds stoichiometrically to the cyanobacterial PSII core complex and enhances oxygen evolution. This finding is significant in that it has confirmed the idea that there is only one species of c550 in cyanobacterial cells and c550 is exclusively associated with PSII as a functional component for OEA (Shen & Inoue, 1993).

Although many significant studies have been completed, it is still not clear if and how the low potential heme of cyt. c550 functions in PSII. Cyt. c550 could have

protective electron transfer function in addition to its structural role in the PSII reaction center. It can be noted that this hemo-protein would unlikely be evolutionarily conserved for such a long time if it was providing no advantage to the cell through a redox function (Kerfeld & Krogman, 1998). Therefore, further investigation into the structure and function of low-potential c550 is imperative.

Redox Properties of Cytochromes

Fermentation, respiration and photosynthesis are the three main bioenergetic mechanisms whereby cells obtain the energy necessary for their metabolic processes. In both of the latter mechanisms, synthesis of ATP is coupled to the electron transfer processes in which oxidoreduction proteins are involved (Dolla, *et al.*, 1994). The wide range of redox potentials found in c-type cytochromes extends from -400mV to +400mV and can be functionally correlated with the involvement of these proteins in various metabolic processes that yield products having a different oxidoreduction powers. The most well characterized class of electron transfer proteins thus far are cytochromes. They are widespread molecules which exist not only in aerobic mitochondrial and bacterial respiratory chains, but also in prokaryotic electron transfer systems including those involved in anaerobic respiration and photosynthesis (Dolla *et al.*, 1994). A cytochrome's electron transfer activity, which involves an association between the heme group and the polypeptide chain, is correlated with the redox potential value of the heme group. One of the main roles of the polypeptide moiety consists of modulating the redox potential of the heme group (Dolla *et al.*, 1994). The polypeptide moiety of c-type cyts. contains the consensus heme binding sequence, C-X-X-C-H, where C represents cysteine,

H represents histidine, and X represents any residue (Fig. 2). Only a few deviations from this consensus sequence have been found (Jungst *et al.*, 1991). Depending on the nature of the sixth axial ligand residue of the heme iron atom, several subclasses of c-type cyts. can be defined. Either a nitrogen atom of a histidine residue or a sulfur atom of a methionine residue can serve to fill the sixth position of the heme iron atom. The differences in the electron donor-acceptor power (ie. the electronegativity) between the ligands in the axial positions will influence the redox potential value (Dolla *et al.*, 1994).

The term redox couple refers to a specific donor-acceptor pair and each couple has a characteristic redox potential difference that depends upon the electron affinities of each member of the couple. The term redox potential refers to the tenancy of a redox group to donate or accept electrons. This value reflects the relative stability of the reduced and oxidized states of a protein. Therefore, any factors which tend to stabilize the oxidized form make the couple a better electron donator and give rise to a more negative redox potential and vice-versa (Moore *et al.*, 1990). Hence, maintaining the redox potential of a cytochrome is one of the main functional roles of the polypeptidic moiety of the molecule. This in turn is imperative for the regulation of the electron flow through the redox partners of the cytochrome (Dolla *et al.*, 1994). In general, it is assumed that midpoint potential is established by several factors; polarity of heme environment (Kassner, 1973), accessibility of heme to solvent (Stellwagen, 1978), strength of axial ligand field (Moore & Williams, 1977), and electrostatic interactions of the heme and its propionates (Moore, 1983). Therefore, it is important to further investigate how each of these factors contributes to the wide range of redox values observed in cytochromes.

Comparison of c-type Cytochromes

When comparing the sequence of cyt. c550 to other c550 cytochromes and cyt. c6, many sequence similarities and conserved residues can be found. As seen in (Fig 3), all of the organisms share the same consensus heme binding sequence (CXXCH) and the His41¹ axial ligand. Also conserved among all but one of the cytochromes (*Anabaena* c6) is the proline residue at position 93. One notable difference between the cytochromes is the sixth axial ligand at position 92. Although all of the represented c550's have a histidine residue at position 92, the cyt. c6 representatives have a methionine residue at this position, therefore leading to histidine-methionine (His-Met) axial ligation of the heme iron instead of histidine-histidine (*bis*-histidine).

Two cyts. that can be studied comparatively to learn more about the factors controlling midpoint potential, are cyt. c550 and cyt. c6 of *Arthrospira maxima*. These two cyts. have been found to share much sequence similarity. Although cyt. c6 and cyt. c550 are not found in higher plants, they are both found in cyanobacteria and algae where they appear to support multiple functions. Cyt c6 functions in PSI to transfer electrons from the membrane bound cyt. b6f complex to PSI, while cyt. c550 is involved in PSII oxygen evolution by functioning as one of the extrinsic subunits.

¹ Numbering system is based upon the mature *Synechocystis* 6803 cyt. c550 sequence.

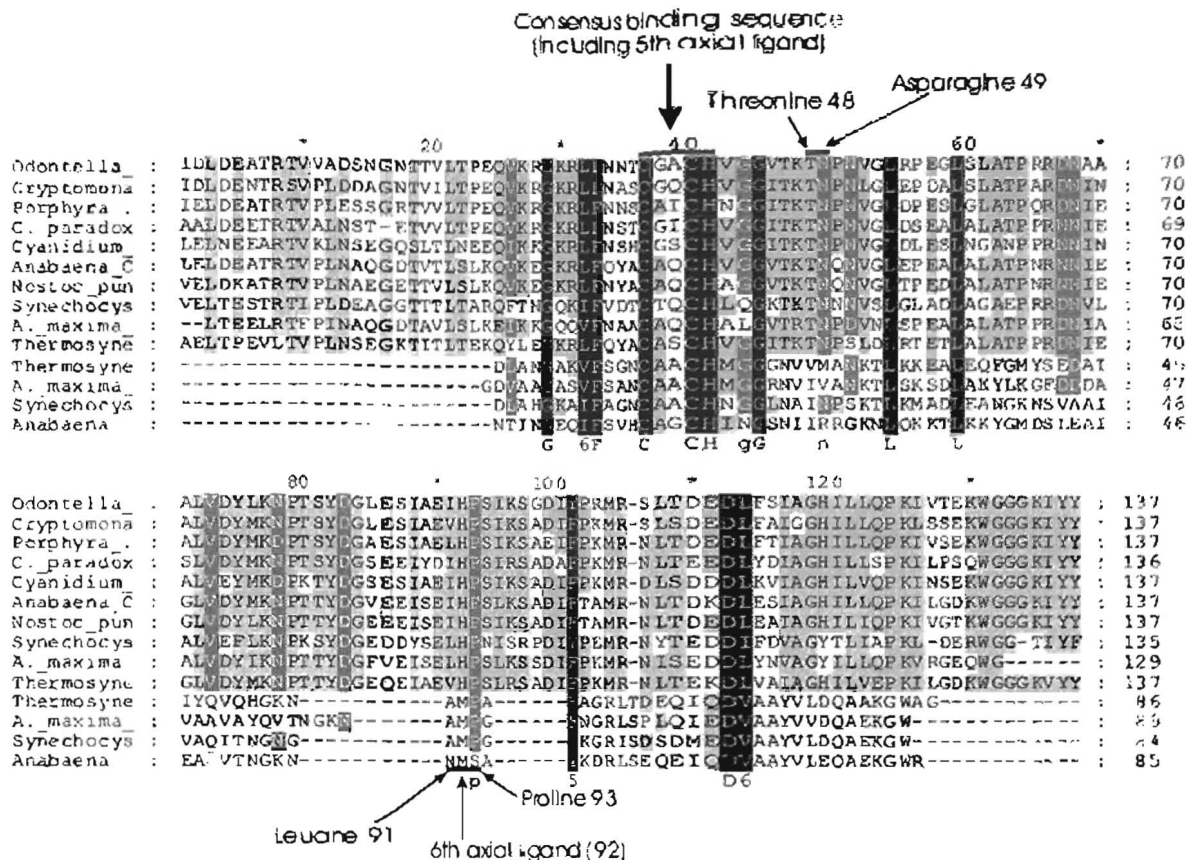


Figure 3: Sequence alignment of cyt. c550 and cyt. c6. Alignment of *Odontella* c550, *Cryptomonas* c550, *Porphyra* c550, *C.paradoxa* c550, *Cyanidium* c550, *Anabaena* c550, *Nostoc punctifo.* c550, *Synechocystis* c550, *A.maxima* c550, *Thermosynechococcus* c550, *Thermosynechococcus* c6, *A. maxima* c6, *Synechocystis* c6 and *Anabaena* c6. Labeled, is the characteristic c-type cyt. CXXCH (C= cysteine, H=histidine, X= any residue) consensus binding sequence that binds the fifth axial histidine ligand to the heme iron. Additionally, at position 92 is the sixth axial ligand of various cytochromes, some consisting of a histidine residue at this position, while others have a methionine residue. Also shown is the evolutionarily conserved Pro93 as well as the other targets for site-directed mutagenesis (T48, N49, and L91).

Both are monoheme cytochromes, and while cyt. c6 is composed of 89 amino acid residues, cyt. c550 is larger with 130 amino acid residues. Two regions of sequence similarity between the primary structures of cyt. c550 and cyt. c6 have led to the suggestion that the two could have descended recently from the same ancestral gene, but diverged to carry out different functions. The most notable difference between the two is

the near 600mV difference in their respective midpoint potentials. Cyt. c550 seems to be extremely more negative with a midpoint potential of -260mV compared to the positive cyt. c6 with a midpoint potential of +314mV.

A prominent difference between the two is the nature of the sixth axial ligand which is His92 in cyt. c550 and Met61 in cyt. c6 (Figs. 3 & 4). However both cyts., c550 and c6, do have the C-X-X-C-H (C= cysteine, H=histidine, X=any residue) heme consensus binding sequence (Figure 3). Both cyts. also have the evolutionarily conserved proline residue at position 93. In addition to having a different sixth axial ligand, cyt. c550 has an additional N-terminal 22 residues as compared to cyt. c6. Also, there is an insert in the primary structure of cyt. c550 that is not found in cyt. c6 between residues 89 and 103.

In addition to sharing sequence similarity, c550 also shares some structural similarity with cyt. c6. The crystal structures of cyt. c6 and cyt. c550 have been determined from the cyanobacterium *Arthrospira maxima* and have been found to be remarkably similar (Figure 4 & 5). Comparison of the two 3-D structures suggests that the difference in midpoint might be attributed to any or all of the following factors: solvent exposure of the heme, electrostatic environment of the heme propionates, and/or heme-iron ligation (Sawaya *et al.*, 2001).

Comparisons of the heme environment of cyt. c550 and cyt. c6 offers several structural clues as to the control of midpoint potential (Fig. 4). Cytochromes with His-Met axial coordination have redox values ranging from +400-0mV while *bis*-histidine

coordinated cyts. typically have potentials ranging from 0 to -400mV (Dolla *et al.*, 1994).

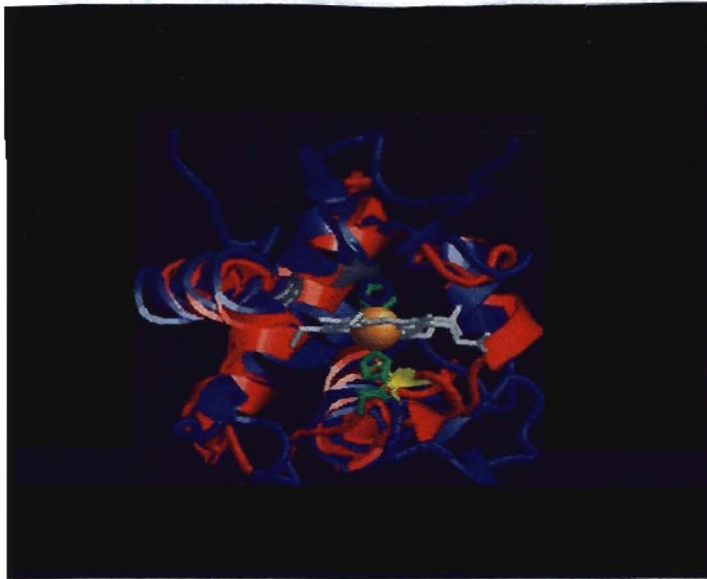


Figure 4. Structural alignment of cyt. c550 of *Synechocystis* sp. PCC6803 and cyt. c6 of *Arthrospira maxima*. Cyt. c550 (blue) (PDB 1E29) and Cyt. c6 (red) (PDB 1F1F). The heme iron (orange sphere) coordinated from the lower axial position by histidine 92 (His92, cyt. c550) or methionine 41 (cyt. c6) colored green and yellow, respectively. Therefore it can be noted that c550 has a *bis*-histidine axial ligation of the heme iron, while c6 has a met-his axial ligation of the heme iron.

Typically, *bis*-histidine (Fig. 4) coordination correlates with a more negative midpoint potential like that of c550. Experimentally it has been found that when Met is substituted for His at the sixth axial position in cyt. c3, there is an increase of 150mV in midpoint potential. This increase is hardly enough to account for the entire 600mV difference between cyt. c550 and cyt. c6 so obviously other factors contribute to midpoint potential (Sawaya *et al.*, 2001). Additionally, the protein backbone conformation in the region adjacent to the sixth axial ligand (His92 in c550 & Met61 in c6) in the two structures are quite dissimilar (Sawaya *et al.*, 2001). It is not clear if the differences are due to insertion or deletion.

Structurally, cyt. c6 is composed of four α -helices which enclose all but 6% of the surface of the heme prosthetic group. The four α -helical core structures of *A. maxima* cyt. c550 and cyt. c6 are very similar. The longest helical segments of the core of cyt. c550 closely superimpose on the four helices of cyt. c6 (Figs. 4 & 5). Additionally, the fold in the vicinity of the first axial ligand (His41 in c550 & His18 in c6) are strikingly similar. When comparing the primary structures of cyt. c550 and cyt. c6, there is a 32% identity between the two while they superimpose (over 263 backbone atoms) with an rmsd of 3.4Å (Figure 4 & 5). When compared with other Class I cytochromes, cyt. c550 superimposes on yeast cyt. c with an rmsd of 4.2Å (over 281 backbone atoms), *Rhodopseudomonas viridis* cyt. c2 with an rmsd of 3.5Å (over 281 backbone atoms), and *Pseudomonas* cyt. c551 with an rmsd of 3.5Å (over 273 backbone atoms). Therefore it would seem that cyts. with very different midpoint potentials are actually close structural relatives (Sawaya *et al.*, 2001).

Besides the nature of the axial ligands, another contributing factor controlling midpoint potential is the polarity of the side chains around the heme. In this respect, the structures of cyt. c6 and cyt. c550 are very similar. There are several hydrophobic amino acids that are conserved structurally in the two proteins: Leu54, Leu59 and Val114 of c550 superimpose on Leu31, Leu36, Val55 and Val77 of cyt. c6 (Sawaya *et al.*, 2001).

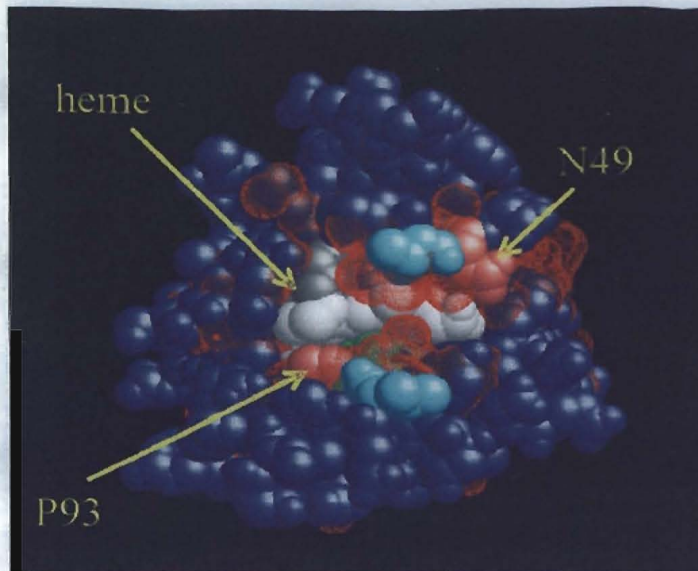


Figure 5. Structural alignment of cyt. c550 of *Synechocystis* sp. PCC6803 and cyt. c6 of *Arthrospira maxima* with spacefill. Cyt. c6 is composed of 89 amino acid residues and cyt c550 is larger with 130 amino acid residues. There is a 32% identity between the two cytochromes, while they superimpose (over 263 backbone atoms) with an rmsd of 3.4Å. The heme is colored white. The hatched red molecular surface of cytochrome c6 occludes the heme edge to a greater extent, where the surface exposure of the heme prosthetic group is 6.6% for cyt. c6, and 9.7% for the more surface exposed cyt. c550. Mutations in threonine 48 (T48) and leucine 91(L91) colored light blue, were originally produced to alter heme exposure, but recent modeling and redox data suggests that these changes do not accomplish this. Proline 93 of cytochrome c550 (P93, pink below heme) hydrogen bonds to the imidazole nitrogen of axial ligand H92. Asparagine 49 (N49, pink above heme) forms hydrogen bonds via its side chain amide nitrogen to heme propionate D oxygen.

Hydrogen bonding to axial ligands is also a likely contributor to midpoint potential, more specifically the hydrogen bond to the N δ atom of the fifth axial ligand. In cyt. c6, the atom forms a hydrogen bond to the carbonyl oxygen atom of Arg22, whereas in cyt. c550, the hydrogen bonds to the same backbone atom of Val45. The electrostatic effects from the side chains of these two residues may contribute to the greater stability of cyt. c6 in its reduced state. The analogous hydrogen bond to the histidine N δ atom in cyt. c2 and mitochondrial cyt. c is formed with the carbonyl oxygen atom of a conserved proline residue. It is unclear why this amino acid side chain in this position is conserved

in these species. It should be noted that in cyt. c550, the carbonyl oxygen atom of conserved Pro93 forms a hydrogen bond with the N δ atom of His92 (Sawaya *et al.*, 2001).

Different solvent exposure of the propionate D oxygen atoms might also differentiate midpoint potentials between various cyts. (Sawaya *et al.*, 2001). The propionate D oxygen environment differs between the two cyts., while in cyt. c550 one of the propionate D oxygen atoms is solvent exposed, in cyt. c6, both propionate D oxygen atoms are surface exposed. This increased exposure of the propionate oxygen atoms may lead to an increase of midpoint potential. However this seems to be opposite of the ideas proposed by and increased heme exposure leading to a reduce midpoint potential. Solvent accessibility of the heme prosthetic group is known to play a role in different midpoint potentials. The surface exposure of the heme prosthetic group of cyt. c6 is 6.6% as compared to the more surface exposed c550 of 9.7%. Typically, increased surface exposure correlates with reduced midpoint potential which is in fact seen in the -260mV value of cyt. c550 as compared to the more positive +340mV of cyt. c6 (Sawaya *et al.*, 2001).

Last, it is proposed that the hydrogen bonding to the propionate D oxygen atoms might also affect midpoint potential. In cyt. c6, the propionate oxygen atoms are hydrogen bonded to the positively charged Lys29 and Lys59. This positive charge may help to stabilize the electron gained by reduction of the heme and thus lead to the higher midpoint potential of c6 as compared to c550. In cyt. c550, the propionate D oxygen atoms are hydrogen bonded to the amide backbone of Tyr82 and water which results in no electrostatic balance for the reduced heme. Mutagenesis studies which alter the electron-withdrawing character of a side chain, hydrogen bonded to a propionate group,

have been shown to change the midpoint potential in mitochondrial cyt. *c* by nearly 50mV (Cutler *et al.*, 1989).

Selection of Mutation Target Sites

A number of target amino acids in cyt. *c*550 were selected for site-directed mutagenesis based on the factors discussed above (Fig. 5). These targeted mutagenesis sites can also be seen in the sequence alignment in (Fig. 3). Threonine 48 as well as Asn49 are involved in shielding the pyrrole A, D, and C rings of the heme and would be surface exposed in a cyt. *c*550 monomer. Leu91 is considered a highly conserved residue and it has a side chain exposed to solvent and is also involved in hydrogen bonding. The interface in the crystal structure of cyt. *c*550 is predominantly hydrophobic, except for a hydrogen bond network formed between Thr48, Asn49, a propionate D oxygen atom, and Glu90. Thr48 and Leu91 were chosen as mutation target sites to try to reduce heme solvent exposure and because of their involvement in the hydrogen bonding network (Fig. 5). Thr48 and Leu91 were both mutated to an isoleucine since it has a non-polar, longer side chain. Asn49 was selected as a target site due to its hydrogen bonding via its side chain amide to the heme propionate D oxygen atom (Fig. 6) (Sawaya *et al.*, 2001). The D propionate forms hydrogen bonds with the solvent-accessible amide of the Asn49 side-chain and three water molecule (Frazao *et al.*, 2001). His92 is the sixth axial ligand contributing to the bis-histidine coordination of the heme prosthetic group, so it was mutated to a methionine which is a common sixth axial ligand in other *c*-type cytochromes (Fig. 7). Pro93 is conserved in cyt. *c*550 and was selected as a target site since it forms a hydrogen bond with the (imidazole) N δ atom of His92 (Fig. 8) (Sawaya

et al., 2001). His92 is actually hydrogen bonded between ND1 of its imidazole ring to carbonyls of Pro93 and Lys45 (Frazao *et al.*, 2001).

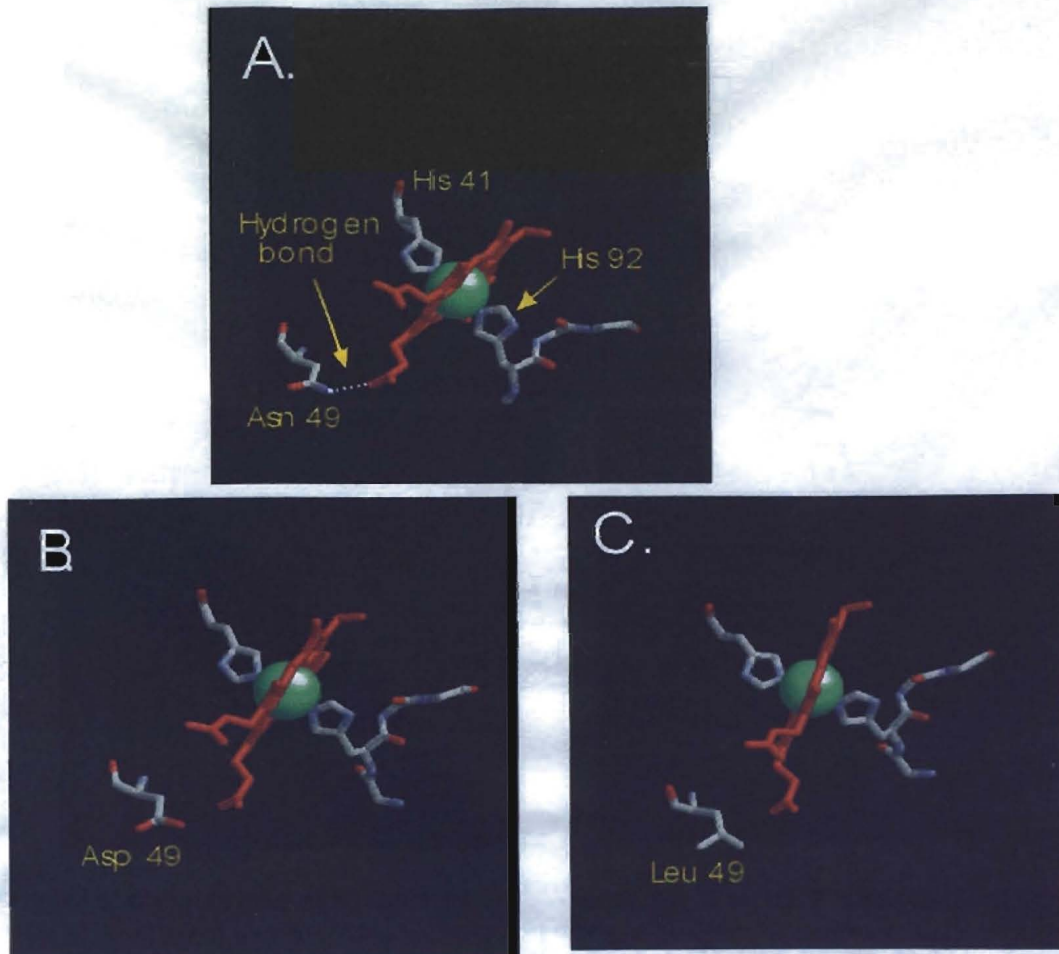


Figure 6. Cytochrome c550 asparagine 49 mutant. **6A:** Cyt. c550 with the axial ligands (His 41 & His92) and the Asparagine (Asn 49) site labeled. The dotted lines represent the hydrogen bond formed between Asn 49's side chain amide to the heme propionate D oxygen atom. **6B:** Is a replication of the picture in 4A, only with an aspartic residue substituted for the asparagine at residue 49. This causes a loss of the hydrogen bond with the heme propionate D oxygen atom. **6C:** Is also a replication of the picture in 4A, only with a leucine residue substituted for the asparagine at residue 49. This also causes a loss of the hydrogen bond with the heme propionate D oxygen atom. (*Mutated amino acids have been substituted into the crystal structure of cyt. c550 (Sawaya *et al.*,) and no molecular simulations of the mutations using energy minimizations have been performed).

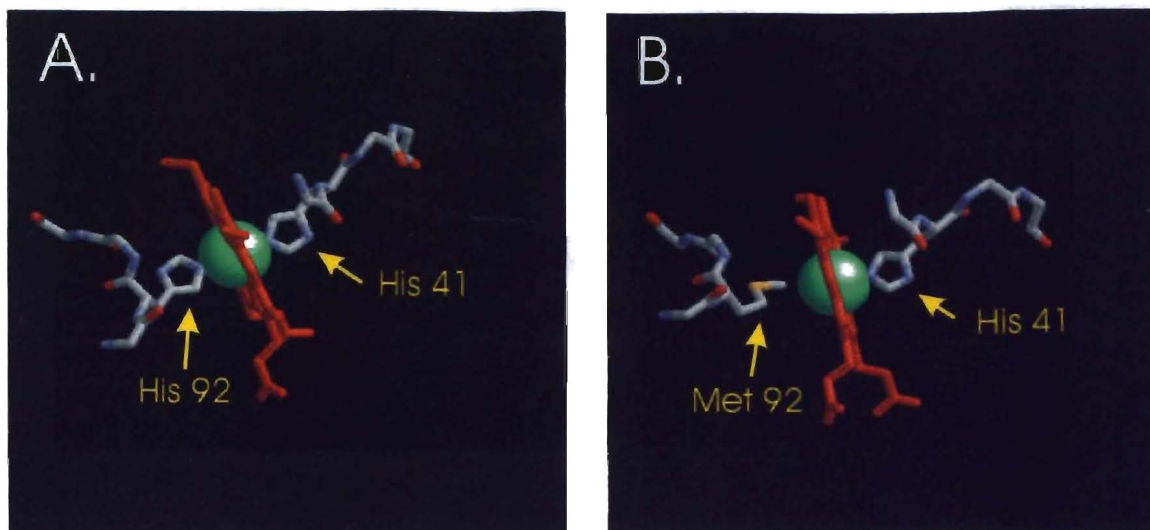


Figure 7. Cytochrome c550 with bis-histidine axial ligation and his-met (H92M) axial ligation. **7A:** Cyt. c550 showing the substitution of a histidine for a methionine at residue 92 (H92M) therefore resulting in a His-Met axial ligation of the heme iron. **7B:** Cyt. c550 showing the wild-type *bis*-histidine (His41 & His92) axial ligation of the heme iron.

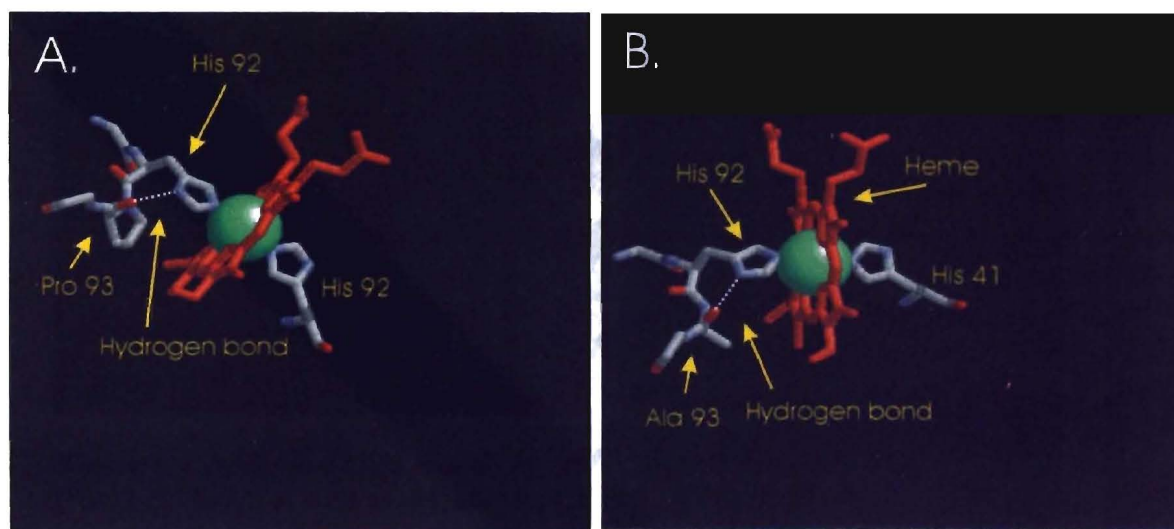


Figure 8. Cytochrome c550 proline 93 mutant. **8A:** Cyt. c550 with the axial ligands (His41 & His92) as well as the wild-type proline (Pro93) site. Pro93 forms a hydrogen bond with the (imidazole) N δ atom of His92 that is shown by the dotted line. **8B:** Cyt. c550 with the proline residue substituted for an alanine at residue 93. Even with the substitution, the hydrogen bond represented by the dotted line is still formed.

CHAPTER 3

OBJECTIVE

The overall objective of my project was to investigate the factors that contribute to the unusually low redox potential of cyt.c550. For this work, five amino acid targets were mutagenized including the sixth axial histidine ligand. Using a binary plasmid system in *Escherichia coli*, these mutations were expressed under varying protocols to find optimal expression and then purified by column chromatography. Using spectroelectrochemistry, each of the cytochromes was analyzed for changes in their redox potential, which may unveil information contributing to an understanding of the functional role of cyt. c550 and basic information regarding redox proteins.

CHAPTER 4

MATERIALS AND METHODS

Construction of pETC550 plasmid vector

The gene encoding cyt. c550, *psbV*, was ligated into the pET-22b(+) vector to give the plasmid pETC550 (Table 1 & Fig. 10). The expression plasmid pET22bC550 was constructed as shown in (Fig. 9) (From Dr. Li, Stillwater, OK). The encoding sequence of mature Cyt. c550 from *Synechocystis* sp. PCC6803 was amplified by PCR using Turbo *Pfu* polymerase (Stratagene, La Jolla, CA). The forward primer 5' GCT CCC ATG GTG GAG TTA ACC GAA AGC 3' which introduced a *Nco I* site (in bold) and the reverse primer 5' GCG CGG ATC CCT AGA AGT AGA TGG TGC C 3' which introduced a *BamH I* site (in bold) were used to amplify the encoding sequence of mature Cyt.c550. The PCR products were inserted into the *Nco I* and *BamH I* sites of the pET-22b (+) vector (Novagen, Madison, WI) to create expression plasmid pET22bC550 (pETC550). The fusion product of the *psbV* gene and the pelB signal sequence allows heterologous expression in *E.coli* under the control of T7 promoter and fast purification by affinity chromatography.

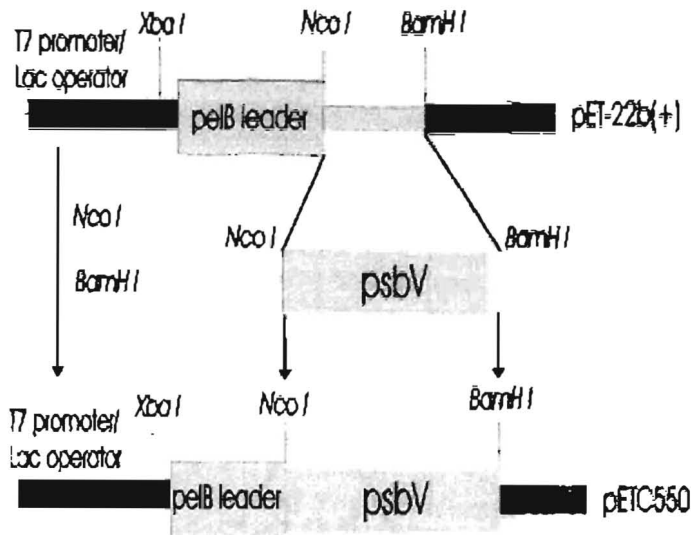


Figure 9. pET22 with *psbV* insert. The ligation of *psbV* into the pET22b(+) plasmid vector to create the plasmid pETC550. The *psbV* gene was ligated into pET22b(+) plasmid vector between the *NcoI* and *BamHI* restriction enzyme sites behind the *pelB* leader and downstream of the T7 promoter/lac operator.

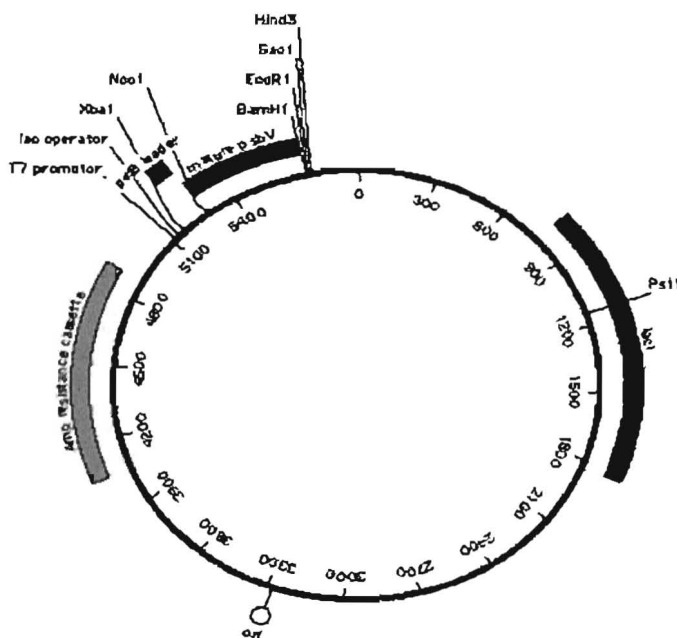


Figure 10. pETC550 plasmid map. Plasmid map of *psbV* ligated into the pET22b(+) plasmid vector to create the plasmid pETC550 which is ~5.9kB. As labeled on the map, there is an ampicillin resistance cassette, a T7 promoter, a *lac* operator, a *pelB* leader sequence, the mature *psbV*, an origin of replication, and a *lacI* site. Also labeled on the map are some various restriction enzyme cut sites.

<u>Plasmids</u>	<u>Description</u>	<u>Reference</u>
pET-22b(+)	Amp ^R , N-terminal pelB signal sequence	Novagen (Madison, WI)
pETC550	Amp ^R , <i>psbV</i> gene	Burnap Lab, (Li <i>et al.</i> , in prep.) (Stillwater, OK)
pEC 86	ccmABCDEFGH cloned into PACYC184, Cm ^R	Thony-Meyer, L. (Zurich, Switzerland), (Arslan <i>et al.</i> , 1998)

Table 1. Plasmids. The table shows the plasmids used for the mutagenesis and expression of cyt. c550.

<u>Bacterial strains</u>	<u>Description</u>	<u>Reference</u>
BL21(DE3) <i>E.coli</i>	Host for heterologous gene expression	Stratagene (La Jolla, CA)
Epicurian Coli XL-1 Blue	Supercompetent cells	Stratagene (La Jolla, CA)

Table 2. Bacterial strains. The table shows the bacterial strains used for the mutagenesis and expression of cyt. c550.

Mutagenic Primer Design.

The mutagenic primers were designed following the Stratagene Quikchange Site-Directed Mutagenesis protocol (La Jolla, CA). Each primer was between 30-45 bases in length with a GC content of at least 40%. Each primer contained at least 10-15 bases of correct sequence on both sides of the engineered mutation and terminated in one or more G or C bases. A silent mutation was also introduced into each of the primers to add an additional restriction enzyme cut site for verification of the mutation after transformation. The DNA oligonucleotide primers were synthesized in approximately 100nmole batches obtained from Integrated DNA Technologies, Inc. (Coralville, Iowa).

Each primer was 5' phosphorylated and was purified by the manufacturer by polyacrylamide gel electrophoresis (PAGE). The primer designs can be seen in (Table 3).

Mutation	Primer Pairs (Forward and Reverse)	Restriction Enzyme
T48I	F -GCACCCAATGTCACCTGCAGGGTAAAACCAAATAATAAACG R -CGTGGGTTACAGTGGACGTCCCATTTTGGTTTTAATTATTATTGC <i>TQCHLQGGKTKINNN</i>	<i>PstI</i>
L91I	F -CTATTCGGAAAATACATCCCAATATTTCTAGACCCGACATCTAC R -GATAAGCCTTTATGTAGGGTTATAAAGATCTGGGCTGTAGATG <i>YSEIHPNISRPDIY</i>	<i>XbaI</i>
P93A	F -GACTATTCGGAGCTCCATGCCAATATTTCC R -CTGATAAGCCTCGAGGTACGGTTATAAAGG <i>DYSELHANIS</i>	<i>SacI</i>
N49L	F -CCAATGTCACCTGCAGGGTAAAACCAAACCTCTTAATAACGTTAG R -GGTTACAGTGGACGTCCCATTTTGGTTTTGAGAATTATTGCAATC <i>QCHLQKTKTLNNVSL</i>	<i>PstI</i>
N49D	F -CCAATGTCACCTGCAGGGTAAAACCAAACCTGATAATAACGTTAG R -GGTTACAGTGGACGTCCCATTTTGGTTTTGACTATTATTGCAATC <i>QCHLQKTKTDNNVSL</i>	<i>PstI</i>
H92M	F -GACTATTCGGAGCTCATGGCCAATATTTCC R -CTGATAAGCCTCGAGTACCGGTATAAAGG <i>DYSELMPNIS</i>	<i>SacI</i>

Table 3. Mutagenic primer design. Sequences of primers and restriction enzyme cut sites used to amplify amino acid mutations in *psbV* of *Synechocystis* sp. PCC 6803. Boldface denotes nucleotides that were mutated while underlines denote restriction enzyme cut sites created by introduction of silent mutations. The intended amino acid sequence after mutagenesis is below each primer set in italics.

Site-Directed Mutagenesis using Polymerase Chain Reaction (PCR)

Directed mutations were introduced into plasmid vector pETC550 using the polymerase chain reaction in conjunction with the mutagenic primers show in Table 3. An outline of this procedure is shown in detail in (Fig. 11). Reactions of 50 μ l were set up separately for the forward and reverse primers of each mutant, and then PCR was run in a two step format. The extension reaction was run for 30s at 95°C, 1' at 55°C, 18' at

68°C, and repeated three times. At the conclusion of the extension reaction, the forward and reverse primers were combined. PCR was continued for the hybridization reaction, that was 30s at 95°C, 1' at 55°C, 18' at 68°C, and was repeated 30 times. PCR products were then analyzed on a 1% agarose gel. After confirmation of the correctly sized fragment, PCR products were digested for four hours at 37°C with 1µl *DpnI*, which was added to digest the methylated, nonmutated parental DNA. After digestion, PCR products were ethanol precipitated in two volumes of ethanol, and then re-suspended in an appropriate amount of TE buffer pH 8.0.

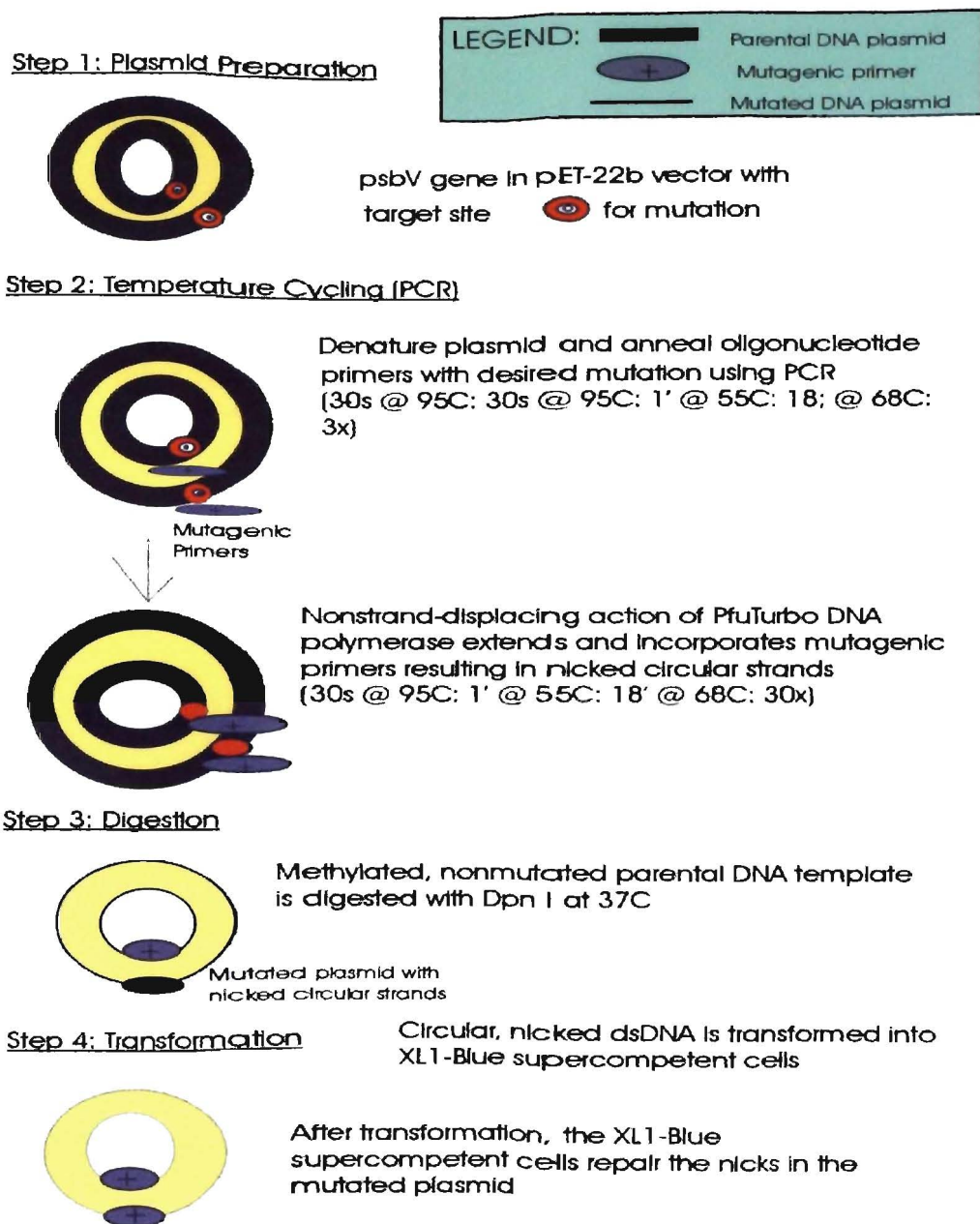


Figure 11. Site-directed mutagenesis flow-chart. The following chart outlines the steps taken in the mutagenesis and PCR, for creating mutations in pETC550 vector. Diagram adapted from Stratagene Quick-Change Site-Directed Mutagenesis Kit.

Transformation of mutant PCR products into *Epicurian Coli XL-1 Blue Supercompetent Cells*

To transform the PCR products into *Epicurian Coli XL-1 Blue Supercompetent cells* (Table 2) (Stratagene, La Jolla, CA), 1 μ L of *DpnI* treated PCR product and 1 μ L of control pETC550 plasmid were aliquoted to 50 μ L of supercompetent XL-1 Blue Cells. The mixture was gently swirled to mix and then incubated on ice for 30 minutes. The transformation mixture was then heat pulsed at 42°C for 45 seconds and then placed on ice for two minutes. Next, 0.5 ml of NZY⁺ broth at 42°C was added and the transformation reactions were allowed to incubate at 37°C for one hour with shaking at 225-250g. The transformation reactions were then plated on Luria Broth (LB) plates containing (100 μ g/ml) Amp. The entire contents of the sample reaction were plated, while 10 μ L of the pETC550 control reaction were plated. Plates were allowed to incubate at 37°C over night. After incubation, successful transformants were counted, and individual colonies were plated on a fresh LB_{Amp} plates in quadrants and allowed to incubate over night.

Mini- Plasmid Preparations

Plasmid DNA was purified using a commercial variant of the alkaline mini-preparation procedure of Sambrook *et al.* Mini-plasmid preparations were performed by inoculating 10 falcon tubes each containing 2ml of LB and 4 μ L (100 μ g/ml) Amp with one colony from separate quadrants of the LB plates described above. The mixture was then incubated at 37°C while shaking at 250g overnight. The following day, 1.5mL of overnight culture was transferred to a microcentrifuge tube and centrifuged at 12,000g for 30 seconds at 4°C to pellet. After removing the supernatant fluid, the pellet was

resuspended in 100 μ l of ice-cold Qiagen solution I by vigorous vortexing. Then 200 μ l of Qiagen solution II was added and mixed by inverting the tube rapidly 5 times. 150 μ l of ice-cold Qiagen solution III was added and mixed by inverting for 10 seconds and then stored on ice for 3-5 minutes. The mixture was then centrifuged at 12,000g for 5 minutes at 4°C and the supernatant fluid was transferred to a fresh tube. The DNA was then precipitated by the addition of two volumes of ethanol at room temperature followed by vortex mixing. After the mixture stood at room temperature for two minutes, it was centrifuged at 12,000g for five minutes at 4°C, followed by removing the supernatant fluid and allowing the pellet to dry. The pellet was rinsed with 1ml of 70% ethanol and centrifuged again. After the pellet was allowed to re-dry, it was resuspended in 50 μ l of TE (pH 8.0) and the plasmid preparations were then analyzed by restriction enzyme cutting and agarose gel electrophoresis.

Restriction Enzyme Digests

To perform restriction enzyme analysis on the plasmid preparations, a master enzyme mix was made containing 24 μ l enzyme, 12 μ l buffer, and 60 μ l ddH₂O (enough for ten reactions, a control and one extra reaction). After 2 μ l of each plasmid was added to ten tubes, 8 μ l of the master mix was added. A control of pETC550 was also made in the same fashion to give a total of 11 tubes. Each of the tubes were vortexed, spun down and then allowed to incubate at 37°C for 4 hours. The digests were then confirmed on a 1% agarose gel. Restriction digests revealing the expected pattern due to the introduction of new cut sites during mutagenesis, were sent to the Oklahoma State University core

facility for DNA sequencing. Preparations that returned from sequencing with the confirmed sequence were stored in 20% frozen glycerol at -20°C.

Transformation into BL-21(DE3) E.coli containing pEC86

Mutants confirmed by DNA sequencing were transformed into the *BL-21(DE3)* *E.coli* vector containing plasmid pEC86 (Tables 1 & 2). Competent cells were prepared using a 0.1M CaCl₂ wash and were resuspended in 0.1M CaCl₂/20% glycerol solution. 1µl of mutant plasmid and 1µl of control pETC550 plasmid were aliquoted to 50µl of BL-21(DE3)/pEC86. The mixture was gently swirled to mix and then incubated on ice for 30 minutes. The transformation mixture was then heat pulsed at 42°C for 45 seconds and then placed on ice for two minutes. Next, 0.5 mL of NZY⁺ broth at 42°C was added and the transformation reactions were allowed to incubate at 37°C for one hour with shaking at 225-250g. The transformation reactions were then plated on LB plates containing (100mg/ml) Amp. The entire contents of the sample reaction were plated, while 10µl of the pETC550 control reaction were plated. Plates were allowed to incubate at 37°C overnight.

The over-expression of pETC550 in BL-21(DE3) E.coli with pEC86.

A unique binary plasmid system was used to over-express cyt. c550 that is responsible for the covalent attachment of the heme to make the mature c550. This plasmid system is discussed in detail in the results section. A 100ml overnight Terrific Broth (TB) culture was inoculated with cells, (30mg/ml) chloramphenicol, (100mg/ml) ampicillin, and depending on the particular mutant, glucose or sucrose. The culture was

incubated overnight while shaking at 250g at the appropriate temperature (37°C or 28°C). The following morning 5ml were transferred to (20) 250ml flasks or (2) 1 liter flasks with 100ml of TB and the appropriate antibiotics and glucose or sucrose. The cultures were then once again incubated with shaking all day. If IPTG was added, it was added when the $OD_{600} = 0.8-1.0$ and the induction was allowed to proceed in the shaker for approximately three-four hours. All cell cultures were combined at the end of the day and placed at 4°C overnight.

Periplasmic fraction preparation.

During production of mature cyt. c550, the PelB leader sequence directs c550 from the cytoplasm into the periplasm (discussed in detail in Chapter 3). Therefore, to obtain the periplasm containing cyt. c550, cells underwent osmotic shock. Cell cultures that were refrigerated at 4°C overnight, were harvested by centrifugation at 4°C, 6000g for ten minutes the following day. Bacterial pellets were incubated in 1ml osmotic buffer (50mM Tris/HCl, pH 8.0, 20% sucrose, 1mMEDTA) per 100ml of cell culture and left on ice for 15 minutes. Nanopure water was then added at the same volume of osmotic buffer and the cell suspension remained on ice for another 15 minutes. The culture was then centrifuged at 4°C and 11,000g for 15 minutes and the supernatant fluid (periplasmic fraction) was collected. The concentration of recombinant cyt. in the periplasmic fraction was then determined by visible spectroscopy. Quantitation relied on the absorbance changes that occur upon reduction of the cyt., when sodium dithionite crystals, which act as a reducing agent, were added to the fraction and the protein was observed for absorbance at 407 nm and 550nm.

Using the spectral data at 550nm, the concentration of protein in the fraction could be estimated by using the following formula: $A = Ebc$. This formula could be rearranged to calculate for the concentration: $C = \frac{(\text{Dilution factor}) (A_{550})}{(E)(b)}$

A= absorbance

b= path length in cm

c = concentration in mM

E= extinction coefficient of cyt. c550 (25×10^3 mole/cm)

The protein was then stored at -20°C until further use.

Crude extract protein preparation

A crude extract of protein was prepared strictly for redox titrations using the following methodology. After the periplasmic fraction was prepared, 10mM, pH 7.0 streptomycin sulfate was added and then the solution was allowed to stir for 1 hour at 4°C . After stirring, the solution was put on ice for 1 hour and then spun down at 11,000g for ten minutes at 4°C . After centrifugation, 75% ammonium sulfate was added and the solution was stirred for 1 hour at 4°C and then spun down once again as above. The resulting pellet was dissolved in 0.1mM sodium phosphate buffer pH 7.0 and concentrated to 2-3ml.

Column chromatography protein purification

Purification of cyt. c550 was completed using a three column chromatography system. First, the protein was dialyzed against 20mM Tris/HCl buffer pH 8.0 and then applied to the DEAE cellulose column (XK 26/20) and Cyt. c550 then was eluted with 0-500mM NaCl gradient in Tris/HCl pH 8.0. The fractions containing cyt. c550 were then collected and concentrated by ultrafiltration (Amicon model 8200 with YM10 membrane) to 10ml. The protein was once again dialyzed against 20mM Tris/HCl pH 8.0 and loaded

into the DEAE sephacel column (XK 16/20). Cyt. c550 was eluted with 150-500mM NaCl gradient in Tris/HCl pH 8.0. The fractions containing cyt. c550 were then collected and concentrated by ultrafiltration (Amicon model 8200 with YM10 membrane) to 2-3ml. Last, the Superdex G-75 gel permeation column was loaded and cyt. c550 was eluted with 50mM Tris/HCl buffer pH 8.0. The fractions containing cyt. c550 were then collected and concentrated by ultrafiltration (Amicon model 8200 with YM10 membrane) to 2-3ml. Then cyt. c550 was exchanged into 0.1mM sodium phosphate buffer pH 7.0 and stored at -80°C until further use.

SDS-PAGE gel analysis

After cyt. c550 was purified through the three column chromatography system, it was analyzed on a 12% acrylamide gel containing 6M urea. A 20ml TMBZ gel soak solution was made by dissolving 26mg of 3',3',5',5' tetramethylbenzidine in 0.5ml DMSO. Then, 4.0ml of 95% ethanol, 100% glacial acetic acid, and 5.5ml of water were added to the TMBZ/DMSO soak solution. The SDS-PAGE gel was then soaked in the TMBZ solution for one hour at room temperature with gentle agitation. The staining reaction is then initiated by adding H₂O₂ to 1% v/v. The reaction was then monitored for the visible blue bands. Once the blue bands were detected, the SDS-PAGE could be viewed for the respective single band representing each purified cytochrome.

Spectroelectrochemistry

Redox titrations for cyt. c550 were completed using a custom-made cell (SEC cell) with a quartz cuvette (1.0 cm path-length) fused to a custom made set of ports through a gradient coupling. (OSU Glass Shop, Stillwater, OK). The cell was comprised

of a platinum working electrode, an Ag/AgCl reference electrode and a magnetic stirrer. A Rotaflow stopcock attached to a Schlenk line served as an inlet for argon to keep the inside of the cell oxygen free. The small port in the front of the cell was for the addition of mediators and protein and was filled with a rubber septum prior to the onset of the titrations. The cell was placed in a cuvette holder (OSU Physics and Chemistry Instrument Shop, Stillwater, OK) with internal channels designed to accept a constant temperature source of 24°C with the aid of a refrigerating circulator. The cuvette holder was on top of a stir plate so constant stirring could be maintained throughout the experiment. Sodium phosphate buffer was added to the cell in addition to the redox mediators added at 20 μM (Table 4), glucose oxidase and catalase. This solution was bubbled with argon for 45 minutes and then 10 μM of protein was added to the cell with a Hamilton gas tight syringe and the cell was sealed with a septum. After the cell was pumped and purged with argon three-four times to remove any residual oxygen, 2M glucose was added to ensure the environment is anaerobic. The titrations were then carried out by adding the appropriate amount of a 1 mM solution of sodium dithionite by syringe, while simultaneously monitoring the UV/VIS spectrum of the protein for shifts at 550nm and taking the respective potential with the voltmeter.

<u>Mediators</u> <i>Compound</i>	<u>Redox Potential</u> <i>(vs. NHE)</i>	<u>(V)</u> <i>Ag/AgCl</i>
1,2-Napthoquinone*	0.157	-0.04
Toluylene Blue*	0.115	-0.082
Duroquinone*	-0.005	-0.192
Pentaaminechlororuthenium (II) di-chloride*	-0.040	-0.237
2,5-dihydroxy- <i>p</i> -benzoquinone	-0.060	-0.257
2-hydroxy-1,4-napthoquinone	-0.130	-0.334
Anthraquinone-2,6-disulfonic acid	-0.180	-0.381
Anthraquinone-2-sulfonic acid	-0.250	-0.449
Methylviologen	-0.440	-0.646
Lumi flavine		

Table 4. Redox mediators used for spectroelectrochemistry. The following are the redox mediators that were added to the cell for the sodium dithionite titrations. *Denotes more positive mediators used only for the titration of Cyt. c550-H92M.

CHAPTER 5

EXPRESSION AND PURIFICATION OF CYTOCHROME c550

I. Introduction

The goal of my overall project was to create mutations in cyt. c550 from *Synechocystis* 6803 which would then be characterized to test the hypothesis: How do these specific mutations effect redox potential? In this chapter, I will describe and discuss the results of all of the steps taken to express cyt. c550 in *E. coli*: mutagenesis, expression and optimization, and purification. I have exhibited how the pET system can be used along with BL21(DE3) *E. coli* housing the pEC86 plasmid, to over-express heme containing protein in *E. coli*. The T7 polymerase-based pET system is one of the most powerful and widely used expression systems available for prokaryotes. This expression system is now widely used because of its ability to mass-produce proteins, the specificity involved in the T7 promoter which only binds T7 RNA polymerase, and also the design of the system which allows for the easy manipulation of how much of the desired protein is expressed and when that expression occurs. (Unger, 1997; Novagen, 2002-2003). Once pETC550 is transformed into the BL21(DE3) *E. coli* harboring the pEC86 plasmid, the binary plasmid system leads to a covalently attached heme and therefore a mature cyt. c550. This process will be discussed in detail in the following section.

Additionally addressed in this chapter will be a number of different strategies that were used to optimize expression conditions for cyt. c550. Since expression levels were not the same for each of the mutagenized cyts., specific expression

protocols had to be re-designed so we could obtain significant yields of each of the proteins for further experimentation. Last, will be the discussion of the purification of cyt. c550 using a three column chromatography purification technique, as well as a crude extract preparation, which proved sufficient for the redox titrations.

II. Results and Discussion

A. Mutagenesis

I have used a PCR-based site-directed mutagenesis procedure to introduce amino acid substitutions into the cyt. c550 protein. The PCR procedure is based upon the Stratagene Quick-change site-directed mutagenesis kit and is outlined in (Fig. 3) of materials and methods. A detailed description of this procedure can also be found in the materials and methods. The PCR resulted in the successful mutagenesis of five of the eight amino acid targets in the pETC550 vector (Table 5). Confirmation was done by 1% agarose gel analysis. After plasmid preparation, approximately 0.10-0.90 $\mu\text{g}/\mu\text{l}$ of DNA was isolated.

<u>Mutant primer</u>	<u>Successful Mutants- (X)</u>	<u>Amount of DNA isolated (μg)</u>
Cyt. c550-T48I	X	67.5
Cyt. c550-L91I	X	45.0
Cyt. c550-P93A	X	52.5
Cyt. c550-P93G		
Cyt. c550-N49L	X	72.3
Cyt. c550-N49D	X	75.1
Cyt. c550-H92M		

Table 5. Successfully mutagenized cytochromes. All mutation target sites attempted and those that were successful after confirmation of two-step PCR by 1% agarose gel analysis. Also shown is the amount of total DNA (μg) isolated after plasmid preparation.

PCR was used for the mutagenic primers to ensure proper elongation and hybridization (Fig. 11). First, PCR was used to denature the pETC550 plasmid and anneal the oligonucleotide primers that contained the desired mutation. At the conclusion of this, the oligonucleotide primers had been annealed separately to the forward and reverse primers, and then were combined. PCR was then used again, and the nonstrand-displacing action of PfuTurbo DNA Polymerase (Stratagene) extended and incorporated the mutagenic primers. The successfully incorporated mutants were confirmed on a 1% agarose gel with pETC550 serving as a control.

Since the PCR regenerates the original plasmid, albeit with a mutation, it is then possible to replicate the products by transformation into *E. coli*. After transformation of the PCR products into competent XL-1 Blue *E. coli* cells (XL1 Supercompetent, Stratagene), individual colonies were grown in culture overnight and were then used for a small plasmid preparation the following morning. After the content of the plasmid preparation was confirmed on a 1% agarose gel, the plasmid samples were digested with the appropriate restriction endonucleases for identification of plasmids containing the mutated sequence. Since a silent mutation was introduced into all of the mutagenic primers, successful transformants showed an additional restriction enzyme cut site when compared to that of the pETC550 control plasmid (Fig. 12). This served as a very efficient marker for successful mutagenesis so we did not proceed with experiments if the mutation was not indeed present.

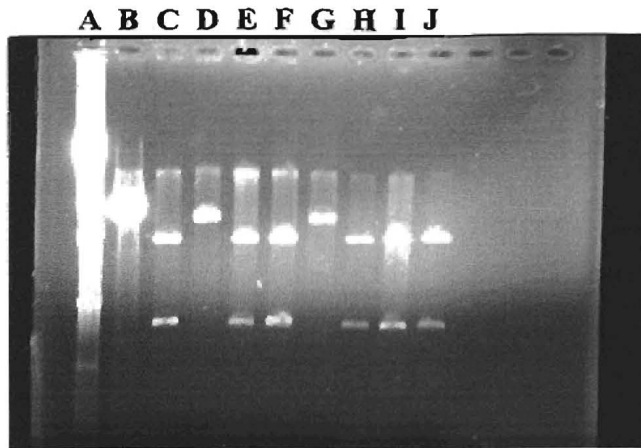


Figure 12. Restriction enzyme digest of *cyt. c550-N49D* with *PstI*. **A:** λ *HindIII* DNA ladder, **B:** pETC550 control, **C-J:** *Cyt. c550-N49D*. Lanes **C,E,F,H,I,** and **J** all show successful mutants that demonstrate the additional cut site introduced with the silent mutation in the mutation target sequence. Therefore there are two fragments of ~1.7kB and 4.2kB (lanes **C,E,F,H,I** and **J**) as compared to the one cut site shown in lanes **B,D,**and **G**.

If a particular plasmid did not show an additional cut site, it was evident that the mutated primer sequence had not been incorporated into the parent plasmid and therefore no further analysis was done. Transformants yielding plasmids with the expected new restriction site were sent to the OSU core facility for DNA sequencing, and results were then compared to the nucleotide sequence of pETC550 for confirmation. It should be noted that although PCR can be erroneous, all sequences were confirmed for the entire *psbV* gene, and therefore the absence of unintended mutations was ensured.

For the initially unsuccessful mutagenesis reactions, some changes to protocol were made in an attempt to optimize PCR conditions. Different volumes of template DNA (0.5 μ l, 1 μ l and 2 μ l) were used in addition to an increased second round annealing temperature of 57 $^{\circ}$ C instead of 55 $^{\circ}$ C without success for the *cyt. c550-MetD* mutant. For *Cyt. c550-P93G* and *cyt. c550-H92M*, the experiment was done in quadruplicate to ensure a higher yield of amplified DNA, and then the entirety of the products were used

to transform into competent XL-1 Blue *E. coli* cells (XL1 Supercompetent, Stratagene). With more DNA present, it was hoped that the competent cells would be more likely to pick it up and incorporate it. However, this did not prove to be any more successful in attaining transformants than doing the procedure following the 1x standard protocol. After transformants were obtained for cyt. c550-P93G and cyt. c550-H92M, restriction analysis indicated that only a few plasmids were positive for carrying the mutated sequence. After the plasmids were sent to sequencing, the confirmed nucleotide sequence indicated that the mutated sequences were actually not present for either Cyt. c550-P93G or cyt. c550-H92M. Since restriction analysis suggested otherwise, we suspected that the problem could be coming from the plasmid preparation. Therefore, the plasmids of cyt. c550-P93G and cyt. c550-H92M were re-prepared using a large scale plasmid preparation protocol (Qiagen, Valencia, CA) which used a column for purification, and then were resent to sequencing. Although the overall DNA nucleotide sequence was more accurate, the mutated sequences were still not present. For the cyt. c550-P93A mutant, the DNA nucleotide sequencing after the small plasmid preparation showed some missing bases throughout the sequence like that of cyt. c550-P93G and cyt. c550-H92M. However, a large plasmid preparation utilizing the column was performed, and then the sequence was accurate when compared to that of the control plasmid pETC550, and additionally contained the mutated sequence. The large plasmid preparation obviously led to a cleaner preparation since it makes use of a filtration column, and therefore a higher yield of purified DNA. After many trials with cyt. c550-MetD, cyt. c550-P93G and cyt. c550-H92M without any success, we continued with the other primers to attain mutants. Many speculations can be made in regards to why only

three of the primers were not amplified using this technique. One possibility exists that these primers did not recognize the annealing site, so therefore they were not incorporated. This could be due to the substitution of some bases, which causes the polymerase to have trouble recognizing the annealing site. The plasmids with a confirmed DNA nucleotide sequence were transformed into the binary expression plasmid BL21(DE3)/pEC 86. The cyt. c550-H92M mutant was obtained from Dr. Li (Burnap Lab, OSU).

B. Overexpression of cyt. c550 using a binary plasmid system in E.coli

For overexpressing cyt. c550, a binary plasmid system in *E.coli* BL21(DE3), consisting of the pEC86 plasmid and the pETC550 plasmid was used. Although a variety of plasmid vectors exist for the overexpression of c-type cytochromes in *E.coli* (Price *et al.*, 2000, Sanders & Lill, 2000), for overexpressing cyt. c550 we used the binary plasmid system consisting of the pEC86 and pETC550 plasmids. The pEC86 plasmid (Fig. 13) is harbored by the *E.coli* BL21(DE3) host strain and was obtained from Dr. Linda Thony-Meyer (Mikrobiologisches Institut, Zurich, Switzerland). Once the mutagenized plasmids were confirmed by sequencing, they could be transformed into the *E.coli* BL21(DE3) strain where they would be housed with the pEC86 plasmid. This system is considered to be binary since both plasmids play a role in producing the covalently attached holo-cyt. c550. The pETC550 plasmid is responsible for the production of apo-cyt. c550 with a cleavable pelB leader sequence that directs the cytochrome across the cytoplasmic membrane and into the periplasm. The pEC86 plasmid contains the genes ccmABCDEFGH cloned in pACYC184 in the direction of the *tet* promoter. It allows for a high copy number expression of the *ccm* genes which are

required for formation of c-type cytochromes. Cytochrome c maturation is actually thought to be catalyzed by the ccm membrane complex consisting of these eight proteins. CcmD is responsible for the delivery of heme to CcmE where heme binds transiently in the periplasm. CcmE then functions as a heme chaperone by facilitating the transfer and preventing aggregation or non-specific interactions of the heme. Once the apo-cyt. c550 has been directed into the periplasm, the heme will become covalently attached to the apo-cyt. c550 via two thioether bonds at the conserved CXXCH binding motif, therefore resulting in holo-cyt. c550 (Arslan *et al.*, 1998).

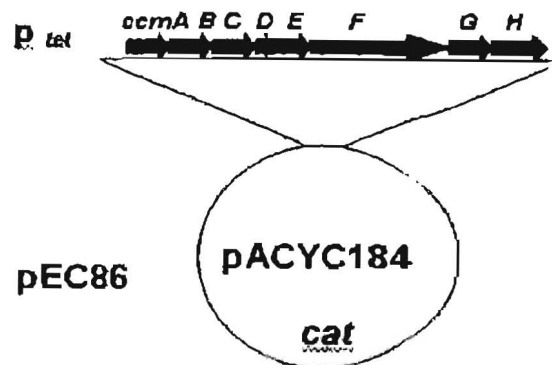


Figure 13. The pEC86 plasmid used to overexpress cyt. c550 in *E.coli*. The genes *ccmABCDEFGH* are cloned in pACYC184 in the direction of the tet promoter (Thony-Meyer *et al.*, 1994 & Fee *et al.*, 2000).. This allows constitutive high copy number expression of the ccm genes, which are required for formation of c-type cytochromes.

C. Optimization of expression

An important goal of the project was to maximize the expression conditions of cyt. c550 in *E.coli* since only variable success has been achieved in the overexpression of c-type cytochromes in *E.coli* thus far (Thony-Meyer, et al., 1994). The combined periplasmic fraction preparations yielded a sufficient amount of recombinant cyt. c550 for protein purification using column chromatography. As discussed below, it was found

that crude protein extracts could also be used for redox potential determinations. The amounts of cyt. in the extracts were determined using the published extinction coefficient for the heme of cyt. c550 (Table 6). Also included in Table 6 are the culturing conditions for cyt. c550 and the cyt. c550 mutants.

<u>Cytochrome c550</u>	<u>Volume (ml)</u>	<u>Concentration (μM)</u>	<u>With IPTG, Sucrose, & Betaine</u>	<u>Without IPTG, Sucrose, & Betaine</u>	<u>With and without IPTG, Sucrose and Betaine</u>
pETC550	420	27			X
Cyt. c550-T48I	500	26		X	
Cyt. c550-L91I	200	20		X	
Cyt. c550-P93A	445	22	X		
Cyt. c550-N49D	200	21	X		
Cyt. c550-N49L	240	29	X		
Cyt. c550-H92M	*	*	X		

Table 6. Expression conditions of cyt. c550. Cyt. c550 and mutants with overall final volume and concentrations obtained from periplasmic fraction preparations. Also included are the expression conditions of the each cyt. *Denotes preparation by Dr. Z.L. Li., OSU).

To culture cyt. c550 in *E.coli*, we used a standard protocol of TB broth with the respective antibiotics and 2M glucose for pETC550, cyt. c550-T48I and cyt. c550-L91I. After being cultured all day, samples were taken out of the shaker and put at 4°C overnight. This seemed to give us a higher yield of covalently attached hemo-protein as compared to cultures that were prepared that evening. It's possible that the longer time is helpful for apo-cyt. c550 export into periplasm and/or heme attachment. After the periplasmic fraction was prepared, we developed a quick test to estimate the amount of recombinant protein present based on the spectroscopic properties of the heme. By adding a small amount of dithionite and then using spectroscopy to scan from 400-700nm

we could use the spectral value at 550nm (α -band) (Fig. 14) and an equation including the extinction coefficient for cyt. c550 to calculate the protein concentration. The dithionite served as a reductant by donating an electron to the heme iron, producing an increase in light absorbance at 550nm. When the population of cyt. molecules in the cuvette are all oxidized, the OD_{550} is minimal, whereas when it is fully reduced, the absorbance is maximized. Because the extinction coefficient for c550 is known, it is possible to quantitate the amount of c550 by the absorbance change, following the addition of excess dithionite.

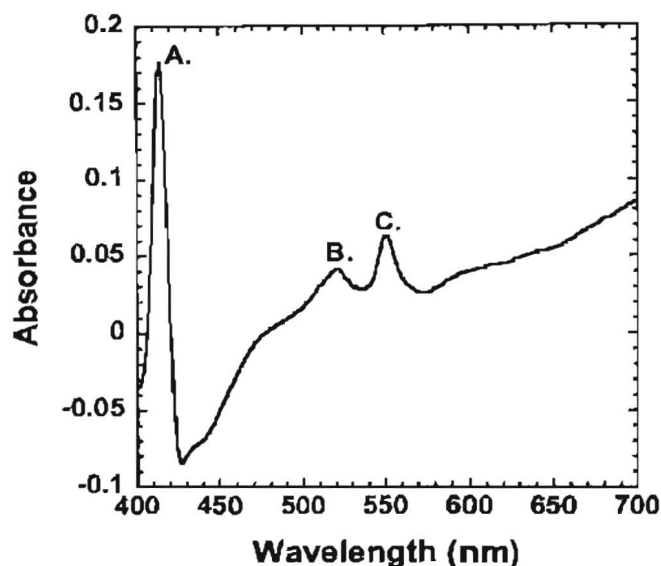


Figure 14. Characteristic difference spectrum of periplasmic fraction preparation after the addition of dithionite. The fraction was scanned from 400 to 700nm so that all three regions of the spectra, A: α -band at 550nm, B: β -band at 522nm, and C: Soret band at 417nm could be viewed. Both the sample and reference cuvettes contained the periplasmic extract. Spectrum was recorded following the addition of sodium dithionite to the sample cuvette.

Although the standard protocol involving the TB, antibiotics and 2M glucose worked for the expression of several of our mutant cyts., some mutant proteins proved more difficult to express in sufficient quantities. Therefore, expression conditions had to

be revisited. A variety of conditions exist for optimizing the expression of covalently attached hemo-proteins. Based on the expression protocol used in our collaborators lab, Dr. Mario Rivera (OSU Chemistry Department), for the expression of cyt. b5, we attempted to induce the growth of cyt. c550 with the addition of 1M IPTG, (100mg/ml) FeSO₄, and (17mg/ml) ALA at O.D.600 =1, but saw no difference in growth as compared to the standard procedure already being employed in our lab. Additionally, we tried to supplement our growth protocol with the addition of FeSO₄ and ALA alone and together, without any IPTG. We found that this actually lowered our yield of protein as compared to the yield of our control preparation with none of the above supplements added. The theory behind the addition of IPTG is that it will induce the T7 RNA polymerase from *E.coli* BL21(DE3) to induce production of the cyt. The pET vector contains a *lac I* gene which codes for the lac repressor, a T7 promoter which is specific to only T7 RNA polymerase (not bacterial RNA polymerase) and a *lac* operator (Blaber, 1998). When the T7 RNA polymerase is present and the *lac* operator is not repressed, transcription proceeds very rapidly as long as the T7 RNA polymerase is present (Campbell, 20003). IPTG is also responsible for displacing the *lac* repressor and initiating the *lac* genes since it is an analogue of lactose (Blaber, 1998). Since there are *lac* operators on both the gene encoding T7 polymerase and *psbV*, IPTG activates both genes (Campbell, 2003). Therefore, when IPTG is added to the cell, the T7 polymerase is expressed, and quickly begins to transcribe *psbV* which is then translated. The FeSO₄ is added as an additional source of iron since heme requires iron in its structure. Last, ALA was added because it serves as a precursor for heme biosynthesis. Without heme biosynthesis, there will be no heme produced, and hence, no holo-cyt. c550.

Since we were having extremely low yields for the expression of cyt. c550-P93A, we then tried to supplement our procedure by inducing growth with only IPTG when O.D 600 = 1, after approximately three-four hours of growth. By varying concentrations of IPTG (0.5mM, 2.5mM, 5mM, and 10mM) we found that 0.5mM IPTG helped to increase the expression of this cyt. c550 three-fold as compared to the control with no IPTG (Fig. 15).

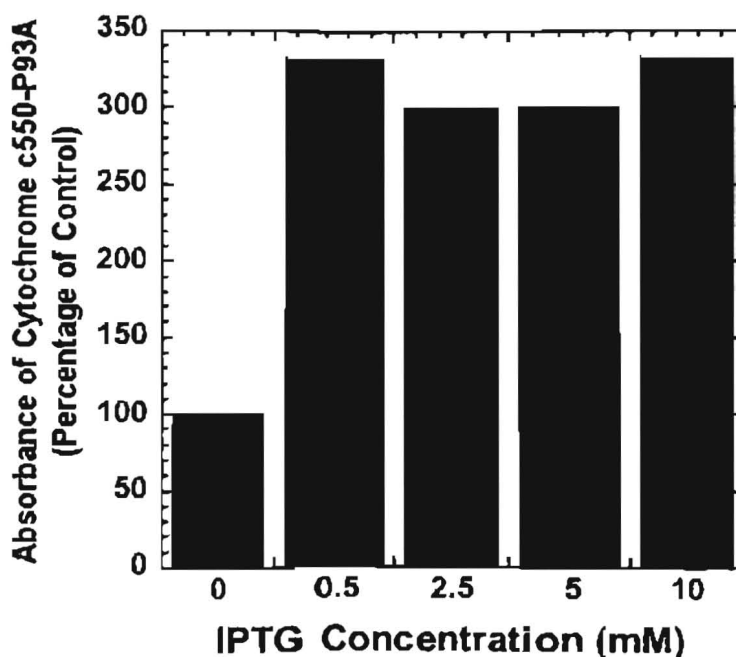


Figure 15. Absorbance of cyt. c550-P93A under varying IPTG conditions as a percentage of the control. When 0.5mM IPTG was added to the culture at an $OD_{600}=1$ after three-four hours of growth, a three fold increase was observed in the expression of cyt. c550 at 37°C, as compared to the control with 0mM IPTG.

It was obvious that the IPTG was indeed inducing the T7 RNA polymerase present in *E.coli* BL21(DE3) therefore leading to the production of more cyt.

c550. Additionally, when we varied the cultivating temperature from 37°C to 28°C with 0.5mM IPTG we saw a three-fold increase in the expression of cyt. c550 (Figs. 16 & 17).

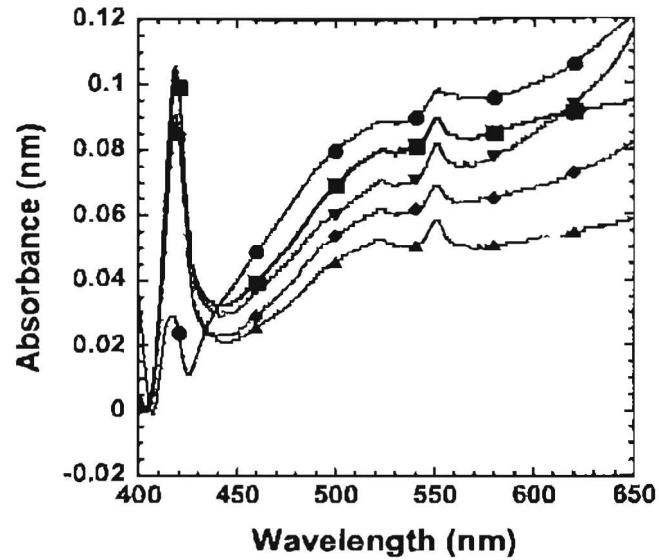


Figure 16. The induction by IPTG given at varying concentration on the expression of cyt. c550-P93A in *E. coli* at 37°C. (●) Control, 0 IPTG, (■) 0.5mM IPTG, (◆) 2.5mM IPTG, (▲) 5mM IPTG, (▼) 10mM IPTG. Induction of 0.5mM IPTG (■) at 37°C showed the best yield. Difference spectra were recorded as in Figure 14.

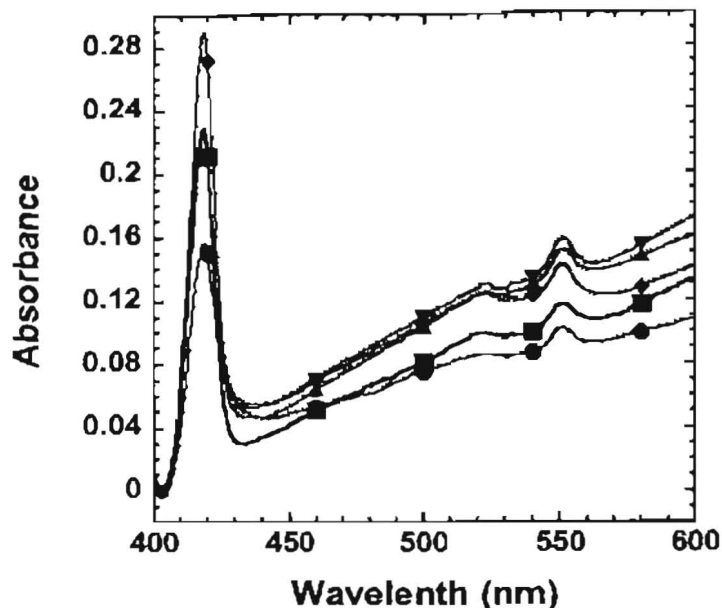


Figure 17. The induction by IPTG given at varying concentrations on the expression of cyt. c550-P93A in *E. coli* at 28°C. (●) Control, 0 IPTG, (■) 0.5mM IPTG, (◆) 2.5mM IPTG, (▲) 5mM IPTG, (▼) 10mM IPTG. Induction of 0.5mM IPTG at 28°C showed the best yield for cyt. c550-P93A giving a near three-fold increase over cyt. c550-P93A grown with 0.5mM IPTG at 37°C. Difference spectra were recorded as in Figure 14.

It was evident that the cyt. c550 mutants had some sensitivity to temperature and preferred to be cultured at 28°C. This was evident as seen in (Fig. 8) when cyt. c550-P93A under induction by 0.5mM IPTG grown at 28°C, as opposed to 37°C, showed a near three-fold increase in expression. Additionally, in the past it had been virtually impossible to express the cyt. c550-H92M mutant since it is so unstable. Once the sixth axial ligand is mutated from a histidine to a methionine, the protein becomes unstable because the covalent attachment of the heme is more difficult to achieve (see below). However, when we supplemented the media with 0.5M IPTG at 28°C we found a four-fold increase in the expression of cyt. c550-H92M as compared to cyt. c550-H92M grown with only 0.5mM IPTG at 37°C (Figs. 18 & 19).

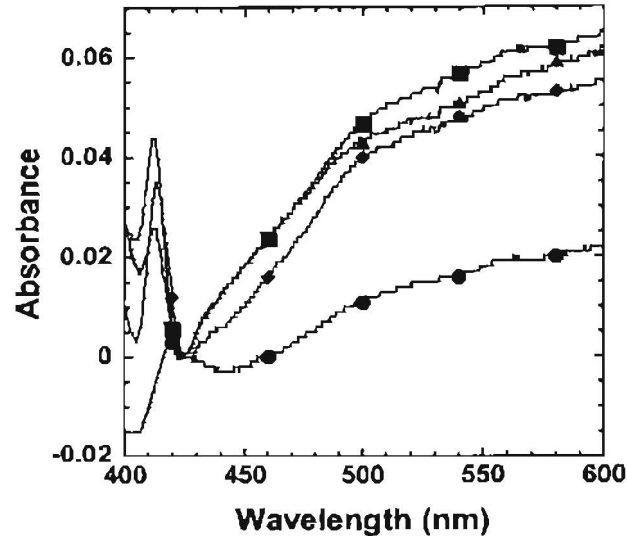


Figure 18. The induction by IPTG on the expression of cyt. c550-H92M in *E. coli* at 37°C. (●) Control, 0 IPTG, (■) 0.5mM IPTG, (◆) 2.5mM IPTG, (▲) 5mM IPTG. There are no peaks observed in the 550nm region at any of the varying concentrations of IPTG. Difference spectra were recorded as in Figure 14.

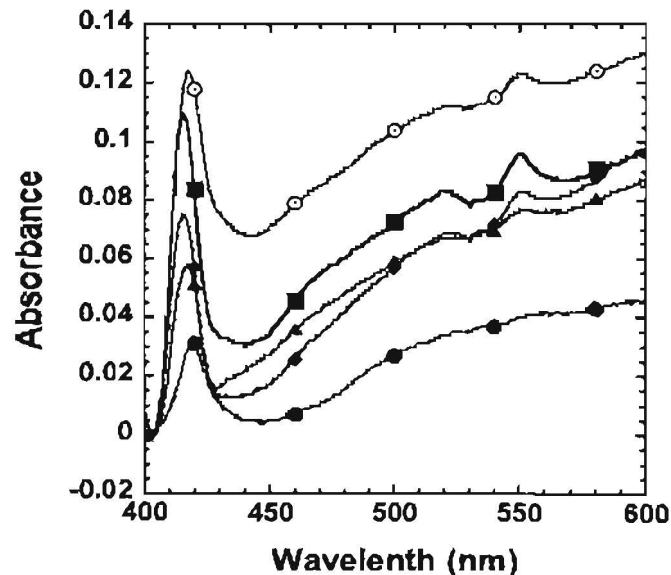


Figure 19. The induction by IPTG on the expression of cyt. c550-H92M in *E. coli* at 28°C. (●) Control, 0 IPTG, (○) 0.1mM IPTG (■) 0.5mM IPTG, (◆) 2.5mM IPTG, (▲) 5mM IPTG. At 28°C, there is a four-fold increase in the expression of cyt. c550-H92M when the media is supplemented with 0.5mM IPTG (■). Difference spectra were recorded as in Figure 14.

Although adding 0.5mM IPTG did increase our expression for cyt. c550-P93A and cyt. c550-H92M, we were still interested in optimizing the conditions further to achieve yields similar to that of pETC550 and the two other mutants cyt. c550-T48I and cyt. c550-L91I. Based on work done by Bourot, *et al.*, and Sosa-Peinado, *et al.*, we additionally supplemented our expression medium with 2.5mM betaine and 300mM sucrose. With the addition of these two osmolytes and 0.5mM IPTG at 28°C, we saw a four-fold increase in the expression cyt. c550-H92M as compared to the control with only 0.5mM IPTG and no betaine or sucrose, (Fig. 20).

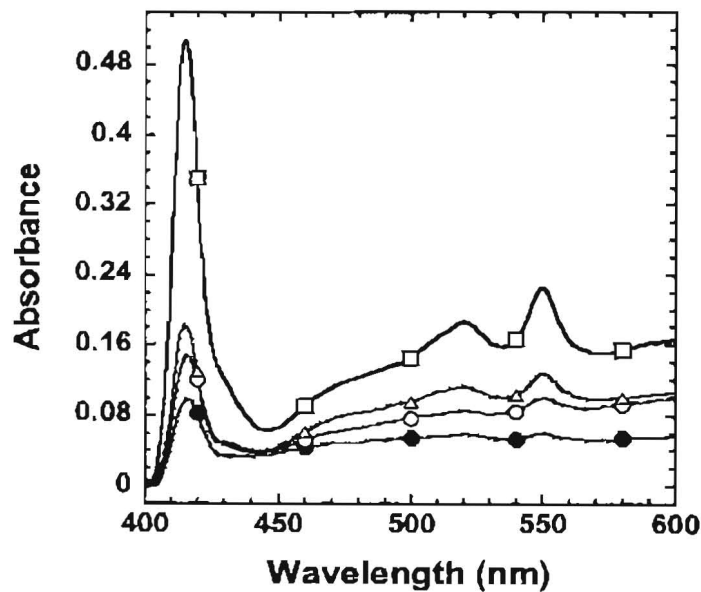


Figure 20. The effects of 0.5mM IPTG, 2.5mM betaine and 300mM sucrose on the expression of cyt. c550-H92M in *E. coli* at 28°C. (●) 0.5mM IPTG, (▲) 0.5mM IPTG, 2.5mM betaine, (△) 0.5mM IPTG, 300mM sucrose, (◻) 0.5mM IPTG, 2.5mM betaine, 300mM sucrose. With the addition of the two osmolytes, betaine and sucrose, and 0.5mM IPTG (◻), a four-fold increase was seen in the expression of cyt. c550-H92M as compared to a control (●) with no addition of osmolytes. Difference spectra were recorded as in Figure 14.

We were also able to see similar results for cyt. c550, cyt. c550-P93A, cyt. c550-N49D and cyt. c550-N49L. It is likely that these two growth additives aid cyt. c550 in protein folding which could in turn result in more protein stability and a stable heme environment and attachment in the holo-cyt. c550. It should be noted that an increase in protein expression was also seen for pETC550 under these same conditions.

Additionally, we found that flask sizes had an influence on the amount of protein expression. All of the mutants seemed to grow better in large 2l flask, with an exception of H92M which grew much better in 20 (100 ml) flask. This likely related to the oxygen requirements of cells expressing each of the different cyt. mutants.

D. Purification

Two purification techniques were utilized to purify the cyt. c550 in *E.coli*, and each yielded a significant amount of protein to perform the redox titrations. The first method purified cyt. c550 by using a three column chromatography system. With this method, the periplasmic fractions could be directly added to the first column, the DEAE cellulose, which is an anion exchange column. Since cyt. c550 is an anion, it bound to the positively charged column matrix, and when rinsed with 500mM NaCl, the Cl⁻ anions released the protein by competing for the positive charge. After fractions were collected and concentrated, they were added to the second column, the DEAE sephacel, which once again allowed cyt. c550 to be purified based on charge differences. The fractions were collected and concentrated from the DEAE sephacel and added lastly to the third column, the G-75 Superdex, which is a gel permeation column. The gel beads in the

column trapped cyt. c550 while allowing larger substances to pass on through. The smaller cyt. c550 was then washed out of the beads and collected as purified protein.

The three column chromatography protein purification was carried out and rendered sufficient yields of cyt. c550 for the redox titrations (Table 7). Characteristic spectras of our collected fractions from each of the three columns can be vjewed in the (Figs. 21-23). Each of the collected fractions were scanned at 280nm and 407nm to detect the protein present in the fraction (280nm) and to detect the soret band (407nm) of cyt. c550. By utilizing this spectral data shown in these figures, we could determine in exactly what part of the fraction our cyt. was, so that we could collect it for concentration.

Cytochrome C550	Protein concentration (mg/ml)	Volume (ml)	Molar concentration (μM)	Yield (μg/l)
<i>Wild Type</i>	1.87	1.95	118	140
<i>T48I</i>	1.88	2.75	118	215
<i>L91I</i>	1.87	1.85	118	247

Table 7: Concentrations and yields of the three column chromatography purification. Shown above are the respective protein concentration, volume, molar concentration and yield for cyt. c550, cyt. c550-T48I and cyt. c550-L91I. Yields for the proteins were sufficient to perform re-dox measurements. Other proteins were purified using the crude extract protein purification procedure for redox titrations.

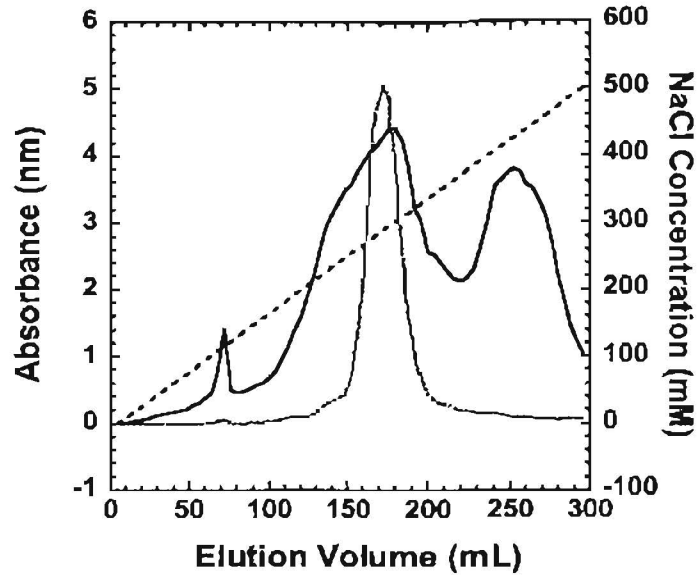


Figure 21. Ion exchange profile with 500mM NaCl salt gradient for cyt. c550 after purification through the DEAE cellulose column. The collected fractions were scanned at 280nm (—) and 407nm (---). The diagonal line (/-) demonstrates the elution of cyt. c550 from 0-500mM NaCl. Fractions were collected where the peaks at 280nm and 407nm coincide (Peak 2 of 280nm).

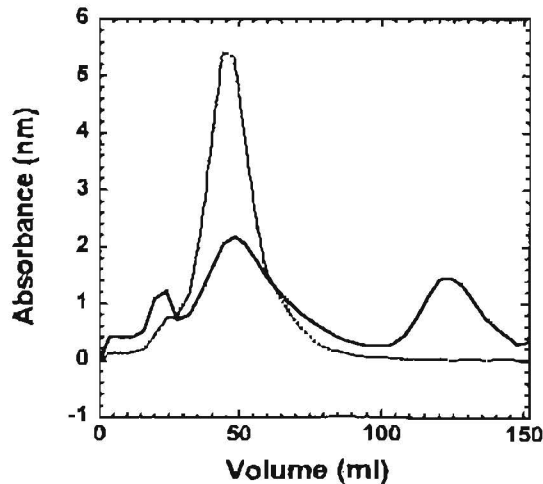


Figure 22. Ion exchange profile for cyt. c550 after purification through the DEAE sephacel column. The collected fractions were scanned at 280nm (—) and 407nm (---). Fractions were collected where the peaks at 280nm and 407nm coincide (Peak 2 of 280nm).

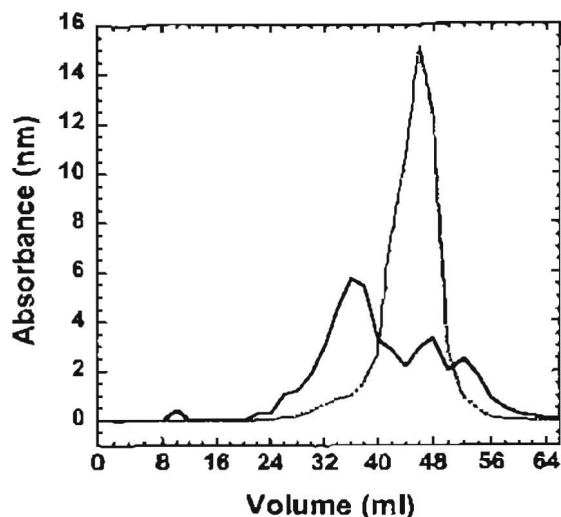


Figure 23. Elution profile of cyt. c550 after purification through the gel permeation column (G-75 Superdex). The collected fractions were scanned at 280nm (—) and 407nm (---). Cyt. c550 was eluted where the peaks at 280nm and 407nm coincide (Peak 2 of 280nm).

The cyts. purified by column chromatography were analyzed on a SDS-polyacrylamide gel with TMBZ and Coomassie Blue staining to confirm the one homologous band representative of purified cyt. c550 (Fig. 24). The first gel (A) is stained only with the Coomassie, while the second gel (B) has been stained additionally by TMBZ. The Coomassie stain is responsible for staining all of the proteins present, while the TMBZ stain is selective for heme-containing proteins. The one homologous band viewed in each of the gels in lanes labeled (E) is representative of the purified Cyt. c550. Since there is only one band present in these lanes, no other heme-containing proteins are likely present, therefore ensuring that our cyts. were purified.

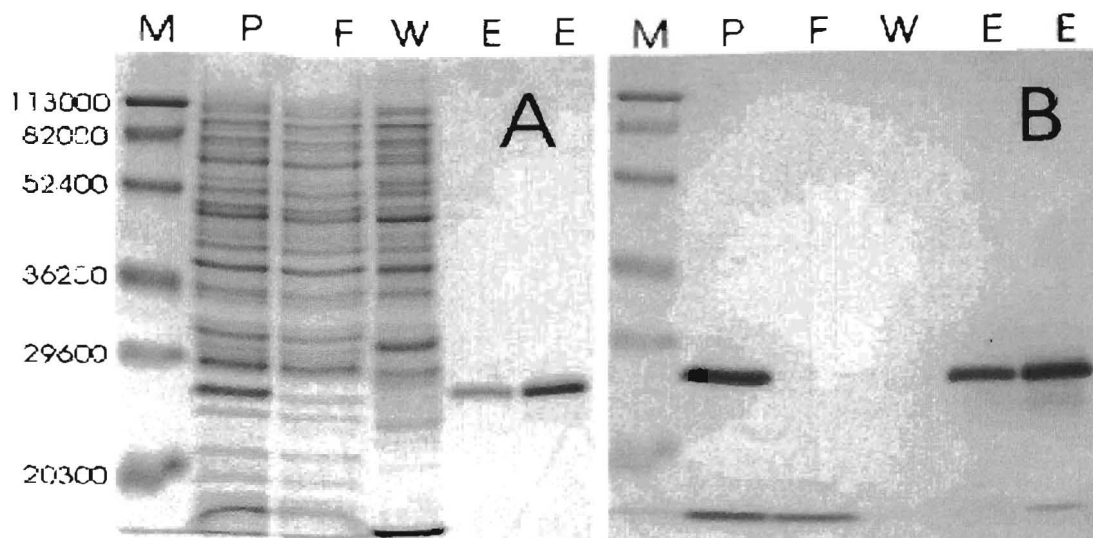


Figure 24. SDS-PAGE: FPLC purification of cyt.C550 on Ni-NTA Superflow. SDS-PAGE was performed at 12% acrylamide including 6M urea. **A:** Coomassie-stained SDS gel; **B:** the same gel with TMBZ staining. **M:** prestained SDS-PAGE standards (Bio-Rad); **P:** periplasmic fraction; **F:** flow through; **W:** wash; **E:** elutes (purified cyt. c550).

In addition to the three column chromatography purification technique, a purification protocol was designed using the crude extracts of the proteins to save time and expense, which yielded a comparable value to that achieved by the columns. It should be noted that the crude extract of protein was prepared strictly for redox titrations and was not used for other procedures. Additionally, the titrations using the crude extract of protein gave us the same results when compared to titrations using the column purified protein. To accomplish this simple purification technique, the periplasmic fraction was prepared, and then streptomycin sulfate was added to precipitate nucleic acids. This was followed by a simple protein purification step involving the same concentration of ammonium sulfate used for our column purified proteins. The procedure is discussed in detail in the materials and methods. Although this procedure was likely not as pure as the protein purified through the three columns, it is unlikely that there were any other

interfering redox proteins present since the entire titration spectra looked identical for the column purified protein and the crude extract purified protein. The concentration of protein obtained from the crude purification can be seen in (Table 8).

Cytochrome c550	Volume (ml)	Concentration(μM)
pET c550	2.85	88
pET Hc550	4	93.6
pETc550H	3.8	118.8
cyt. c550- P93A	4.8	106
cyt. c550- N49D	3.4	101
cyt. c550-N49L	4.3	112.5
cyt. c550- H92M	3.5	96

Table 8. Concentration of proteins after crude extract purification. Shown are the overall volumes and concentrations that were obtained after the crude purification of the periplasmic fraction preparation. Crude purified protein was used only for electrochemistry.

CHAPTER 6

REDUCTION-OXIDATION (Redox) PROPERTIES OF CYTOCHROME c550 AND c550 MUTANTS

Introduction

Redox titrations can be carried out to determine the concentration and midpoint potential(s) of one or more species in a solution. A titration is done to obtain quantitative information about the sample, by adding a certain volume of reactant whose concentration is known. By adding a known concentration of reactant, at consistent intervals, data can be collected to make a titration curve. To determine the formal reduction potential of cyt. c550, we used the reactant sodium dithionite. Sodium dithionite serves as a reductant by adding electrons to the electrochemical cell, which are then picked up by the redox mediators in the cell that in turn, transfer the electrons to the heme iron of cyt. c550. During this process, the redox potential in the titration cell becomes progressively more negative which is measured with a Ag/AgCl electrode. This is a stepwise process, which allows for a gradual reduction of cyt. c550 with each addition of sodium dithionite, so sufficient data can be collected at each progressively more negative potential. As the cyt. becomes reduced it undergoes absorbance changes which allow us to determine the fraction of the cyt. population in the solution that has become reduced. It was very important for us to have the correct balance of mediators for each of the different proteins, so they could provide a buffering capacity around the actual redox value of the respective protein, and electrons could be slowly delivered to the heme iron of the cyt.

As sodium dithionite was added to each titration, the concentration of the reduced and oxidized states of the redox protein in the cell, are determined from the optical absorption spectrum of the solution in the cell. Each new spectrum following each addition of sodium dithionite to the cell was saved, and the absorbance value at 550nm was documented. As more sodium dithionite was gradually added to the cell, the peak at 550nm went from completely oxidized (flat) to partially oxidized (semi-curved), to completely reduced (curved) as can be seen in (Fig. 25).

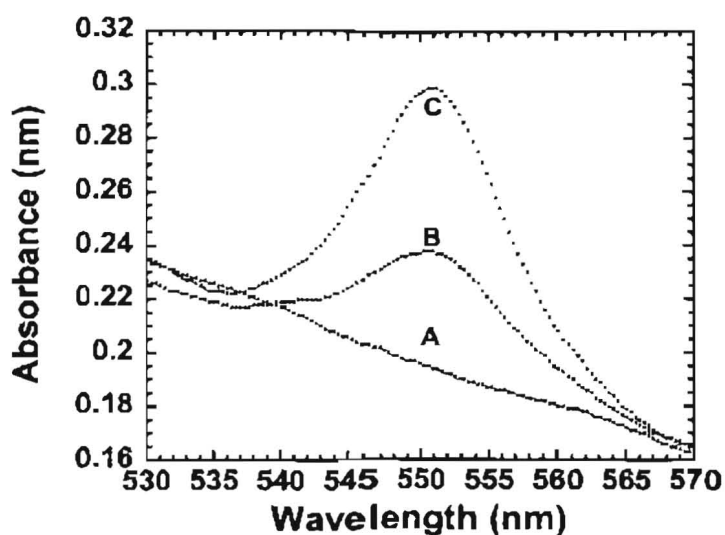


Figure 25. Redox titration spectrum at 550nm. Shown in this figure is the absorbance at 550nm for A: the fully oxidized protein, B: the partially oxidized protein, and C: the completely reduced protein.

The spectral information from each addition of dithionite is then correlated with the simultaneously determined reduction potential of the cell, as measured by the electrode, in which the values were recorded from the potentiostat. Therefore, each data point on the titration curve represents the absorption spectrum of the titration solution at

550nm and the respective redox potential at that absorption. Once it was ensured that the solution in the cell was completely reduced, these two pieces of information were interpreted through the Nernst equation (Eq. 1) to find the formal redox potential (E) by determining the ratio of $[ox]/[red]$ at the electrode surface.

Equation 1. $E(mV) = E^{\circ} + 59 \log[ox]/[red]$

In calculating the formal reduction potential, we had to convert our potential values obtained from our Ag/AgCl reference electrode to the standard NHE reference value, since this value is usually used in the literature and since our Ag/AgCl electrode was giving us a midpoint potential in regards to the affinity for electrons to Ag/AgCl, whereas the NHE value indicates the affinity for protons and electrons to make hydrogen. The following formula describes the relationship between the Ag/AgCl value and the NHE value:

Equation 2. (NHE) formal redox potential = (Ag/AgCl) redox potential - 197mV

Results and Discussion of Redox Titrations

The reduction potential of cyt. c550 and eight mutants have been measured using an anaerobic spectroelectrochemical cell, by adding the reductant sodium dithionite. Before beginning experiments for cyt. c550 and mutants, cyt. b5 from Dr. Mario Rivera's lab was measured. Since potentiometric titrations had been performed on cyt. b5 before, and their value published, this served as a control for our experiments. After the published redox value for cyt. b5 of -100mV was obtained using the potentiometric procedure, the titrations for cyt. c550 were begun. After a struggle with a number of different redox mediators and keeping the environment in the electrochemical

cell completely anaerobic, we determined that the potentiometric titration (i.e. using a working electrode to supply electrons instead of dithionite) would not work for cyt. c550. This could be due to a number of reasons, but because of cyt. c550's extremely negative potential, it was always very difficult and time consuming to get cyt. c550 to its completely reduced state. If a completely reduced state was achieved, the protein would gradually re-oxidize spontaneously leading us to conclude that there was also some interference with oxygen, despite repeated efforts to improve the sealing of the system. Therefore, I decided to use a different, but still reliable method employed by other groups (Navarro *et al.*, 1995), to do the titrations, by scrupulously adding small amounts of a stock solution of 1mM sodium dithionite to the cell and not applying any potential (voltage). This seemed to work much more efficiently in achieving the desired titration results, and we were able to get cyt. c550 fully reduced much more rapidly and reliably, than with the potentiometric titrations. The overall results of the spectroelectrochemical titrations using sodium dithionite proved to be very interesting and can be seen in (Table 9). The results and discussion for each specific cyt. that was measured will follow.

<u>Cytochrome</u>	<u>C550</u>	<u>T48I</u>	<u>L91I</u>	<u>HC550</u>	<u>C550H</u>
Trial 1	-250.00	-253	-253	-243	-245
Trial 2	-253.00	-253	-251	-240	-253
Trial 3	-253.00	-253	-253	-241	-253
<u>Average Potential</u>	-252.00	-253.00	-252.33	-241.33	-250.33
Standard Deviation	2.12	0.00	1.41	2.12	5.66
Difference from wild type	0.00	1.00	0.33	-10.67	-1.67
<u>Cytochrome</u>	<u>P93A</u>	<u>N49D</u>	<u>N49L</u>	<u>H92M</u>	
Trial 1	-238	-242	-239	-178	
Trial 2	-233	-241	-234	-176	
Trial 3	-238	-246	-233	-178	
Trial 4		-243		-175	
<u>Average Potential</u>	-236.33	-243.00	-235.33	-177.33	
Standard Deviation	3.54	0.71	3.54	1.41	
Difference from wild type	-15.67	-9.00	-16.67	-74.67	

Table 9. The results of the sodium dithionite titrations of cyt. c550 and mutants. Included for each cyt. are the average potential, standard deviation and difference in redox potential from the wild type redox potential. All titrations were carried out with ~10mM protein in 200mM sodium phosphate buffer pH 8.0, 24C°. The titrations were monitored by following the intensity of the absorbance of the oxidized α - band (550nm) of the cyt. being measured and the equilibrium potential resulting from each addition of 1mM sodium dithionite (measured by the potentiostat).

Cytochrome c550

The average midpoint potential determined for cyt. c550 was -252 ± 2.12 mV vs. NHE. I was very pleased to get this value because it agrees with previously published redox values for cyt. c550 by Roncel *et al.*, and Navarro *et al.* This therefore proves that cyt. c550 can be expressed in *E.coli* and the product produced is consistent with native cyt. purified from native sources, as indicated in the literature (Navarro *et al.*, 1995,

Roncel *et al.*, 2003). Additionally, this replicated redox value indicated that I had been able to achieve the same thioether linkage to the heme by expression in *E. coli*. This result is also supported by SDS-page of the protein purified from *E. coli* that resembles the wild-type and shows no unbound heme (Fig. 24). Last, the redox value indicates that the same hydrogen bonding interactions are intact in the *E. coli* expressed protein, as are present in the native expressed protein (Sawaya *et al.*, 2001).

A characteristic sigmoidal titration curve can be seen for cyt. c550 in (Fig. 26A). The sigmoidal curve for cyt. c550 and each of the other cyts. was fitted (as indicated in each figure) using the Nernst equation so that the slope of the curve was a consistent value of 59mV for each Cyt. (Eq. 1). The sigmoidal curve is significant because it relates the fraction of the oxidized mediators to the reduction cell, controlled at the indicated potentials. The formal redox potential can be obtained from the titration curve by going about half-way up the (y-axis) fraction oxidized (~0.5), and then straight over on the (x-axis) titration curve to read the potential value.

The entire spectra of the sodium dithionite titration of cyt. c550. can also be seen in (Fig. 26B). There are two regions in the spectrum that can be focused on to monitor the reduction of the protein. The first region of the spectrum indicating the reduction of cyt., is a shift in the solet band from 407nm to 417nm. The shift in this region is shown in figure 12, where the fully oxidized protein has a peak at 407 nm, while the fully reduced protein has a peak 417 nm. The second region that can be observed in the spectrum is that of the α -band at 550nm. This was the region of focus for cyt. c550 because the absorbance values at 550 nm were recorded in conjunction with the respective potential. In (Fig. 26B), the big peak is representative of the fully reduced

protein and the fully oxidized protein is the flat curve at the bottom. The inset of (Fig. 26B) is a logarithmic Nernst plot for cyt. c550 where the potential vs. the $\log[\text{ox}]/[\text{red}]$ has been plotted. By plotting this information, a straight line is obtained with a slope equal to 59mV (Eq. 1) and the y-intercept, at zero, equal to the formal midpoint potential of the redox couple in solution.

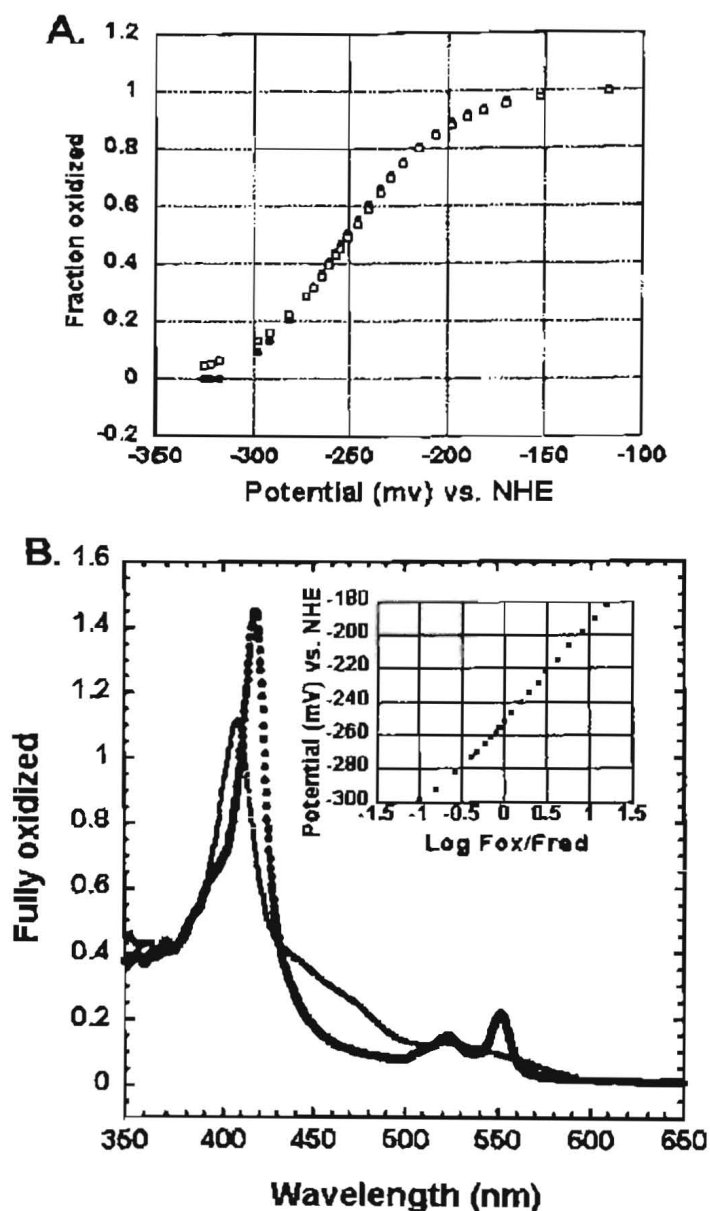


Figure 26. Graphs of spectroelectrochemical titration of cyt. c550 using sodium dithionite. ($\sim 10\mu\text{M}$ protein in 200mM sodium phosphate buffer pH 8.0, 24° C).

A. Titration curve of cyt. c550. The fraction of oxidized cyt. c550 is plotted against the corresponding potential at that time during the titration (●). The Nernst equation was used to fit the titration curve with a consistent slope of 59mV (□). After three trials, the redox potential of cyt. c550 was determined to be -252 ± 2.12 mV vs. NHE.

B. Complete spectrum showing the completely oxidized form of cyt. c550 (—) with no peak at 550nm, and the completely reduced form of cyt. c550 (—) with a large peak at 550nm. The inset of the figure is a logarithmic Nernst plot derived from the change in absorbance at 550nm which also indicates a redox potential of ~ -252 mV vs. NHE.

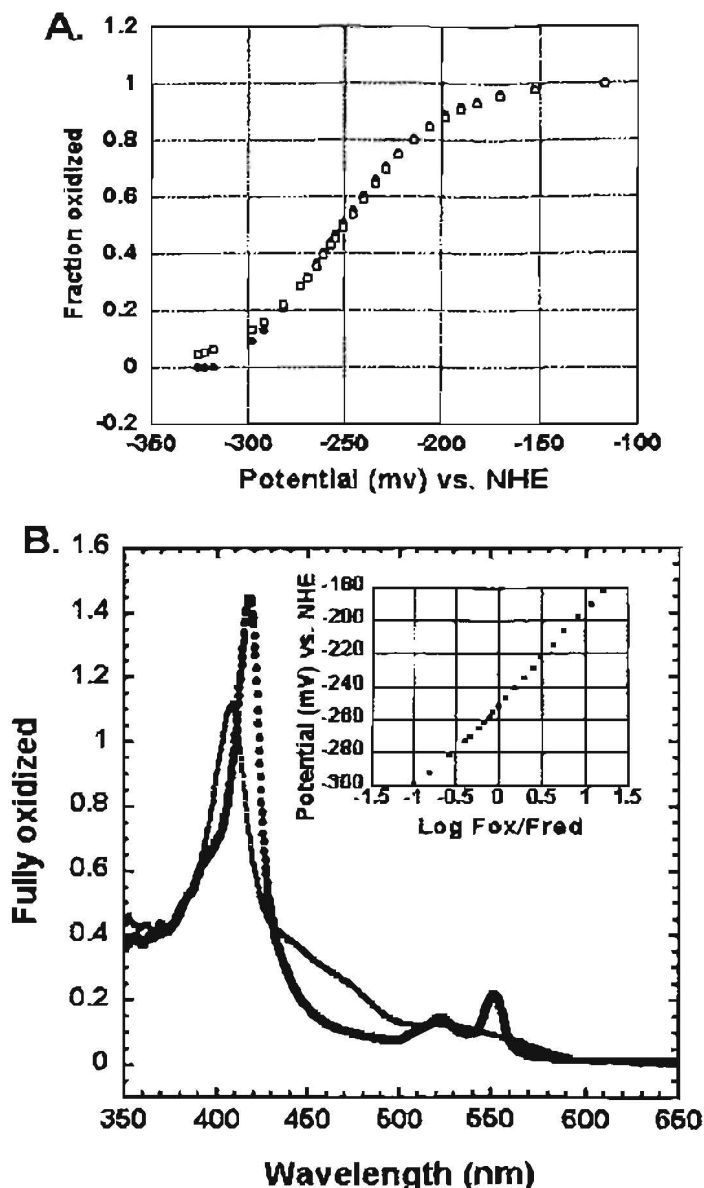


Figure 26. Graphs of spectroelectrochemical titration of cyt. c550 using sodium dithionite. (~10 μ M protein in 200mM sodium phosphate buffer pH 8.0, 24 $^{\circ}$ C).

A. Titration curve of cyt. c550. The fraction of oxidized cyt. c550 is plotted against the corresponding potential at that time during the titration (●). The Nernst equation was used to fit the titration curve with a consistent slope of 59mV (□). After three trials, the redox potential of cyt. c550 was determined to be -252 \pm 2.12 mV vs. NHE.

B. Complete spectrum showing the completely oxidized form of cyt. c550 (---) with no peak at 550nm, and the completely reduced form of cyt. c550 (—) with a large peak at 550nm. The inset of the figure is a logarithmic Nernst plot derived from the change in absorbance at 550nm which also indicates a redox potential of ~-252 mV vs. NHE.

Cytochrome c550-T48I

The average midpoint potential for cyt. c550-T48I was $253 \pm 0 \text{ mV}$ vs. NHE, which was very consistent with the cyt. c550 value of $-252 \pm 2.12 \text{ mV}$ vs. NHE. Although heme solvent exposure has long been recognized as a major contributing factor to midpoint potential (MP), Mao *et al.*, indicate that it is probably multiple factors that lead to a change in MP where solvent exposure is concerned. They also note that typically the addition of surface groups covering the heme will raise the MP, because the heme will now be buried and the MP will increase irregardless of solvent. However, the T48I target, which was selected primarily to aid in covering the solvent exposed heme, (Fig. 27), did not allow for significant enough coverage to result in a change in midpoint potential upon the substitution of threonine for isoleucine. Additionally, Mao *et al.* indicate that mutations of charged surface groups usually yield changes in MP of only $\sim 15 \text{ mV}$, if at all, since solvent screening makes their electrostatic potential negligible at the heme. The surface charges are instead needed for binding the correct reaction partners (Tiede *et al.*, 1993).

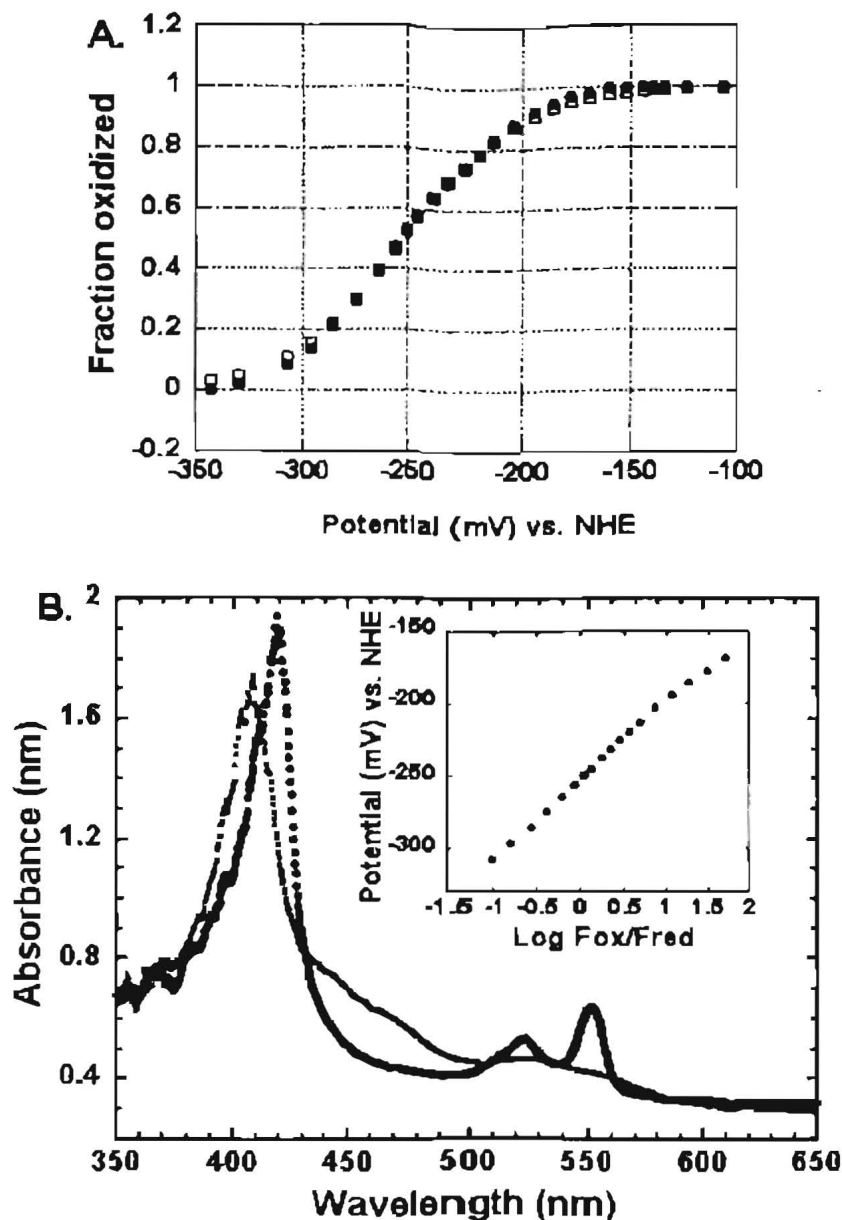


Figure 27. Graphs of spectroelectrochemical titration of cyt. c550-T48I using sodium dithionite. (~10 μ M protein in 200mM sodium phosphate buffer pH 8.0, 24° C). **A.** Titration curve of cyt. c550-T48I. The fraction of oxidized cyt. c550-T48I is plotted against the corresponding potential at that time during the titration (●). The Nernst equation was used to fit the titration curve with a consistent slope of 59mV (□). After three trials, the redox potential of cyt. c550-T48I was determined to be -253 \pm 0 mV vs. NHE. **B.** Complete spectrum showing the completely oxidized form of cyt. c550-T48I (—) with no peak at 550nm, and the completely reduced form of cyt. c550-T48I (■) with a large peak at 550nm. The inset of the figure is a logarithmic Nernst plot derived from the change in absorbance at 550nm which also indicates a redox potential of ~-253 mV vs. NHE.

Cytochrome c550-L91I

Cyt. c550-L91I which had a midpoint potential of -252.33 ± 1.41 mV vs. NHE, was once again nearly the same as cyt. c550. The L91I site was also selected to try to cover the heme from solvent exposure (Fig. 28), but obviously the substitution of leucine for isoleucine did not help in the coverage significantly enough to render a change in redox value for the same reasons as the c550-T48I mutant.

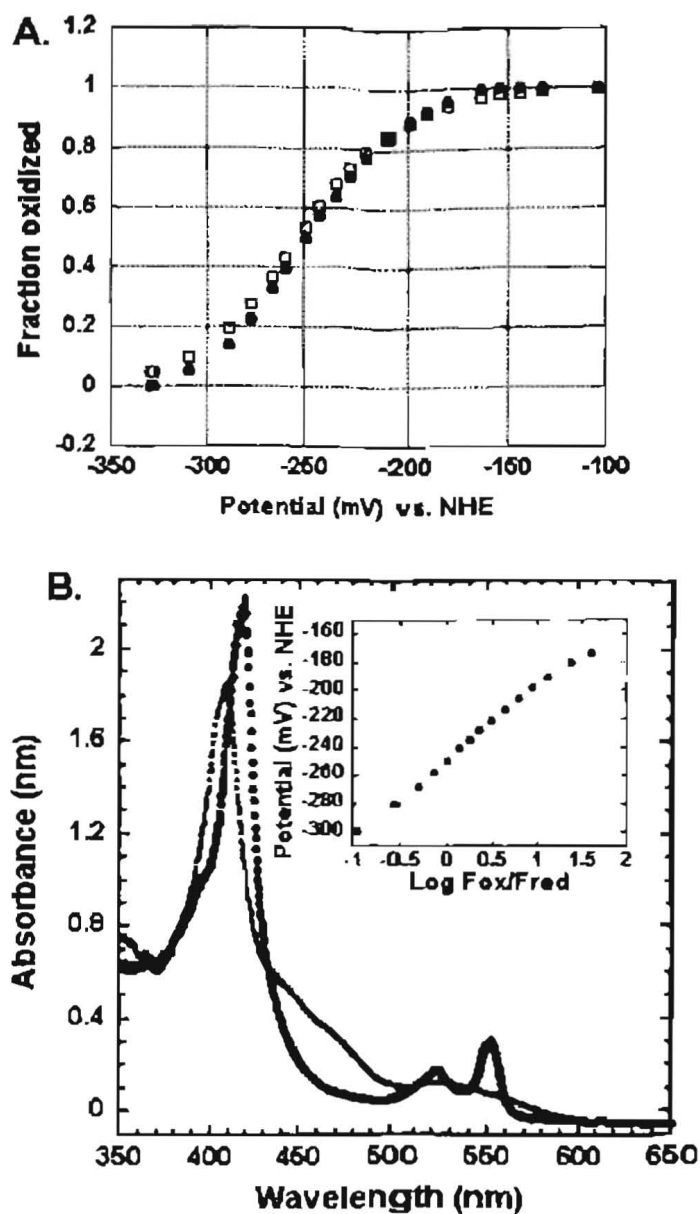


Figure 28. Graphs of spectroelectrochemical titration of cyt. c550-L91I using sodium dithionite. ($\sim 10\mu\text{M}$ protein in 200mM sodium phosphate buffer pH 8.0, 24° C).
A. Titration curve of cyt. c550-L91I. The fraction of oxidized cyt. c550-L91I is plotted against the corresponding potential at that time during the titration (\bullet). The Nernst equation was used to fit the titration curve with a consistent slope of 59mV (\blacksquare). After three trials, the redox potential of cyt. c550-L91I was determined to be -252.33 ± 1.41 mV vs. NHE. **B.** Complete spectrum showing the completely oxidized form of cyt. c550-L91I (—) with no peak at 550nm, and the completely reduced form of cyt. c550-L91I (—) with a large peak at 550nm. The inset of the figure is a logarithmic Nernst plot derived from the change in absorbance at 550nm which also indicates a redox potential of ~ 252 mV vs. NHE.

Cytochrome c550H

Out of curiosity, we tested cyt. c550H (from Dr. Li), which was His-tagged at the C-terminus. Cyt. c550H, was also much like cyt. c550, as it resulted in a midpoint potential of -250.33 ± 5.66 mv vs. NHE as seen in (Fig. 29). This was anticipated since it would not be likely that a His-tag would change the redox potential of a protein. Additionally, the SDS-page of the cyt. c550H protein showed a band that was identical to the wild-type cyt. c550 (Fig. 30). However, I did not see the same results when I tested the N-terminal His-tagged c550.

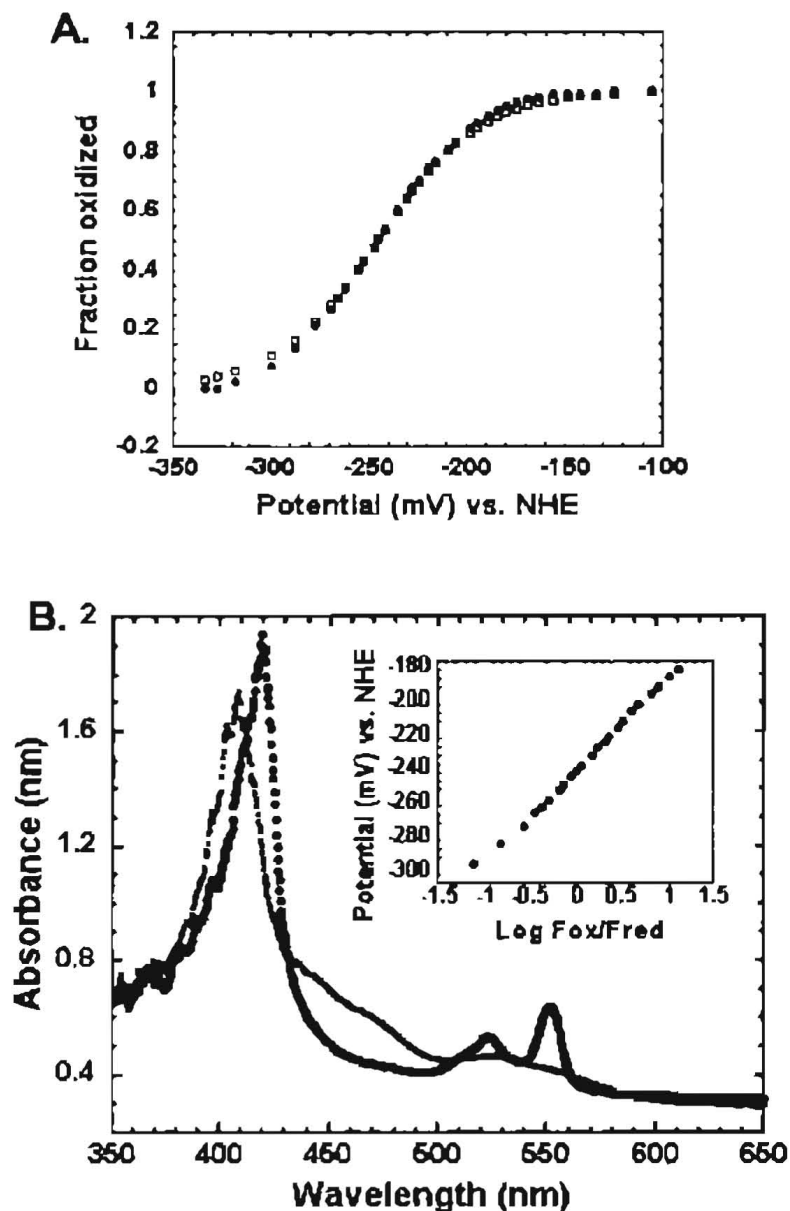


Figure 29. Graphs of spectroelectrochemical titration of cyt. c550H using sodium dithionite. (~10 μ M protein in 200mM sodium phosphate buffer pH 8.0, 24 $^{\circ}$ C).

A. Titration curve of cyt. c550H. The fraction of oxidized cyt. c550H is plotted against the corresponding potential at that time during the titration (●). The Nernst equation was used to fit the titration curve with a consistent slope of 59mV (□). After three trials, the redox potential of cyt. c550H was determined to be -250.33 +/- 5.66 mV vs. NHE.

B. Complete spectrum showing the completely oxidized form of cyt. c550H (—) with no peak at 550nm, and the completely reduced form of cyt. c550H (—) with a large peak at 550nm. The inset of the figure is a logarithmic Nernst plot derived from the change in absorbance at 550nm which also indicates a redox potential of ~250 mV vs. NHE.

Cytochrome Hc550

A somewhat unexpected result was found for cyt. Hc550 which yielded a midpoint potential of $-241.33 \pm 2.12 \text{ mV}$ vs. NHE, a near -10.67 vs. NHE difference from the midpoint potential of wild-type cyt. c550 (Fig. 31). Obviously in this situation, the His-tag was responsible for this small, but significant shift in midpoint. We speculate that the His-tag destabilizes the three-dimensional structure such that hydrogen bonding to the heme is altered. Data supporting this conjecture was seen on the SDS-page (Fig. 30B), where there was a shift in the mobility of the N-terminus His-tagged protein as compared to the band of wild-type cyt. c550 and the C-terminus His-tagged c550. Additionally seen in (Fig. 30A), is the 2 conformations of cyt. c550H, the reduced and oxidized form, upon the addition of dithiothreitol.

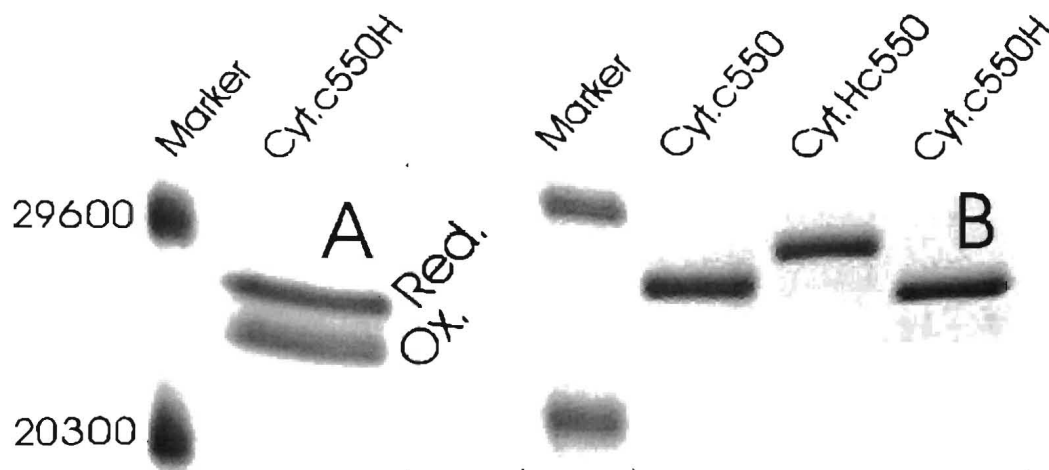


Figure 30. Effects of dithiothreitol concentration and the position of his-tag on the electrophoretic behavior of cyt. c550. SDS-PAGE was performed at 12% acrylamide including 6M urea, the gel was stained by Coomassie Brilliant Blue R-250. **A:** profile of cyt.c550H in the presence of 40 mM DTT, Red., reduced cyt.c550H, Ox., oxidized cyt.c550H; **B:** profile of native and His-tagged cyt.c550 protein in the presence of 150 mM DTT. Cyt.c550: cytochrome c550; cyt.c550H: His-tag located at C-terminus of cytochrome c550; cyt.Hc550: His-tag located at N-terminus of cytochrome c550. Prestained SDS-PAGE standards (Bio-Rad) was used as molecular weight marker and 1 μg protein was loaded (Dr. Li, OSU).

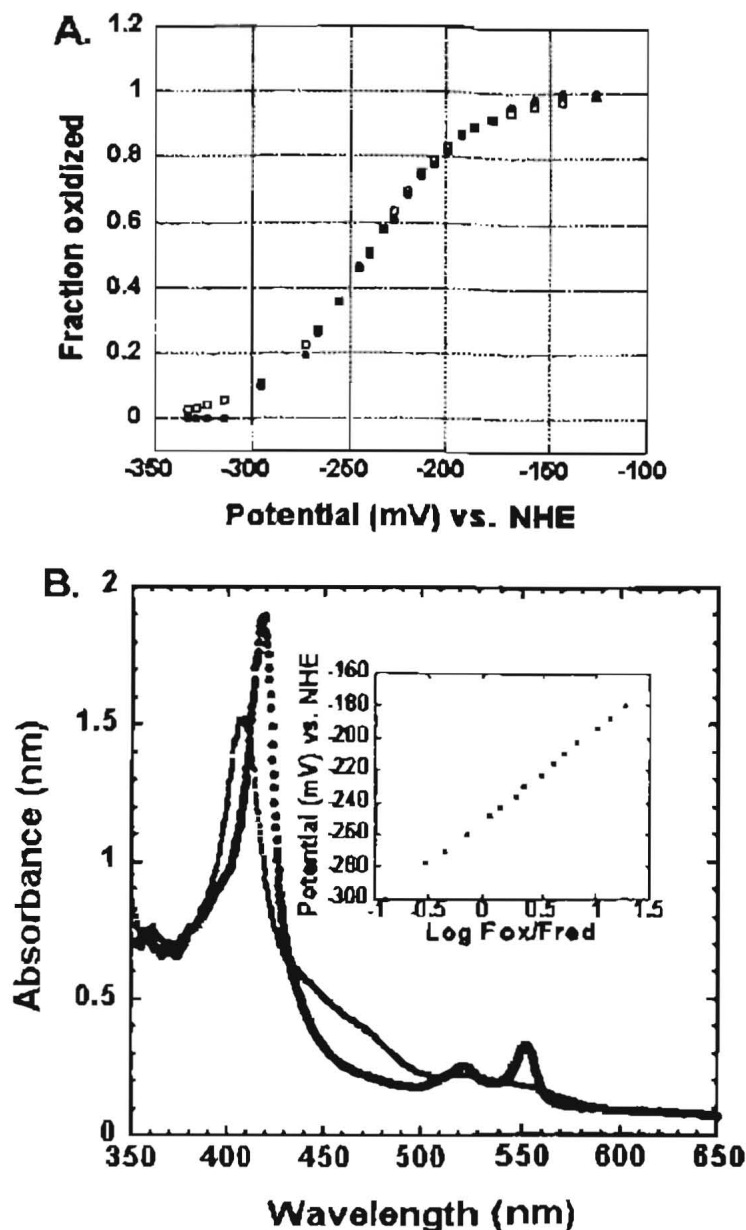


Figure 31. Graphs of spectroelectrochemical titration of cyt. Hc550 using sodium dithionite. (~10 μ M protein in 200mM sodium phosphate buffer pH 8.0, 24 $^{\circ}$ C).

A. Titration curve of cyt. Hc550. The fraction of oxidized cyt. Hc550 is plotted against the corresponding potential at that time during the titration (●). The Nernst equation was used to fit the titration curve with a consistent slope of 59mV (□). After three trials, the redox potential of cyt. c550H was determined to be -241.33 \pm 2.12 mV vs. NHE.

B. Complete spectrum showing the completely oxidized form of cyt. Hc550 (—) with no peak at 550nm, and the completely reduced form of cyt. Hc550 (—) with a large peak at 550nm. The inset of the figure is a logarithmic Nernst plot derived from the change in absorbance at 550nm which also indicates a redox potential of ~241 mV vs. NHE.

Based on this information, we can conclude that Hc550 may have two discrete mobility forms that possibly correspond to two conformations of the protein, which could additionally attribute to the difference seen in redox potential. Consequently, there is no difference in mass when compared to cyt. c550H as determined by MALDI-TOF (Dr. Li) (Fig. 32). So although the two His-tagged proteins have the same molecular mass, placement of the His-tag at the alternative ends of the polypeptide likely results in differences in the secondary or tertiary structure of the two proteins. This evidence is supported by Mao *et al.*, who report how cytochromes with different folds control heme redox potentials, based on differences in stabilization of the buried, cationic, oxidized heme by proteins in different motifs (Churg *et al.*, 1983).

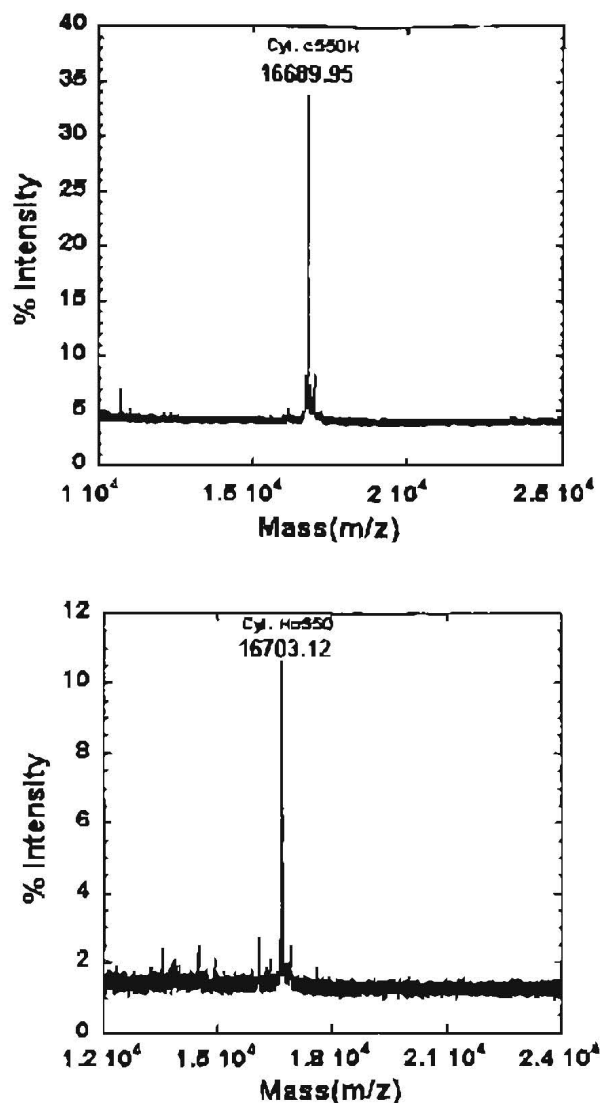


Figure 36. MALDI-TOF Mass Spectra of cyt.c550 with a C-terminal His-tag and a N-terminal His-tag from *Synechocystis* sp. PCC6803. Matrix-Assisted Laser Desorption/Ionization Time-of-Flight (MALDI-TOF) mass spectrometric analyses were carried out with a Applied Biosystems Voyager DE-PRO mass spectrometer (PerSeptive Biosystem, Framingham, USA) using a 25kV accelerating voltage. The samples were run in the linear mode. The protein solutions (50 mM MES, pH6.5) were diluted 1:1 (v/v) with the matrix solution of sinapinic acid at 10 mg/ml in 50% acetonitrile containing 0.1% TFA, 1 μ l of the mixture was deposited on the sample target and then allowed to air-dry. Bovine serum albumin (664299 Da) was used for external calibration. The spectrum was acquired in the linear mode. Predicted molecular mass for both His-tag forms is 16688.5 daltons (Dr. Li, OSU).

Cytochromes c550-P93A & c550-P93G

Cyt. c550-P93A yielded a midpoint potential of $-236.33 \pm 3.54 \text{ mV}$ vs. NHE as shown in (Fig. 33). This value was different from the wild-type cyt. c550 by -15.67 mV vs. NHE. Although this particular mutation was initially selected for its involvement in hydrogen bonding (Fig. 8A), since proline forms a hydrogen bond to the N δ atom of His92, upon the substitution of proline93 for an alanine (Fig. 8B), this hydrogen bond is not lost since the peptide backbone carbonyl is involved and not the side-chain. The alanine substitution for proline does not remove the hydrogen bond, however it may change the geometry of the hydrogen bonding, which may force a carbonyl oxygen location that is undesirable, therefore accounting for the -15.67 mV vs. NHE shift in redox potential. As evidenced by Mao *et al.*, cyts. with different folds and protein conformations can lead to changes in MP for a number of reasons. They report that nonpolar residues change MP indirectly by helping define the protein conformation, limiting the position of polar residues, and keeping water out of the protein core. However, they go on to state that changes in the backbone geometry, site ionization, or burial of polar or charged groups can lead to unpredictable effects where hydrophobic residues are changed. Since proline is hydrophobic, as is alanine, the change in MP is likely not due to the positioning of the residues, but the new backbone geometry that the cytochrome assumes upon the mutation. Since the internal hydrogen bonds of a protein provide a structural basis for its native folding pattern, if a protein folds in a way that prevents some of its internal h-bonds from forming, their free energy would be lost and such conformations would be less stable.

Although I was unable to get the *cyt. c550-P93G* mutant, it likely would have had less effect on the redox potential because glycine has a hydrogen side-chain as opposed to the methyl side-chain of alanine. A hydrogen side-chain would have likely allowed backbone rearrangements more easily than the methyl group of alanine.

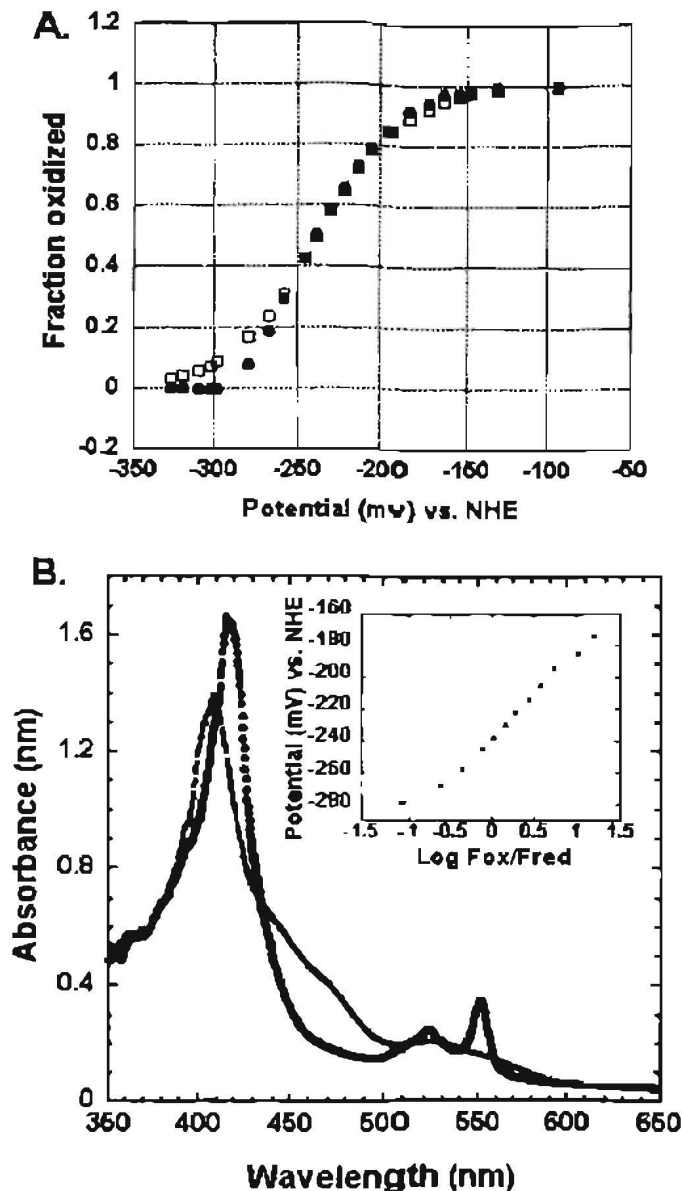


Figure 33. Graphs of spectroelectrochemical titration of cyt. c550-P93A using sodium dithionite. ($\sim 10\mu\text{M}$ protein in 200mM sodium phosphate buffer pH 8.0, 24° C).

A. Titration curve of cyt. c550-P93A. The fraction of oxidized cyt. c550-P93A is plotted against the corresponding potential at that time during the titration (●). The Nernst equation was used to fit the titration curve with a consistent slope of 59mV (□). After three trials, the redox potential of cyt. c550-P93A was determined to be -236.33 ± 3.54 mV vs. NHE.

B. Complete spectrum showing the completely oxidized form of cyt. c550-P93A (—) with no peak at 550nm, and the completely reduced form of cyt. c550-P93A (—) with a large peak at 550nm. The inset of the figure is a logarithmic Nernst plot derived from the change in absorbance at 550nm which also indicates a redox potential of ~ 236 mV vs. NHE.

Cytochromes c550-N49L & c550-N49D

In addition to the shift in midpoint potential seen in the cyt. c550-P93A mutant, the cyt c550- N49L and cyt. c550-N49D mutants also resulted in a shift in midpoint. The cyt. c550-N49L mutant yielded a midpoint potential of -235.33 ± 3.54 mV vs. NHE which was a difference from the wild-type cyt. c550 of -16.67 mV vs. NHE as shown in (Fig. 34). This is in accordance to claims that changes in the propionate ionization are the most important response to oxidation in many cytochromes (Rogers *et al.*, 1995). This was a significant difference that could be attributed to Asn49's involvement in the hydrogen bonding network that shields the pyrrole A, D, and C rings of the heme (Fig. 6A). Additionally Asn49 is solvent exposed and involved in the hydrogen bonding network to a propionate D oxygen atom. Asn49's amide side-chain is hydrogen bonded to the D propionate. Therefore upon the mutation of asparagine (Asn) to leucine (Leu) (Fig. 6C), the polar amide side-chain of Asn is lost and now the nonpolar ethyl side-chain of Leu is left to hydrogen bond to the propionate D oxygen atom instead. Since propionates are always close to the heme ($\sim 8 \text{ \AA}$), and partially buried in the protein, they usually do modify MP based on differences in their ionization states and solvent exposure (Mao *et al.*, 2003). Since leucine is nonpolar, it might actually assume a position closer to the core of the protein, which could aid in solvent exposure of the heme.

A change in midpoint potential was also observed for the cyt. c550-N49D mutant, which yielded a midpoint potential of -243 ± 0.71 mV vs. NHE which was -9 mV different from the midpoint potential of wild-type cyt. c550 (Fig. 35). The difference in midpoint potential seen from the substitution of Asn to aspartate (Asp) (Fig. 6B) is a little less than the value seen upon the substitution for Asn to Leu, but once again, Asp has a charged

polar ester side-chain, which would be capable of hydrogen bond formation in contrast to the Leu's nonpolar ethyl side-chain. However, since Asp is polar, it might not be buried as well as the nonpolar leucine.

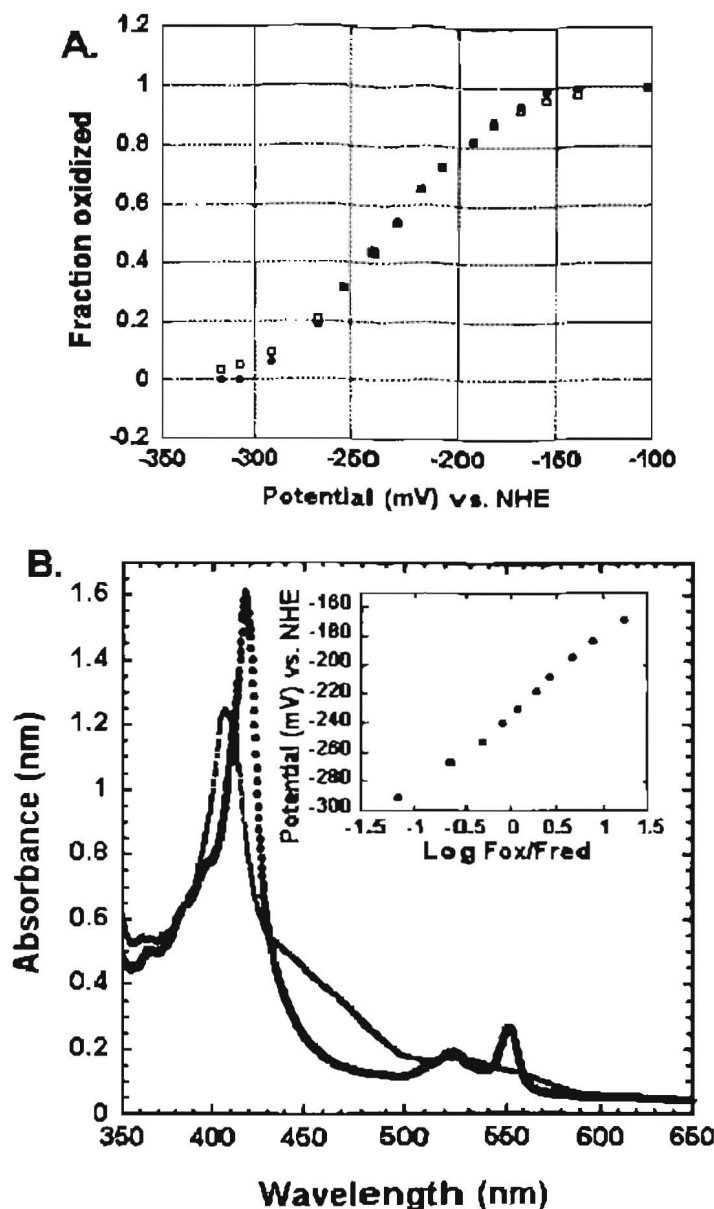


Figure 34. Graphs of spectroelectrochemical titration of cyt. c550-N49L using sodium dithionite. (~10 μ M protein in 200mM sodium phosphate buffer pH 8.0, 24 $^{\circ}$ C).

A. Titration curve of cyt. c550-N49L. The fraction of oxidized cyt. c550-N49L is plotted against the corresponding potential at that time during the titration (●). The Nernst equation was used to fit the titration curve with a consistent slope of 59mV (□). After three trials, the redox potential of cyt. c550-N49L was determined to be -235.33 +/- 3.54 mV vs. NHE. **B.** Complete spectrum showing the completely oxidized form of cyt. c550-N49L (—) with no peak at 550nm, and the completely reduced form of cyt. c550-N49L (—) with a large peak at 550nm. The inset of the figure is a logarithmic Nernst plot derived from the change in absorbance at 550nm which also indicates a redox potential of ~235 mV vs. NHE.

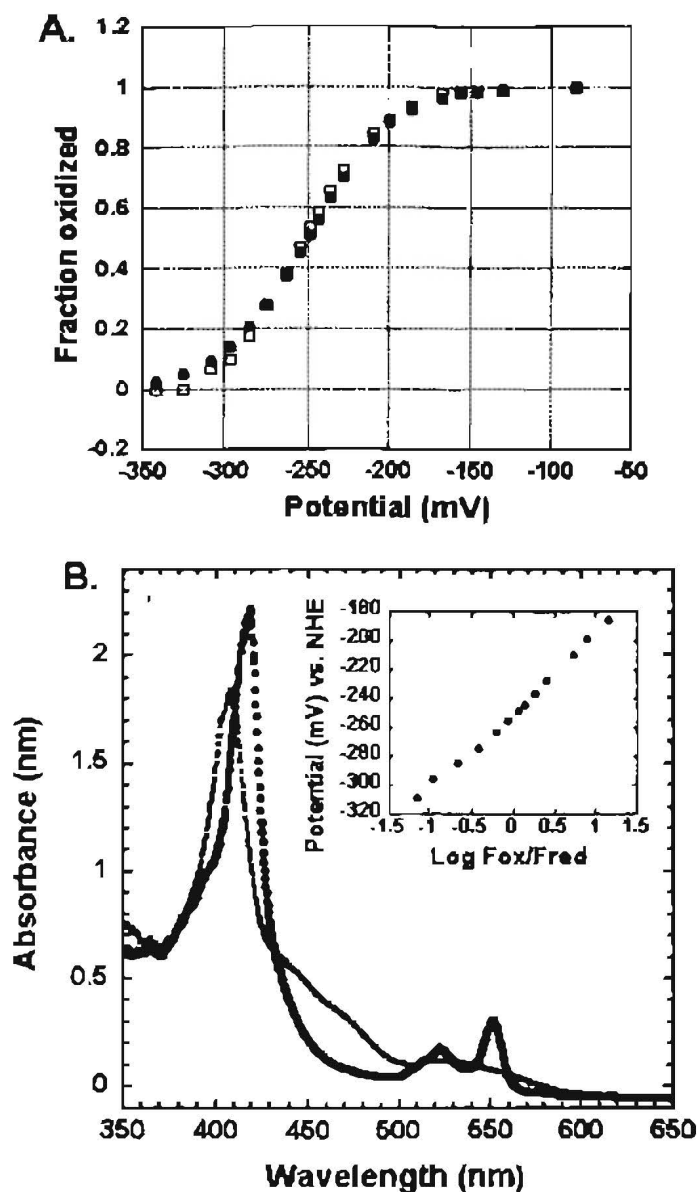


Figure 35. Graphs of spectroelectrochemical titration of cyt. c550-N49D using sodium dithionite. (~10 μ M protein in 200mM sodium phosphate buffer pH 8.0, 24 $^{\circ}$ C).

A. Titration curve of cyt. c550-N49D. The fraction of oxidized cyt. c550-N49D is plotted against the corresponding potential at that time during the titration (●). The Nernst equation was used to fit the titration curve with a consistent slope of 59mV (□). After three trials, the redox potential of cyt. c550-N49D was determined to be -243 +/- 0.71 mV vs. NHE. **B.** Complete spectrum showing the completely oxidized form of cyt. c550-N49D (—) with no peak at 550nm, and the completely reduced form of cyt. c550-N49D (—) with a large peak at 550nm. The inset of the figure is a logarithmic Nernst plot derived from the change in absorbance at 550nm which also indicates a redox potential of ~243 mV vs. NHE.

Cytochrome c550-H92M

Lastly, and most significantly, was the change in midpoint potential observed in the Cyt. c550-H92M mutant. The H92M substitution (Fig. 7B) resulted in a midpoint potential of -177.33 ± 1.41 mV vs. NHE (Fig. 36) which was -74.67 vs. NHE different from the wild-type cyt. c550 value (Fig. 7A). Obviously this value can be attributed somewhat to the fact the His92 is the sixth axial ligand, and as reported in literature (Dolla *et al.*, 1994), substitution of Met for His at the sixth axial position usually results in a positive shift in midpoint potential. Axial ligands are assumed to influence heme MP primarily through bonding, not electrostatic interactions. The heme-ligand complex is treated as a single unit to be modified as a whole by the protein (Mao *et al.*, 2003). His-ligands in proteins are found to lie in a narrow range of orientations, which maximizes the hydrogen bonding at the distal positions (Zaric *et al.*, 2001). It appears that Met is electron withdrawing, which increases MP, while His is electron donating. This is justified since Met has a higher affinity for Fe (II) than Fe (III), while His has the opposite preference (Nesset *et al.*, 1996), therefore accounting for the positive shift in MP upon substitution of His for Met. It was expected to see a shift of close to -150 mV as reported by Dolla *et al.*, in Cyt. c3, but the shift that I got was about half of that. There may have been less of a positive shift in midpoint as a result of much of cyt. c550's heme still being exposed to solvent, versus the heme of Cyt. c3 (Dolla *et al.*, 1994). It is also possible that the new conformation of the protein assumed upon the change in axial ligation (from *bis*-histidine to His-Met), or the new orientation of the heme, did not allow for that large of an increase in MP.

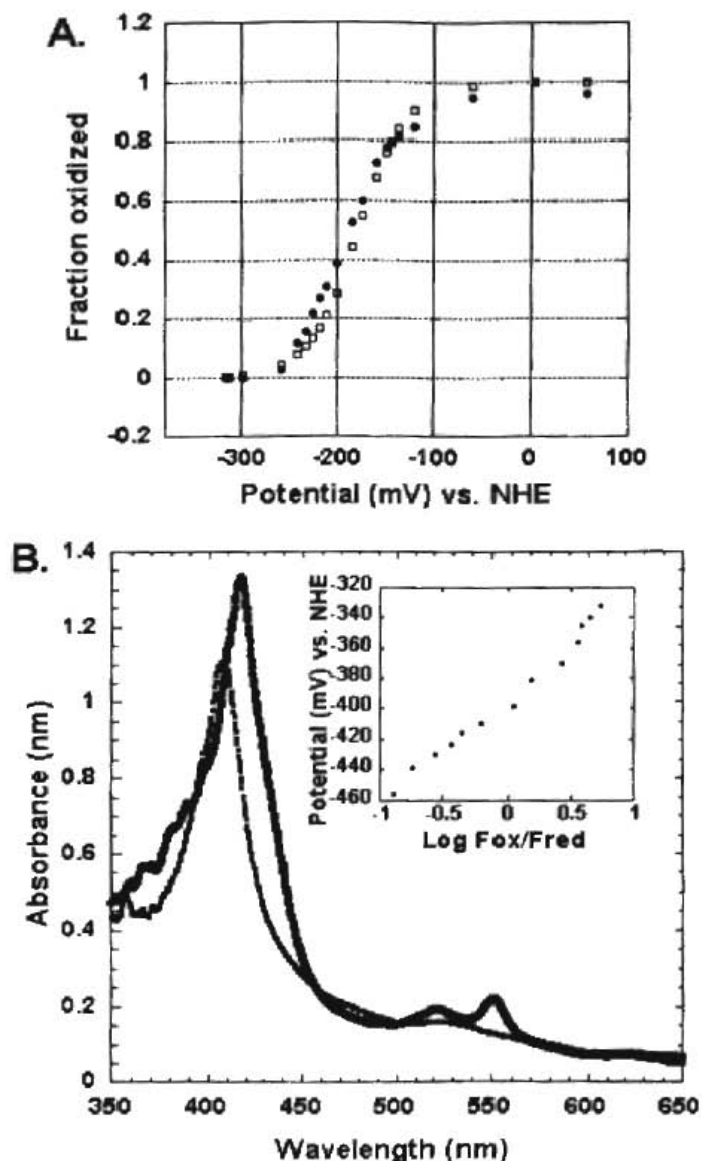


Figure 36. Graphs of spectroelectrochemical titration of cyt. c550-H92M using sodium dithionite. ($\sim 10\mu\text{M}$ protein in 200mM sodium phosphate buffer pH 8.0, 24°C).

A. Titration curve of cyt. c550-H92M. The fraction of oxidized cyt. c550-N49D is plotted against the corresponding potential at that time during the titration (\bullet). The Nernst equation was used to fit the titration curve with a consistent slope of 59mV (\square). After three trials, the redox potential of cyt. c550-H92M was determined to be -177.33 ± 1.41 mV vs. NHE. **B.** Complete spectrum showing the completely oxidized form of cyt. c550-H92M ($-$) with no peak at 550nm, and the completely reduced form of cyt. c550-H92M (\equiv) with a large peak at 550nm. The inset of the figure is a logarithmic Nernst plot derived from the change in absorbance at 550nm which also indicates a redox potential of ~ 177 mV vs. NHE.

CHAPTER 7

SUMMARY

The most well-characterized class of electron transfer proteins thus far are cytochromes. They are widespread molecules which exist not only in aerobic mitochondrial and bacterial respiratory chains, but also in prokaryotic electron transfer systems including those involved in anaerobic respiration and photosynthesis (Dolla *et al.*, 1994). Cytochrome c550 of *Synechocystis* 6803 functions in PSII of photosynthesis and is encoded for by the *psbV* gene. Cyt. c550 is a very unique cytochrome because it has a single heme with *bis*-histidine axial ligation, and an unusually negative redox potential of -250mV.

Since c550's unique low redox potential raises fundamental questions on the factors governing redox potential in heme proteins, we have successfully mutagenized several amino acid target sites to further investigate the factors controlling redox potential. A number of factors such as axial ligation, hydrogen bonding, heme solvent exposure and heme propionates are all known to contribute to redox potential. Therefore amino acid sites were selected to target each of these governing factors. The cyt. c550-T48I and cyt c550-L91I mutants were selected to help cover the heme and shield it from solvent exposure, while cyt. c550-P93A was selected because of its hydrogen bond to the sixth axial his ligand. The cyt. c550-N49D and cyt. c550-N49L mutants were selected because of their hydrogen bonding to the heme propionate D oxygen atom. Additionally, we tested cyt. c-550 with a His-tag on the C-terminus and c-550 with a His-tag on the N-

terminus, simply out of curiosity of the effects of His-tags on proteins. PCR was used to successfully amplify each of these mutations in the plasmid vector pETC550.

Following the successful amplification of each mutant, we were able to demonstrate how a c-type cytochrome can be over-expressed using a binary plasmid system in *E.coli*.

While over-expressing the various cyt. c550 mutants in *E.coli*, we were forced to optimize some of our expression conditions so we would get significant yields of each protein. We found that by supplementing our growth medium with 0.5mM IPTG for three-four hours until $OD_{600}=1$, adding 2.5mM betaine, and 300mM sucrose that our expression levels were increased nearly four-fold. We also found that after the culturing process was complete, instead of immediately preparing the periplasmic fraction, leaving it at 4°C over-night increased expression levels. It is likely that allowing the culture to sit in the cold over-night facilitates the covalent attachment of the heme, therefore leading to a more stable protein. To purify the protein, column chromatography was used as well as a crude extract protein purification technique using only ammonium sulfate. Since the column chromatography was so time-consuming, and significant amounts of protein were needed for the spectroelectrochemistry, we used a crude extract purification technique to obtain protein strictly for redox titration experiments. The crude-purified protein showed the same redox values as protein purified by the columns, and therefore provided us a reliable alternative.

The spectroelectrochemical titrations using sodium dithionite yielded some very interesting results. We were able to obtain a redox potential value for cyt. c550 of -252mV vs. NHE which was in agreement with the value in the literature (Roncel *et al.*, & Navarro *et al*). The cyt. c550-T48I and cyt. c550-L91I mutants that were

selected to shield the heme from solvent exposure seemed to have no effect redox potential, as both of them yielded values nearly identical to wild-type c550. It was interesting to find that the N-terminal His-tagged protein showed a redox value nearly the same as the wild-type, while the C-terminal His-tagged protein showed a redox potential nearly 11mV more positive. This is likely attributed to differences in the secondary or tertiary structures of the two proteins. The cyt. c550-P93A mutant gave a redox value of -236.66mV vs. NHE which was nearly 16mV more positive than the wild-type. Although this site was selected because of the hydrogen bond to the sixth axial ligand, His 92, the alanine substitution for proline doesn't remove the hydrogen bond. However, it may change the geometry of the hydrogen bonding, which may force a carbonyl oxygen location that is undesirable, therefore accounting for the change in redox. Cyt. c550-N49D gave a redox value of -242 mV vs. NHE while cyt. c550-N49L gave a value of -235.33mV vs. NHE. We were expecting to see a change in redox at this location because of the relationship of the N49 site with the propionate D oxygen atom of the heme. Last, and most significant, was the change in redox that occurred upon the substitution of the sixth axial ligand from histidine to methionine. The cyt. c550-H92M mutant gave a redox value of -177.33 mV vs. NHE which was 75mV more positive than the wild-type. Although we were expecting to see more of a positive shift upon this mutation, it is possible that the new conformation of the protein assumed upon the change in axial ligation (from *bis*-histidine to His-Met), or the new orientation of the heme, did not allow for that large of an increase in MP.

Overall this research is significant for a number of reasons; first, site-directed mutagenesis can be used to create mutations, by PCR amplification, in cytochrome c550, second, cyt. c550 can be over-expressed in a binary-plasmid vector, responsible for the synthesis of apo-cytochrome and the covalent attachment of the heme, harbored in *E. coli* BL-21(DE3), third, protein expression conditions can be enhanced with the addition of IPTG, betaine and sucrose, and after protein purification, spectroelectrochemical redox titrations, using the reductant sodium dithionite, can be done to acquire data to make a redox titration curve and therefore determine the redox potential.

The selection of the mutation target sites in cytochrome c550 did allow the verification of a number of factors controlling redox potential: hydrogen bonding to propionate oxygen atoms, hydrogen bonding to axial ligands, and the nature of the axial ligation itself (*bis*-histidine or histidine-methionine). This is significant because it contributes to previous findings that these factors are important in redox potential. Additionally, future research may allow for different amino acids to be substituted into the mutation target sites in cyt. c550, or other cytochromes could be mutagenized, to find out if these same factors govern redox potential in other cytochromes, as they do in c-type cytochromes.

However, the function of cyt. c550 still remains enigmatic as the findings of this study alone do not unveil enough information to make a conclusion. The redox findings, albeit significant to this study, can not verify that c550 plays a role in electron transport. Other studies in our lab by Dr. Li have shown that cyt. c550 effects the calcium requirement of the water oxidation reaction. It is possible that cyt. c550 binds something

toxic, like superoxide, which would be facilitated if one of the histidine ligands would leave the heme iron and allow the toxicant to bind. To test this hypothesis, the cyt. c550 spectrum was monitored at different pH's (3.5-9.0) (Appendix), but there was no change observed at any of these values. If one of the histidine ligands would have become protonated at a low pH, a change in the spectrum would have been evident. However, we did not see anything to indicate that either histidine ligand got protonated in the spectrum, so without further analysis, we cannot conclude that cyt. c550 functions to bind toxicants. Insight could possibly be gained as to a functional role of cyt. c550 if the mutants created in this study were actually put back into the wild-type cyt. c550. Hopefully with future experiments such as this, more light will be shed on the actual function of this very unique and evolutionarily conserved protein.

BIBLIOGRAPHY

- Alam, J., Sprinkle, M.A., Hermodson, M.A., & Krogmann, D.W. (1984). Characterization of cytochrome c550 from cyanobacteria. *Biochim. Biophys. Acta.* **766**, 317-321.
- Arslan, E., Schulz, Henk, Z., Rachel, Kunzler, P., & Thony-Meyer, L. (1998). Overproduction of the *Bradyrhizobium japonicum* c-type cytochrome subunits of the cbb₃ oxidase in *Escherichia coli*. *Biochem. Biophys. Res.* **251**, 744-747.
- Bertrand, P., Mbarki, O., Asso, M., Blanchard, L., Guerlesquin, F., & Tegoni, M. (1995). Control of the redox potential in c-type cytochromes: Importance of entropic contribution. *Biochemistry.* **34**, 11071-11079.
- Betts, S.D., Ross, J.R., Hall, K.U., Pichersky, E. & Yocum, C.F. (1996). Functional reconstitution of photosystem II with recombinant manganese-stabilizing proteins containing mutations that remove the disulfide bridge. *Biochim. Biophys. Acta.* **1274**, 135-142.
- Cho, Y.S., Pakrasi, H.B., & Whitmarsh, J. (2000). Cytochrome Cm from *Synechocystis* 6803. *Eur. J. Biochem.* **267**, 1-8.
- Churg, A.K., Weiss, R.M., Warshel, A., & Takano, T. (1983). On the action of cytochrome c: correlating geometry changes upon oxidation with activation energies of electron transfer. *J. Phys. Chem.* **87**, 1683-1694.
- Cohn, C.L., Sprinkle, J., Alam, J., Hermodson, M., Meyer, T.E. & Krogmann, D.W. (1989). The amino acid sequence of low-potential cytochrome c550 from the cyanobacterium *Microcystis aeruginosa*. *Arch. Biochem. Biophys.* **270**, 227-235.
- Cutler, R.L., Davies, A.M., Creighton, S., Warshel, A., Moore, G.R., Smith, M., & Mauk, G. (1989). Role of arginine-38 in regulation of the cytochrome c oxidation-reduction equilibrium. *Biochemistry.* **28**, 3188-3197.
- Debus, R.J. (2000). The polypeptides of photosystem II and their influence on manganotyrrosyl-based oxygen evolution. *Metal Ions in Biological Systems.* Marcel Dekker, Inc. New York. **37**, 679-680.
- Diner, B.A. & Babcock, G.T. (1996) Structure, dynamics, and energy conversion efficiency in photosystem II. *Oxygenic photosynthesis: the light reactions.* (Ort, D.R. and Yocum, C.F., eds) p. 213-247. Kluwer Academic Publishers.

- Dolla, A., Florens, L., Bianco, P., Haladjian, P., Voordouw, G., Forest, E., Guerlesquin, F., & Bruschi, M. (1994). Characterization and oxidoreduction properties of cytochrome c3 after heme axial ligand replacements. *J. Biol. Chem.* **269**, 6340-6346.
- Dolla, A., Blanchard, L., & Guerlesquin, M.B. (1994). The protein moiety modulates the redox potential in cytochromes c. *Biochemistry.* **76**, 471-479.
- Drogmann, D.W. (1991). The low-potential cytochrome c of cyanobacteria and algae. *Biochemi. Biophys. Acta.* **1058**, 35-37.
- Enami, I., Murayama, H., Ohta, H., Kamo, M., Katsuyoshi, M., & Shen, J.R. (1995). Isolation and characterization of a Photosystem II complex from the red alga *Cyanidium caldarium*: association of cytochrome c-550 and a 12 kDa protein with the complex. *Biochim. Biophys. Acta.* **1232**, 208-216.
- Fee, J.A., Chen, Y., Todaro, T.R., Bren, K.L., Patel, K.M., Hill, M.G., Gomez-Moran, E., Loehr, T.M., Ai, J., Thony-Meyer, L., Williams, P.A., Stura, E., Sridhar, V., & McRee, D.E. (2000). Integrity of thermus thermophilus cytochrome c552 synthesized by *Escherichia coli* cells expressing the host-specific cytochrome c maturation genes, ccmABCDEFGH: biochemical, spectral, and structural characterization of the recombinant protein. *Protein Sci.* **11**, 2074-84.
- Finazzi, G., Buschlen, S., de Vitry, C., Rappaport, F., & Joliet, P. (1997). Function directed mutagenesis of the cytochrome b6/f complex in *Chlamydomonas reinhardtii*: involvement of the cd loop of cytochrome b6 in quinol binding to the Qo site. *Biochemistry.* **36**, 2867-74.
- Frazao, C., Enguita, F.J., Coelho, R., Sheldrick, G.M., Navarro, J.A., Hervas, M., De la Rosa, M.A., & Carrondo, M.A. (2001). Crystal structure of low-potential cytochrome c549 from *Synechocystis* sp. PCC 6803 at 1.21 Å resolution. *J. Biol. Inorg. Chem.* **6**, 324-332.
- Gust, D. (1996). Why study photosynthesis? Arizona State University. <http://photoscience.la.asu.edu/photosyn/study.html> Accessed September 15, 2002.
- Jungst, A., Wakabayashi, S., Matsubara, H., & Aurnft, W.G. (2001). The nirSTBM region coding for cytochrome cd1-dependent nitrite respiration of *Pseudomonas stutzeri* consists of a cluster of mono, di, and tetraheme proteins. *FEBS Lett.* **279**, 205-209.
- Ho, K.K., Ulrich, E.L., Krogmann, D.W. & Gomez-Lojero, C. (1979). Isolation of photosynthetic catalysts from cyanobacteria. *Biochim. Biophys Acta.* **545**, 236-248.
- Hunte, C., Solmaz, S., & Lange, C. (2002). Electron transfer between yeast cytochrome bc1 complex and cytochrome c: a structural analysis. *Biochem. Biophys. Acta.* **1555**, 21-28.

Kang, C., Chitnis, P.R., Smith S. & Krogmann, D.W. (1994). Cloning and sequence analysis of the gene encoding the low potential cytochrome c of *Synechocystis* PCC 6803. *FEBS Lett.* **344**, 5-9.

Kassner, R.J. (1973). A theoretical model for the effects of local nonpolar heme environments on the redox potentials in cytochromes. *J. Am. Chem. Soc.* **95**: 2674-2677.

Katoh, H., Itoh, S., Shen, J., & Ikeuchi, M. (2001). Functional analysis of *psbV* and a novel c-type cytochrome gene *psbV2* of the thermophilic cyanobacterium *Thermosynechococcus elongatus* strain BP-1. *Plant Cell Physiol.* **42**(6), 599-607.

Kerfeld, C.A. & Krogman, D.W. (1998). Photosynthetic cytochromes c in cyanobacteria, algae and plants. *Annu. Rev. Plant Physiol. Plant Mol. Biol.* **49**, 397-425.

Kienzl, P.F., & Peschek, G.A. (1983). Cytochrome c-549: A cofactor of cyclic photophosphorylation in *Anacystis nidulans*. *FEBS Lett.* **162**, 76-80.

Krogmann, D.W. (1991). The low-potential cytochrome c of cyanobacteria and algae. *Biochim. Biophys. Acta.* **1058**, 35-37.

Kuhl, H., Rogner, M., van Breemen, J.F. & Boekema, E.J. (1999). Localization of cyanobacterial photosystem II donor-side subunits by electron microscopy and the supramolecular organization of photosystem II in the thylakoid membrane. *Eur. J. Biochem.* **266**, 453-459.

Lee, B., & Richards, F.M. (1971). The interpretation of protein structures: estimation of static accessibility. *J. Mol. Bio.* **55**, 370-400.

Mao, J., Hauser, K., & Gunner, M.R. (2003). How cytochromes with Different folds control heme redox potentials. *Biochemistry.* **42**(33), 9829-40.

Meetam, M., Keren, N., Ohad, I. & Pakrasi, H.B. (1999). The *psbY* protein is not essential for oxygenic photosynthesis in the cyanobacterium *Synechocystis* sp. PCC 6803. *Plant Phys.* **121**, 1267-1272

Moore, G.R., & Williams, R.J.P. (1977). Structural basis for the variation in redox potential of cytochromes. *FEBS Lett.* **79**, 229-232.

Moore, G.R. (1983). Control of redox properties of cytochrome c by special electrostatic interactions. *FEBS Lett.* **161**, 171-183.

Moore, G.R., & Pettigrew, G.W. (1990). Cytochromes c: Evolutionary, Structural and Physicochemical Aspects. SpringerVerlag, Berlin - Heidelberg - New York.

- Morgan, T.R., Shand, J.A., Clarke, S.M. & Eaton-Rye, J.J. (1998). Specific requirements for cytochrome c-550 and the manganese-stabilizing protein in photoautotrophic strains of *Synechocystis* sp. PCC 6803 with mutations in the domain Gly-351 to Thr-436 of the chlorophyll-binding protein CP47. *Biochemistry*. **37**, 14437-14449.
- Navarro, J.A., Hervas, M., De la Cerda, B. & De la Rosa, M.A. (1995). Purification and physiochemical properties of the low-potential cytochrome c549 from the cyanobacterium *Synechocystis* sp. PCC 6803. *Archives of Biochem. and Biophys.* **318**, 46-52.
- Neset, M.J.M., Shokhirev, M.V., Enemark, P.D., Jacobson, S.E., & Walker, F.A. (1996). Electronic effects in transition metal porphyrins. 10. Effect of ortho substituents on the temperature dependence of the NMR spectra of a series of spin-admixed perchloratoiron (III) tetrakis(2,6- or 2,4,6-phenyl substituted)porphyrinates. *Inorg. Chem.* **35**, 5188-5200.
- Novagen. (2002-2003). Protein Expression: Prokaryotic Expression: pETBlue and pET System Overview. Novagen 2002-2003 Catalog. p 84-91.
http://www.novagen.com/SharedImages/Novagen/05_PROEXP.pdf. Accessed 2003 Aug 13.
- Odom, J.M. & Peck, H.D. (1984). Hydrogenase, electron-transfer proteins, and energy coupling in the sulfate-reducing bacteria *Desulfovibrio*. *Annu. Rev. Microbiol.* **38**, 551-592.
- Pakrasi, H.B., Reithman, H.C., & Sherman, L.A. (1985). Organization of pigment proteins in the photosystem II complex of the cyanobacterium *Anacystis nidulans* R2. *Pro. Nat. Acad. Sci.* **82**, 6903.
- Price, N.J., Brennan, L., Faria, T.Q., Vijgenboom, E., Canters, G.W., Turner, D.L. & Santos, H. (2000). High yield of *Methylophilus methylotrophus* cytochrome c by coexpression with cytochrome c maturation gene cluster from *Escherichia coli*. *Protein Exp. Purif.* **3**, 444-50.
- Reincke, B., Thony-Meyer, L., Dannehl, C., Odenwald, A., Aidim, M., Witt, H., Ruterjans, H. & Ludwig, B. (1999). Heterologous expression of soluble fragments of cytochrome c552 acting as electron donor to the *Paracoccus denitrificans* cytochrome c oxidase. *Biochem. et Biophys. Acta.* **1411**, 114-120.
- Roncel, M., Boussac, A., Zurita, J.L., Bottin, H., Sugiura, M., Kirilovsky, D., & Ortega, J.M. (2003). Redox properties of the photosystem II cytochromes b559 and c550 in the cyanobacterium *Thermosynechococcus elongatus*. *J Biol Inorg Chem.* (1-2), 206-16.
- Rogers, N.K., Moore, G.R., & Sternberg, M.J. (1985). Electrostatic interactions in globular proteins: calculation of the pH dependence of the redox potential of cytochrome c551. *J. Mol. Biol.* **182**, 613-616.

- Rutherford, A.W. & Faller, P. (2001). The heart of photosynthesis in glorious 3D. *Trends in Biochem. Sciences.* 26(6), 341-344.
- Sambrook, J., Fritsch, E.F., & Maniatis, T. (1989). *Molecular Cloning: A laboratory manual.* Cold Spring Harbor Laboratory Press. 1(2), 1.25.
- Sanders, C. & Lil, H. (2000) Expression of prokaryotic and eukaryotic cytochromes c in *Escherichia coli.* *Biochim. Biophys. Acta.* 1459(1),131-8.
- Sawaya, M.R., Krogman, D.W., Serag, A., Ki Ho, K., Yeates, R.O. & Kerfeld, C.A. (2001). Structures of cytochrome c-549 and cytochrome c6 from the cyanobacterium *Arthrospira maxima.* *Biochemistry.* 40(31), 9215-25.
- Seidler, A. (1996). The extrinsic polypeptides of Photosystem II. *Biochim. Biophys. Acta.* 1277, 35-60.
- Shen, J.R., Ikeuchi, M., & Inoue, Y. (1992). Stoichiometric association of extrinsic cytochrome c550 and 12 kDa protein with a highly purified oxygen-evolving photosystem II core complex from *Synechococcus vulcanus.* *FEBS Lett.* 301, 145-149.
- Shen, J. & Inoue, Y. (1993). Cellular localization of cytochrome c550. *J.Biol. Chem.* 268(27), 20408-20413.
- Shen, J.R. & Inoue, Y. (1993). Binding and functional properties of two new extrinsic components, cytochrome c-550 and a 12-kDa protein, in cyanobacterial photosystem II. *Biochemistry.* 32, 1825-1832.
- Shen, J.R., Vermaas, W.F.J. & Inoue, Y. (1995). The role of cytochrome c-550 as studied through reverse genetics and mutant characterization in *Synechocystis* sp. PCC 6803. *J. Biol. Chem.* 270, 6901-6907.
- Shen, J.R., Burnap, R.L. & Inoue, Y. (1995). An independent role of cytochrome c-550 in cyanobacterial photosystem II as revealed by double-deletion mutagenesis of the *psbO* and *psbV* genes in *Synechocystis* sp. PCC 6803. *Biochemistry.* 34, 12661-12668.
- Shen, J., Vermaas, W., & Inoue, Y. (1995). The role of cytochrome c-550 as studied through reverse genetics and mutant characterization in *Synechocystis* sp. PCC 6803. *J. Biol. Chem.* 270(12), 6901-6907.
- Shen, J.R., Qizn, M., Inoue, Y. & Burnap, R.L. (1998). Functional characterization of *Synechocystis* sp. PCC 6803 *psbU* and *psbV* mutants reveals important roles of cytochrome c-550 in cyanobacterial oxygen evolution. *Biochemistry.* 37(6), 1551-1558.
- Stellwagen, E. (1978). Haem exposure as the determinate of oxidation-reduction potential of haem proteins. *Nature.* 275, 73-74.

- Thony-Meyer, L., Ritz, D., & Hennecke, H. (1994). Cytochrome c biogenesis in bacteria: a possible pathway begins to emerge. *Mol Microbiol.* **12**(1),1-9.
- Tiede, D.M., Vashishta, A.C., & Gunner, M.R. (1993). Electron-transfer kinetics and electrostatic properties of the Rhodobacter sphaeroides reaction center and soluble c-cytochromes. *Biochemistry.* **32**, 4515-4531.
- Unger, T.F. 1997. Show Me The Money: Prokaryotic Expression Vectors and Purification Systems. The Scientist 11(17). http://www.the-scientist.com/yr1997/sept/profile2_970901.html. Accessed 2003 Aug 13.
- Williams, J.G.K. (1988). Construction of specific mutations in photosystem II photosynthetic reaction center by genetic engineering methods in *Synechocystis* 6803. *Methods in Enzymology.* **167**, 766-778.
- Wirtz, M., Oganessian, V., Zhang, X., Studer, J., & Rivera, M. (2000). Modulation of redox potential in electron transfer proteins: Effects of complex formation on the active site microenvironment of cytochrome b5. *Faraday discuss.* **116**, 221-234.
- Zaric, S.D., Popovic, D.M., & Knapp, E.W. (2001). Factors determining the orientation of axially coordinated imidazoles in heme proteins. *Biochemistry.* **40**, 7914-7928.
- Zouni, A., Witt, H.T., Kern, J., Fromme, P., Kraub, N., Saenger, W. & Orth, P. (2001). Crystal structure of photosystem II from *Synechococcus elongatus* at 3.8 Å resolution. *Nature.* **409**, 739-743.

APPENDIX

pH experiment

A general experiment was performed to see if alterations in pH had any effect on the spectrum of cyt. c550. To perform the experiment, 20 μ L of cyt. c550 was added to 580 μ L of each buffer and scanned from 260-700nm. None of the different pH values had an effect on the spectrum of cyt. c550 as compared to the control at pH 7.0, which preliminarily indicates that there are no ionizable groups that change the coordination of the heme. The following table shows the pH buffers used to test cyt. c550 absorbance.

<u>pH value</u>	<u>Buffer</u>	<u>Effect on spectrum of Cyt. c550</u>
3.5	Citrate and Sodium Citrate	None
4.5	Citrate and Sodium Citrate	None
5.5	Citrate and Sodium Citrate	None
6.5	Phosphate	None
7.0	Phosphate	None
8.0	Phosphate	None
9.0	TAPS/KOH	None

Table 1. Effect of different pH's on the absorbance of cyt. c550 from 260-700nm. From the pH values of 3.5-9.0, there was no effect on the spectrum of cyt. c550 as compared to the control at pH 7.0

VITA



Heather L. Andrews

Candidate for the degree of

Master of Science

Thesis: STRUCTURE AND FUNCTION OF CYTOCHROME *c*550 OF *SYNECHOCYSTIS* sp. PCC6803: FACTORS CONTROLLING REDOX POTENTIAL

Major field: Microbiology, Cell and Molecular Biology

Biographical:

Personal Data: Born on Jan. 8, 1977 in Colorado Springs, CO USA, the daughter of Al and Carolyn Andrews.

Education: Graduated from Bartlesville High School in Bartlesville, Oklahoma 1995; Received Bachelor of Science in Biology from Missouri Southern State University in Joplin, Missouri in 2000; completed the requirements for Master of Science Degree in Microbiology, Cell and Molecular Biology at Oklahoma State University in Stillwater, Oklahoma in December 2003.

Experience: Teaching Assistant, School of Arts and Sciences, Oklahoma State University, August 2000 through May 2002; Graduate Research Assistant, Department of Microbiology and Molecular Genetics, Oklahoma State University, June 2002 through November 2003.

Professional organizations: Microbiology and Molecular Genetics Graduate Student Association